

STRUCTURAL AND BIOCHEMICAL STUDIES OF
MULTIPLE IMPORTIN-HISTONE INTERACTIONS

APPROVED BY SUPERVISORY COMMITTEE

Yuh Min Chook, Ph.D.

Jose Rizo, Ph.D.

Youxing Jiang, Ph.D.

Joel Goodman, Ph.D.

Bing Li, Ph.D.

DEDICATION

I would like to thank my mentor Yuh Min Chook for her assistance and guidance throughout my graduate career. She has not only taught me how to design and perform experiments, but also how to approach scientific problems and manage a laboratory. She is one of the most passionate scientists and works hard to get the best out of her students. Her passion for her work not only drove me throughout my project but also continues to drive me to reach my goal of being a PI.

I would also like to thank all the members of the Chook lab. All of the members (past and present) made it a very enjoyable and collaborative environment to come to work everyday and do science. I would like to also thank the members all the members of my dissertation committee: Dr. Jose Rizo, Dr. Bing Li, Dr. Joel Goodman, and Dr. Youxing Jiang for their support and guidance through my project.

I would like to thank my family for their support and for providing me with a stable foundation that allowed me to pursue my degree. I especially want to thank my mom and dad for not only introducing me but also always keeping my interest in science by taking me to the science museums and NASA throughout my life.

Most importantly, I would like to thank my wife, Julia. You were my support and encouragement throughout this journey especially through the challenges of graduate school. Words cannot express how much I love, admire, and respect you.

STRUCTURAL AND BIOCHEMICAL STUDIES OF
MULTIPLE IMPORTIN-HISTONE INTERACTIONS

by

MICHAEL MAURICE SONIAT II

DISSERTATION/THESIS

Presented to the Faculty of the Graduate School of Biomedical Sciences

The University of Texas Southwestern Medical Center at Dallas

In Partial Fulfillment of the Requirements

For the Degree of

DOCTOR OF PHILOSOPHY

The University of Texas Southwestern Medical Center

Dallas, Texas

May, 2016

STRUCTURAL AND BIOCHEMICAL STUDIES OF
MULTIPLE IMPORTIN-HISTONE INTERACTIONS

MICHAEL MAURICE SONIAT II, Ph.D.

The University of Texas Southwestern Medical Center at Dallas, 2016

Supervising Professor: Yuh Min Chook, Ph.D.

ABSTRACT

Multiple Importins can bind the N-terminal tails of histones H3 and H4, and import them into the nucleus to be assembled into the nucleosomes. However, it is not known what sequence elements in the histone tails are recognized by each of the Importins. Through structural and quantitative biochemical analysis, I identified binding determinants in the N-terminal tails of

histones H3 and H4 for each of seven different human Importins (Imp α , Imp β , Kap β 2, Imp4, Imp5, Imp7, Imp9). Crystal structure of the H3 tail bound to Kap β 2 identified H3 tail residues 11-27 as the important binding element, which resembles a PY-NLS that is missing the canonical proline-tyrosine motif. This same N-terminal basic segment of H3 is also important for binding Imp β , Imp4, Imp5, Imp7, Imp9, and Imp α . In addition, a C-terminal IK-NLS-like motif at residues 35-40 of H3 is also used to bind Imp5, Imp7, Imp9 and Imp α . Interactions of the H4 tail with the same Importins show a similar trend of relative affinities as the H3 tail, though at least 10-fold weaker. Similar to the H3 tail, the H4 tail also uses one or two basic regions to bind the Importins. I also studied the effects of histone tail acetylation on Importin-histone interactions and showed that acetylation of Lys14 of the H3 tail impairs binding to all six Importins and Imp α while acetylation of Lys18 of H3 tail and acetylation of Lys5 and Lys12 of the H4 tail had only mild effects on binding to the Importins. Lastly, I studied Importin binding to the H3/H4 dimer and showed that only one Importin molecule binds each H3/H4 dimer. Furthermore, the Importin-binding trend with the H3/H4 dimer is very different than with the N-terminal tails alone suggesting additional interactions with the histone fold domains of H3 and H4. Overall, I have mapped Importin-binding determinants for the H3 and H4 and revealed acetylation effects on Importin-histone binding.

TABLE OF CONTENTS

CHAPTER 1	
INTRODUCTION.....	1
Nuclear Transport and Karyopherins: Introduction.....	1
Classical NLS.....	6
PY-NLS.....	7
Recognition by Kap β 2.....	7
New Kap β 2-PY-NLS or cargo structures.....	8
Newly Identified PY-NLS and non-PY-NLS cargoes.....	9
Kap121p-Specific Lys-Rich NLS.....	12
RS repeat NLS.....	15
Summary.....	19
NLSs and Nuclear Import by other Kap β s.....	21
Importin-4.....	21
Importin-7.....	22
Importin-9.....	22
Histones.....	23
Chromatin.....	23
Nucleosomes and Histones.....	23
Histone Variants.....	24
Post-translational modification and Histone modifying enzymes.....	26
Histone Chaperones.....	27
Nucleosome Biogenesis.....	28
Nuclear Import of Histones.....	31
CHAPTER 2	
KARYOPHERIN- β 2 RECOGNITION OF A PY-NLS VARIANT THAT LACKS THE PROLINE-TYROSINE MOTIF.....	33
Abstract.....	33
Introduction.....	34
Materials and Methods.....	35
Cloning, Expression, and Purification of H3 and Kap β 2.....	35
Structure determination of Kap β 2 bound to the H3 tail.....	37
Measuring dissociation constants with isothermal titration calorimetry.....	38
Results.....	38
Structure of the Kap β 2-Histone H3 tail complex.....	39
Interactions between H3 tail and Kap β 2.....	43
Mutagenic analysis of the Kap β 2-Histone H3 tail interactions.....	44
Discussion.....	46
CHAPTER 3	
RECOGNITION ELEMENTS FOR THE HISTONE H3 AND H4 TAILS FOR SEVEN DIFFERENT IMPORTINS.....	54
Abstract.....	54
Introduction.....	55
Materials and Methods.....	57
Plasmids.....	59

Expression and purification of histones and Importins.....	60
Pull-down binding assays.....	61
Measuring dissociation constants with isothermal titration calorimetry.....	62
Results.....	63
Seven different human Importins bind the H3 and H4 tails.....	63
Interactions of the basic segment within residues 11-27 of H3 tail with other Importins.....	65
A C-terminal IK-NLS-like epitope in the H3 tail.....	68
The Histone H4 tail also contains basic epitope(s) for binding multiple importins.....	71
Acetylation of H3 and H4 tails affects Importin binding.....	74
Discussion.....	75
The N-terminal basic segments of H3 and H4 tails are used to bind all seven Importins.....	76
NLSs in the histone tails for different Importins.....	77
Importin recognition beyond the histone tails.....	79
Acetylation of H3 Lys14 Impairs Importin binding.....	80

CHAPTER 4

BIOCHEMICAL AND BIOPHYSICAL ANALYSIS OF THE IMPORTIN-ASF1-H3/H4 COMPLEX.....

Abstract.....	85
Introduction.....	86
Materials and Methods.....	87
Purification and assembly of Asf1-H3/H4 complexes.....	87
Purification and assembly of the Imp4-Asf1-H3/H4.....	87
X-ray Crystallography of the Imp4-Asf1-H3/H4.....	88
Small-angle X-ray Scattering (SAXS) Analysis.....	88
Pull-down binding assays.....	88
Results.....	89
Purification and analysis of Imp4-H4/H4 complex.....	89
Only one Imp4 molecule binds the Asf1-H3/H4 complex.....	90
Importin binding trend with Asf1-H3/H4 complex is different from the trend with the histone tails.....	93
Asf1-H3/H4 complex is dissociated from Importins by RanGTP.....	94
Complex formation and crystallization of Imp4-Asf1-H3/H4 complex.....	95
Discussion.....	95

CHAPTER 5

CRYSTAL STRUCTURE OF HUMAN KARYOPHERIN β 2 BOUND TO THE PY-NLS OF SACCHAROMYCES CEREVISIAE NAB2.....

Abstract.....	97
Introduction.....	98
Materials and Methods.....	99
Protein expression, purification, and complex assembly.....	99
Crystallization and structure determination of the Kap β 2-Nab2 PY-NLS complex.....	100
Results and Discussion.....	101

CHAPTER 6

CONCLUSIONS AND FUTURE PERSPECTIVES.....	106
BIBLIOGRAPHY.....	113

PRIOR PUBLICATIONS

Soniat, M., Sampathkumar, P., Collett, G., Gizzi, A., Banu, N., Bhosle, R., Chamala, S., Chowdhury, S., Fiser, A., Glenn, A.S., Hammonds, J., Hillerich, B., Khafizov, K., Love, J. D., Matikainen, B., Seidel, R., Toro, R., Kumar, P.R., Bonanno, J., Chook, Y. M.¹, Almo, S. C. Crystal Structure of human Kap β 2 bound to the PY-NLS of *Saccharomyces cerevisiae* Nab2. *Journal of Structural and Functional Genomics*. **2013**, 14(2), 31-35.

Soniat, M. and Chook, Y.M. Nuclear Localization Signals for Four Distinct Karyopherin- β Nuclear Import Systems. *Biochemical Journal* **2015**, 468(3), 353-362.

LIST OF FIGURES

Figure 1-1.....	6
Figure 1-2.....	8
Figure 1-3.....	15
Figure 1-4.....	17
Figure 1-5.....	24
Figure 1-6.....	26
Figure 1-7.....	28
Figure 2-1.....	38
Figure 2-2.....	42
Figure 2-3.....	44
Figure 2-4.....	49
Figure 2-5.....	50
Figure 2-6.....	51
Figure 3-1.....	65
Figure 3-2.....	67
Figure 3-3.....	70
Figure 3-4.....	73
Figure 3-5.....	75
Figure 3-6.....	82
Figure 3-7.....	83
Figure 3-8.....	84
Figure 4-1.....	90

Figure 4-2.....	92
Figure 4-3.....	93
Figure 4-4.....	94
Figure 4-5.....	95
Figure 5-1.....	101
Figure 5-2.....	104

LIST OF TABLES

Table 1-1.....	4
Table 1-2.....	11
Table 1-3.....	12
Table 2-1.....	41
Table 2-2.....	45
Table 2-3.....	52
Table 3-1.....	68
Table 4-1.....	91
Table 5-1.....	105

LIST OF ABBREVIATIONS

ATP	adenosine triphosphate
β -ME	β -mechaproethanol
DTT	dithiothreitol
<i>E.coli</i>	<i>Eschericheria coli</i>
EDTA	ethylenediamine tetra-acetic acid
GAP	GTPase activating protein
GDP	guanosine 5'-diphosphate
GEF	guanine nucleotide exchange factor
GST	glutathione S-transferase
GTP	guanosine 5'-triphosphate
HEAT	Huntington, Elongation factor 3, α ' subunit of protein phosphatase-2A, and TOR1
HEPES	4-(2-hydroxyethyl)-1-piperizine-ethanesulfonicacid
hnRNP	heterogeneous nuclear ribonucleoprotein
IPTG	isopropyl β -D-thiogalactoside
ITC	isothermal titration calorimetry
Kap	karyopherin
Kap α	Karyopherin alpha
Kap β 1	Karyopherin beta-1
Kap β 2	Karyopherin beta-2
Imp	Importin
Imp4	Importin-4

Imp5	Importin-5
Imp7	Importin-7
Imp9	Importin-9
K _D	dissociation constant
kDa	kilo Dalton
MBP	maltose binding protein
NES	nuclear export signal
NLS	nuclear localization signal
NPC	nuclear pore complex
OD ₆₀₀	optical density at 600 nm
PCR	polymerase chain reaction
PY-NLS	proline-tyrosine nuclear localization signal
SDS-PAGE	sodium dodecyl sulfate polyacrylamide gel electrophoresis

CHAPTER 1

INTRODUCTION

Nuclear Transport and Karyopherins¹

Introduction

Transport of macromolecules between the cytoplasm and the nucleus occurs through the nuclear pore complex (NPC). The NPC allows passive passage of ions and small molecules between the nucleus and cytoplasm but larger proteins require binding to nuclear transport factors to traverse the permeability barrier of the NPC. With the exception of mRNA export, much of nuclear-cytoplasmic transport of macromolecules is mediated by the Karyopherin- β (Kap) family of proteins, which are also known as Importins and Exportins. Protein cargos for the Kaps contain nuclear localization signals (NLSs) and/or nuclear export signals (NESs) within their polypeptide chains that direct them either in or out of the nucleus, respectively (Gorlich and Kutay 1999; Chook and Blobel 2001; Conti and Izaurralde 2001; Weis 2003; Cook et al. 2007; Tran et al. 2007a; Xu et al. 2010; Chook and Suel 2011). In addition to binding NLSs or NESs of cargos, Kaps also bind nucleoporins in the NPC for translocation. Because of their interactions

¹ Pages 1-20 were originally published in Biochemical Journal **2015**, 468(3), 353-362. Copyright by the Biochemical Society.

with large numbers of diverse functioning proteins and their roles in controlling protein localization, Kaps are also critically involved in many cellular processes such as gene expression, signal transduction, immune response, oncogenesis, and viral pathogenesis (Dormann and Haass 2011; Ito et al. 2011; Fung and Chook 2014; Mor et al. 2014; Yarbrough et al. 2014).

At least twenty homologous human Kaps and fourteen *S. cerevisiae* Kaps have been identified. Each Kap appears to recognize and transport a distinct set of proteins even though some cargos can be imported into the nucleus by multiple Importins (Chook and Suel 2011). Kaps share low sequence homology (sequence identity of 8-15%), similar molecular weights, isoelectric points and architecture (Quan et al. 2008; O'Reilly et al. 2011). The Kap proteins are made up almost entirely of HEAT repeats, each composed of two antiparallel helices A and B, which are arranged into superhelical or ring-like structures (Chook and Blobel 2001; Conti and Izaurralde 2001; Lee et al. 2005; Suel et al. 2006; Cook et al. 2007). All Kaps bind the GTPase Ran, which controls transport directionality, and all Kaps bind weakly to phenylalanine-glycine (FG) repeats in nucleoporins to target Kap-cargo complexes to the NPC (Kraemer et al. 1995; Moroianu et al. 1995; Gorlich 1998; Mosammaparast and Pemberton 2004; Pemberton and Paschal 2005; Conti et al. 2006).

Nuclear-cytoplasmic localization of cargos by the Kaps is controlled by the Ran nucleotide cycle (reviewed in (Gorlich 1998; Mosammaparast and Pemberton 2004; Pemberton and Paschal 2005; Conti et al. 2006)). Ran is mostly in the GDP state in the cytoplasm and mostly in the GTP state in the nucleus because of asymmetric localization of RanGAP in the cytoplasm and exchange factor RCC1 in the nucleus. Kaps bind selectively to RanGTP but not to RanGDP. Importins bind RanGTP and cargos with negative cooperativity. In the cytoplasm where

RanGTP is scarce, Importins are able to bind cargos and translocate across the NPC. In the nucleus where RanGTP is abundant, Importins bind RanGTP and release their cargos. Importin-RanGTP complexes then translocate back through the NPC to the cytoplasm for the next cycle of nuclear import. In contrast, Exportins bind export cargos (in the nucleus) and RanGTP cooperatively. After translocation through the NPC, RanGTP is hydrolyzed causing release of export cargos from Exportins into the cytoplasm.

Eleven of the twenty human Kaps have been shown to import proteins into the nucleus or participate in bidirectional transport. These Importins and bidirectional Kaps (Importin- β , Karyopherin- β 2, Importin-4, Importin-5, Importin-7, Importin-8, Importin-9, Importin-11, Trn-SR, Importin-13 and Exportin-4) are thought to recognize distinct classes of NLSs in their import cargos (Table 1-1; reviewed in (Chook and Suel 2011)). An NLS is generally defined as the portion of an import cargo that is necessary and sufficient for nuclear import, and is transferable to direct nuclear import in another protein (Dingwall et al. 1982; Kalderon et al. 1984a; Lanford and Butel 1984). NLSs should bind directly to their specific Importins or bind to adaptor proteins for Importins (such as Importin- α proteins, which are specific adaptors for Importin- β). Therefore, nuclear import of NLS-bearing proteins should be abolished when their Importins are disabled. NLSs can be linear or conformational signals. The former are motifs that are usually contiguous in sequence and thus can be described using consensus sequences (Lange et al. 2007). Linear signals tend to bind Kaps in extended conformations, as isolated helices or combinations thereof (Cingolani et al. 1999; Cingolani et al. 2002; Lee et al. 2006; Dong et al. 2009; Suel and Chook 2009; Guttler et al. 2010; Zhang and Chook 2012). Linear NLSs can often accommodate large variations in sequence and thus are usually prevalent in the proteome and can be categorized into classes of NLSs. Conformational NLSs are folded protein domains with surface

patches that interact with their Importins. So far, only a few examples of different folded domains are known to bind Importin-13 and Imp β (see below).

Table 1-1. Karyopherin- β proteins that are involved in nuclear import and bidirectional transport.

Kap Superfamily	Human Kaps (alternate names)	Gene name (alternate names)	Uniprot Entry	<i>S. cerevisiae</i> Kaps (alternate names)
IMB1	Importin- β 1 (Kap β 1)	KPNB1 (NTF97)	Q14974	Kap95
IMB2	Transportin-1 (Kap β 2, Imp- β 2)	TNPO1 (KPNB2, TRN)	Q92973	Kap104
	Transportin-2	TNPO2	O14787-1	
	Transportin-2 Isoform 2 (Kap β 2b)		O14787-2	
IMB3	Importin-5 (Kap β 3, Imp- β 3, RanBP5)	IPO5 (KPNB3, RANBP5)	O00410	Kap121 (Pse1)
IMB4	Importin-4 (Imp-4b, RanBP4)	IPO4 (IMP4B, RANBP4)	Q8TEX9	Kap123 (YRB4)
IPO8	Importin-7 (RanBP7)	IPO7 (RANBP7)	O95373	Kap119 (Nmd5)
	Importin-8 (RanBP8)	IPO8 (RANBP8)	O15397	Kap108 (Sxm1)
IMB5	Importin-9 (RanBP9)	IPO9 (IMP9, RANBP9)	Q96P70	Kap114 (Imp- β 5, Kap- β 5)
KA120	Importin-11 (RanBP11)	IPO11 (RANBP11)	Q9UI26	Kap120
TNPO3	Transportin-3 (Transportin-SR, Imp-12)	TNPO3 (IPO12)	Q9Y5L0	Mtr10 (Kap111)
	Transportin-SR2 (Isoform 2 of Trn-SR)			
	Importin-13 (Kap13, RanBP13)	IPO13 (RANBP13)	O94829	Kap122 (Pdr6)
XPO4	Exportin-4	XPO4	Q9C0E2	

Isolated cargos or cargo segments that bind Importin-13 and Imp β (directly, without binding to Imp α) have also been studied. Imp β binds directly with many functionally diverse cargos. The lengths and sequences of Imp β binding segments within its cargos coupled with structures of Imp β in complex with the Imp α IBB, the Snurportin1 IBB, SREBP-2, a segment of PTHrP, and Snail, all suggest that Imp β recognizes structurally diverse targeting elements in the cargos by using multiple distinct binding sites (Cingolani et al. 1999; Lam et al. 1999; Cingolani et al. 2002; Lee et al. 2003; Mitrousis et al. 2008; Forwood et al. 2010; Marfori et al. 2011; Choi et al. 2014). Importin-13 is a bidirectional transporter that imports more than 10 cargos by binding folded domains (such as homeodomains and histone fold domains) of its cargos (Mingot et al. 2001; Ploski et al. 2004; Kahle et al. 2005; Kahle et al. 2009; Walker et al. 2009; Bono et al. 2010). We will not cover cargo recognition by Imp13 or Imp β in the present review since these findings have already been reviewed recently.

Most importantly, structures of the yeast karyopherin Kap121 (homologous to human Importin-5 or Imp5) bound to fragments of import cargos Ste12, Pho4 and the cargo mimic Nup53 were reported in 2013 by the Matsuura group (Kobayashi and Matsuura 2013). The structure of Transportin-SR2 (Trn-SR2; also known as TNPO3 or Trn-3) in complex with its cargo ASF1/SF2 was also reported recently (Maertens et al. 2014). Both sets of studies have provided new knowledge about two new classes of NLSs, recognized by Kap121 and Trn-SR2, respectively. The present review summarizes the classical-NLS briefly, provides updates about PY-NLSs and provides an in-depth review of the two newly discovered classes of NLSs that are recognized by Kap121 and Trn-SR2.

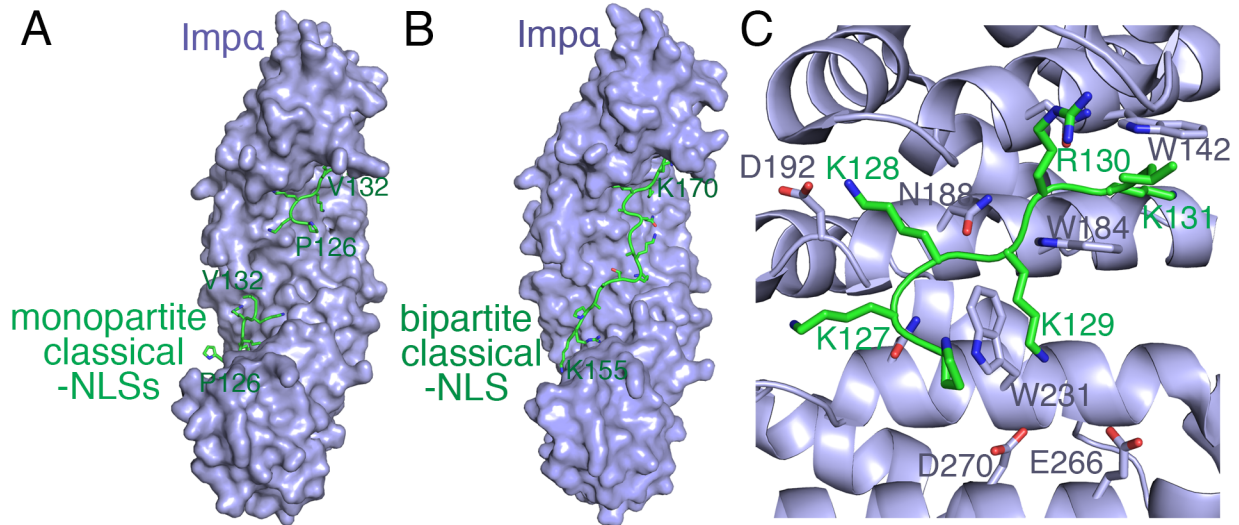


Fig 1-1. The recognition of classical-NLSs by Imp α . The ARM domain of Imp α (blue) in complex with (A) monopartite classical NLS peptides (green) from the SV40 T antigen (PDB: 1EJL), and (B) the bipartite classical-NLS (green) of nucleoplasmin (PDB:1EJY). (C) The major NLS binding site of Imp α (blue), showing the SV40 T antigen monopartite classical-NLS residues (green) and interacting Imp α sidechains (PDB:1EJL).

Classical-NLS

The first NLS peptides were discovered in the 1980s (Dingwall et al. 1982; Kalderon et al. 1984b; Lanford and Butel 1984). These signal sequences were later found to bind the adaptor karyopherin Imp α , which in turn binds Imp β (Adam and Adam 1994; Gorlich et al. 1994; Radu et al. 1995; Lange et al. 2007). The short basic NLSs are now known as classical-NLSs to distinguish them from other distinct classes of NLSs that bind directly to Imp β and to the other ten Kaps that perform nuclear import (Lange et al. 2007; Lott and Cingolani 2011; Marfori et al. 2012). Since the 1980s, classical NLSs have been identified in many cargos mostly through independent studies of the individual cargos. More recently, systematic approaches including peptide library, proteomic and yeast two-hybrid studies have increased the number of cargos that bind Imp α and contain classical-NLSs (Blazek and Meisterernst 2006; Kosugi et al. 2009a; Yang et al. 2010; Fukumoto et al. 2011; Ly-Huynh et al. 2011; Park et al. 2012; Kimura et al. 2013b; Miyamoto et al. 2013). Classical-NLSs contain either one (monopartite) or two (bipartite)

clusters of positively charged amino acids. The consensus sequence for monopartite classical-NLS is K-K/R-X-K/R whereas that for the bipartite signal is (K/R)(K/R)X₁₀₋₁₂(K/R)_{3/5}, where X is any amino acid and (K/R)_{3/5} represents three lysine or arginine residues out of five consecutive amino acids. Structural analyses of karyopherin-NLS complexes have been critical in explaining how the signals are recognized by their receptors. All reported Imp α -classical-NLS structures show the signals binding in extended conformations and making similar interactions with Imp α at two separate sites of its armadillo (ARM) domain (Figures 1-1A and 1-1B) (Conti et al. 1998; Cingolani et al. 1999; Kobe 1999; Fontes et al. 2000; Catimel et al. 2001; Fontes et al. 2003a; Fontes et al. 2003b; Matsuura et al. 2003; Chen et al. 2005; Matsuura and Stewart 2005; Cutress et al. 2008; Dias et al. 2009; Giesecke and Stewart 2010; Yang et al. 2010; Hirano and Matsuura 2011; Lott et al. 2011; Mynott et al. 2011; Takeda et al. 2011; Chang et al. 2012; de Barros et al. 2012; Marfori et al. 2012; Chang et al. 2013; Roman et al. 2013; Rona et al. 2013; Pumroy et al. 2015; Trowitzsch et al. 2015). Polar and acidic side chains of Imp α make electrostatic and polar interactions with basic NLS side chains, conserved Imp α tryptophan sidechains make hydrophobic interactions with the aliphatic portions of NLS side chains, and asparagine sidechains hydrogen bond with the NLS main chains (Figure 1-1C) (Conti et al. 1998). Detailed reviews of Imp α recognition of classical-NLSs are covered in (Marfori et al. 2011; Pumroy and Cingolani 2015).

PY-NLS

Recognition by Kap β 2

Kap β 2 and its yeast homolog Kap104 bind PY-NLS signals in their cargos. The PY-NLS is defined by a set of physical criteria, which include loose sequence motifs (N-terminal hydrophobic or basic motifs and a C-terminal R/K/H-X₂₋₅-P-Y motif), structural disorder and

overall basic charge (Lee et al. 2006). PY-NLSs can be divided into two subclasses: the hydrophobic PY-NLS or the basic PY-NLS, depending on the composition of their N-terminal motifs (Lee et al. 2006; Cansizoglu and Chook 2007; Cansizoglu et al. 2007; Suel et al. 2008; Suel and Chook 2009; Zhang et al. 2011). PY-NLSs also usually use three structurally conserved and energetically important but sequence diverse binding epitopes to bind a large and relatively flat concave surface of Kap β 2 (Figures 1-2A and 1-2B) (Lee et al. 2006; Cansizoglu and Chook 2007; Cansizoglu et al. 2007; Imasaki et al. 2007; Suel et al. 2008; Suel and Chook 2009; Niu et al. 2012; Zhang and Chook 2012; Soniat et al. 2013). Kap β 2-PY-NLS interactions were previously reviewed in (Xu et al. 2010; Chook and Suel 2011).

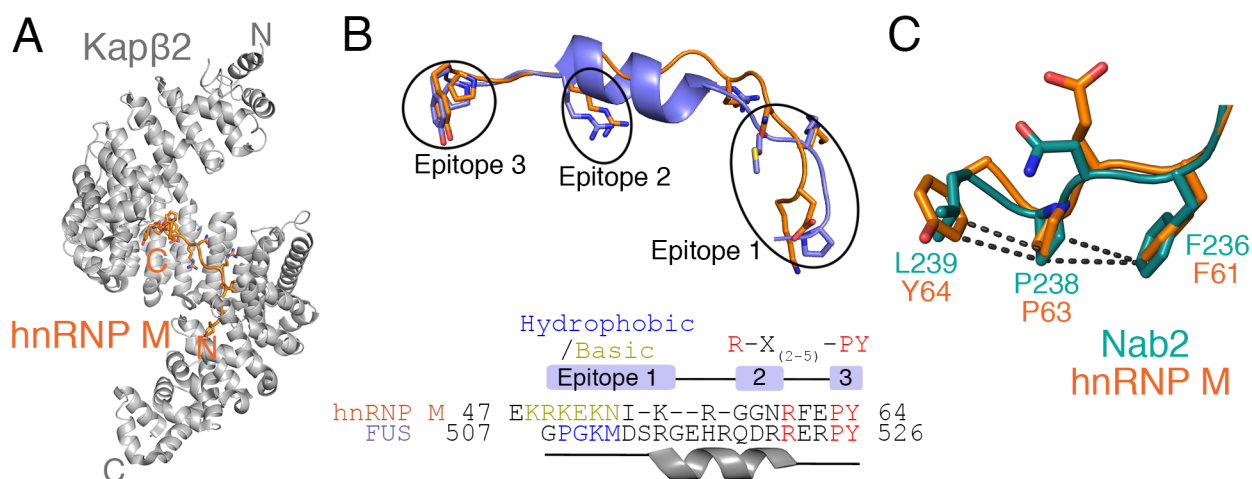


Fig 1-2. The recognition of PY-NLSs by Kap β 2. (A) Kap β 2 (gray) in complex with the PY-NLS of hnRNP M (orange; PDB:2OT8). (B) The PY-NLSs of hnRNP M (orange) and FUS (purple; PDB:4FDD) when bound Kap β 2s are superimposed. Epitopes 1, 2 and 3 of both peptides are structurally conserved and separated by linkers. A schematic with the secondary structure of the FUS PY-NLS highlights a central helix in the peptide. (C) C-terminal residues of PY-NLSs of hnRNP M (orange) and Nab2 (green; PDB:4JLQ), showing contacts between the three hydrophobic sidechains that likely pre-organize the PY or PL motifs for Kap β 2 binding.

New Kap β 2-PY-NLS or cargo structures

Between 2006 and 2011, structures of Kap β 2 in complex with seven different PY-NLSs, all containing C-terminal PY dipeptide motifs, were published (Lee et al. 2006; Cansizoglu and

Chook 2007; Cansizoglu et al. 2007; Imasaki et al. 2007). Structures of Kap β 2 bound to two new PY-NLSs were published in the last three years (Figures 1-2B and 1-2C) (Zhang and Chook 2012; Soniat et al. 2013). One of them is of the PY-NLS of yeast protein Nab2, which has a homologous PL in place of the C-terminal PY dipeptide (Soniat et al. 2013). The C-terminal ²³⁵RFNPL²⁴⁰ motif of the Nab2 PY-NLS interacts with Kap β 2 much like RX₂₋₅PY motifs of other PY-NLSs (Figure 1-2C). The phenylalanine residue Phe236, just N-terminal of the PL, is close to the proline and adopts a conformation similar to hydrophobic residues in equivalent positions in several other PY-NLSs, which all seem to pre-organize the PY/PL motifs for Kap β 2 binding (Figure 1-2C). The other recent Kap β 2-PY-NLS structure is of the PY-NLS of cargo Fused in Sarcoma or FUS (Figure 1-2B) (Zhang and Chook 2012). Unlike other PY-NLSs, which are entirely extended when bound to Kap β 2, the FUS PY-NLS contains a central 2.5-turn α -helix, which is induced upon Kap β 2 binding (Figure 1-2B) (Niu et al. 2012; Zhang and Chook 2012). The Kap β 2-FUS PY-NLS structure suggests that PY-NLSs, though mostly extended, may also include small helical elements.

A third recent structure of a Kap β 2 cargo is of the protein Symportin 1, alone and in complex with ribosomal proteins Rpl5-Rpl11 (Kressler et al. 2012). Symportin 1 is a Kap104 adaptor, which contains an N-terminal basic PY-NLS (also with a PL instead of PY motif). Although the Symportin1 PY-NLS was not observed in the structures, biochemical studies showed that the signal was sufficient for Kap104 binding. Kap104 binds the PY-NLS of Symportin 1 and imports the Symportin1-Rpl5-Rpl11 complex into the nucleus allowing for simultaneous import of three proteins by Kap104 (Kressler et al. 2012).

Newly identified PY-NLS and non-PY-NLS cargos

A previous review listed 30 different PY-NLS containing Kap β 2 cargos (Chook and Suel 2011). Twelve additional PY-NLS containing Kap β 2 cargos or binding partners were reported recently. The new Kap β 2 cargos or binding partners in Table 1-2 are involved in many biological processes including Hedgehog signaling (Ci/Gli), viral pathogenesis (HCMV UL79), and also implicated in neurodegenerative diseases amyotrophic lateral sclerosis, Huntington's and Parkinson's diseases. Ten of the new cargos have PY-NLSs with C-terminal PY motifs, and the other two, Symportin 1 and cilia kinesin-2 motor KIF17, have homologous PL motifs instead (Dishinger et al. 2010; Hurd et al. 2011; Neumann et al. 2011; Desmond et al. 2012; Dormann et al. 2012; Kressler et al. 2012; Shin et al. 2012; Wang et al. 2012; Mallet and Bachand 2013; Twyffels et al. 2013; Bernis et al. 2014; Bjorkblom et al. 2014; Shi et al. 2014). Only three of the twelve newly identified PY-NLS containing proteins have been tested for direct binding to Kap β 2.

There have also been reports of Kap β 2 cargos that do not contain recognizable PY-NLSs (Table 1-3) (Favre et al. 2008; Fritz et al. 2009; Lee et al. 2009; Janiszewska et al. 2010; Huang et al. 2013; Kimura et al. 2013a; Putker et al. 2013; Tai et al. 2013; Barraud et al. 2014). It is currently unknown how these proteins bind Kap β 2 – are their binding elements completely distinct from PY-NLSs and bind different sites on Kap β 2, or are they variants of PY-NLSs with PY motifs that have diverged to be unrecognizable or entirely lost? A few of the cargos with no recognizable PY-NLSs, such as SRP19, c-Jun and rpL23a, are imported by multiple Kaps, and one cargo rpL23a does not seem to compete with the PY-NLS of hnRNP A1 for Kap β 2 binding (Jakel and Gorlich 1998; Dean et al. 2001; Waldmann et al. 2007). Other cargos like the human RNA-editing enzyme adenosine deaminase acting on RNA or ADAR1 are imported by Kap β 2 alone (Fritz et al. 2009; Barraud et al. 2014). NMR and biochemical studies of ADAR1 mapped

its NLS to two disordered fragments that flank its second double strand RNA binding domain (dsRBD2) (Barraud et al. 2014). Neither fragment contains a PY or PΦ motif (Φ is hydrophobic amino acid) but the studies suggested that these fragments are positioned by the dsRBD into the PY-NLS site of Kapβ2 in an RNA-sensitive manner, and bind Kapβ2 in a mode similar to PY-NLSs (Figure 1-2A) (Fritz et al. 2009; Barraud et al. 2014). Structures of Kapβ2 in complex with the ADAR1 PY-NLS-like NLS will be important to understand this potentially unusual but perhaps also familiar mode of recognition by Kapβ2.

Another non-PY-NLS cargo is the FOXO4/DAF-16A protein, which seems to bind Kapβ2 in a very unusual manner (Putker et al. 2013). Upon accumulation of reactive oxygen species (ROS), Kapβ2 imports FOXO4 into the nucleus where it stimulates transcription of ROS-detoxifying enzymes. High ROS levels were shown to induce a disulfide bond between a cysteine in the C-terminus of FOXO4 with an unidentified cysteine in Kapβ2. The disulfide bond is subsequently reduced in the nucleus where the redox potential is lower, and FOXO4 is released.

Table 1-2. Recently reported PY-NLS containing cargos of Kapβ2.

New Cargos with PY-NLSs	
Cargo	NLS Region
DJ-1	50-67 (Bjorkblom et al. 2014)
Ci/Gli	197-222 (Shi et al. 2014)
ELYS*	2359-2408 (Lau et al. 2009)
GSK-3β	109-117 (Shin et al. 2012)
HCMV UL79	66-92 (Wang et al. 2012)
Huntington	174-207 (Desmond et al. 2012)
PABPN1*	259-306 (Mallet and Bachand 2013)
Symportin 1*	1-18 (Kressler et al. 2012)
TAF15	567-589 (Neumann et al. 2011; Dormann et al. 2012)
TIS11	165-190 (Twyffels et al. 2013)
KIF17 ^Δ	1003-1029 (Dishinger et al. 2010)
RP2 ^Δ	78-120 (Hurd et al. 2011)

* Cargos that have had tested for direct binding to Kapβ2.

^Δ interacts with Kap β 2 in ciliary transport.

Table 1-3. Recently reported cargos of Kap β 2 that have no recognizable PY-NLSs.

Cargos with no recognizable PY-NLS	
Cargo	NLS Region
ADAR1	708-801 (Fritz et al. 2009; Barraud et al. 2014)
CD44 (ICD)	671-697 (Janiszewska et al. 2010)
FOXO4	200-505 (Putker et al. 2013)
JMJD5	134-151 (Huang et al. 2013)
PLK1	396-433 (Lee et al. 2009)
RPL7	1-54 (Tai et al. 2013)
TCP-1- γ	ND (Favre et al. 2008)
U1 snRNP A	ND (Kimura et al. 2013a)
U2 snRNP A	ND (Kimura et al. 2013a)

ND, not determined.

The Kap121-specific Lys-rich NLS

Kap121 (also known as Pse1) is one of the four Kaps that are essential for cell viability in *S. cerevisiae*. The other three essential yeast Kaps are Kap60 (Imp α homolog), Kap95 (Imp β homolog) and CRM1 (also known as Xpo1) (Rout et al. 1997; Makhnevych et al. 2003). Kap121 mediates nuclear import of diverse functioning cargos, which include cell cycle regulators, transcription factors, core histones, and ribosomal proteins (reviewed in (Chook and Suel 2011)). Kap121 shows functional redundancy to Kap123 and appears to be a backup Importin for many Kap123 cargos. Importin-5 (Imp5; also known as RanBP5 or Kap β 3) is the human homolog of Kap121 (Yaseen and Blobel 1997). Some Imp5 cargos are similar to Kap121 cargos and these include core histones and ribosomal proteins (Rout et al. 1997; Baake et al. 2001; Muhlhauser et al. 2001; Mosammaparast et al. 2002b; Blackwell et al. 2007). Only ~20 different cargos have been identified for Imp5 and most have also been shown to be imported by other Kaps (Kaffman

et al. 1998; Chaves and Blobel 2001; Delahodde et al. 2001; Isoyama et al. 2001; Leslie et al. 2002; Ueta et al. 2003; Leslie et al. 2004; Cairo et al. 2013).

A few Kap121 and Imp5 cargos have been mapped for their Kap binding segments, and they tend to be located within disordered regions and are enriched in lysine residues. No clear consensus sequence could be derived for these isolated NLS sequences until the recent availability of Kap121-cargo structures. Kobayashi and Matsuura reported structures of Kap121 bound to fragments of yeast cargos Ste12, Pho4, and cargo mimic Nup53 (Figures 1-3A-C) (Kobayashi and Matsuura 2013). Pho4 and Ste12 are both transcription factors (Kaffman et al. 1998; Leslie et al. 2002). The nucleoporin Nup53 binds Kap121 during mitosis to sequester it to the NPC and prevent it from importing cargos (Lusk et al. 2002; Makhnevych et al. 2003). Kap121 was crystallized with large 50-70 residue fragments of Pho4, Ste12 and Nup53, but electron density was observed for only 8-12 residues of each cargo (Ste12p residues 606-617, Pho4p residues 141-150, Nup53p residues 405-412) (Kobayashi and Matsuura 2013). All three NLS peptides adopt extended conformations when bound to Kap121, interacting with the concave surface of central HEAT repeats 7-12 of Kap121 (Figure 1-3A and 1-3B).

Structure-based alignment of the short cargo fragments of Pho4, Ste12 and Nup53 revealed a consensus motif K-V/I-x-K-x_{1,2}-K/H/R for the Kap121 specific NLSs (Figure 1-3B) (Kobayashi and Matsuura 2013). Correspondingly, the NLS binding site of Kap121 is composed of an electrostatically neutral pocket, which is surrounded by negatively charged residues (Figure 1-3C). The lysine residues of the lysine-rich NLSs make salt bridges with acidic residues of Kap121 while the valine or isoleucine residue in the second consensus position of the NLS fits into the neutral pocket on Kap121. Mutagenesis, pull-down binding and nuclear localization assays to determine contributions of the conserved NLS residues showed the first three

conserved positions of the consensus, K-V/I-x-K, were the most important for binding and nuclear import while some variability in the fourth conserved position is tolerated (Kobayashi and Matsuura 2013). Kap121 residues that interact with the lysine-rich NLSs are highly conserved in its human homolog Imp5, suggesting that many Imp5 cargos likely use similar lysine-rich Kap121-specific NLS.

Kobayashi and Matsuura used the K-V/I-x-K-x_{1,2}-K/H/R consensus to predict lysine-rich Kap121-specific NLSs in ten other Kap121 cargos but the predicted NLSs have not yet been experimentally verified (Kobayashi and Matsuura 2013). Interestingly, only three of the predicted NLSs fit the consensus perfectly, supporting the ability of Kap121 to accommodate variations in the K-V/I-x-K-x_{1,2}-K/H/R consensus. Identification of additional Kap121 or Imp5 cargos and their NLSs will allow refinement of the current lysine-rich NLS consensus, and facilitate development of computational predictors for this new class of NLS. Finally, although the lysine-rich Kap121-specific NLS motif is likely to contribute most of the Kap121-cargo binding energy, the small motif may not always act alone. Observance of stable structure for only small fractions of the large 50-70 residue fragments of cargos Pho4, Ste12 and Nup53 that were used in structure determination (presumably mapped as optimal binding units) (Kobayashi and Matsuura 2013) may suggest additional cargo epitopes that make important energetic contributions to binding but are dynamic thus not observed in the crystal structures. Careful dissection of energetic contributions by the small lysine-rich Kap121-specific NLSs compared to full length cargos may reveal additional binding determinants for the Kap121 import system.

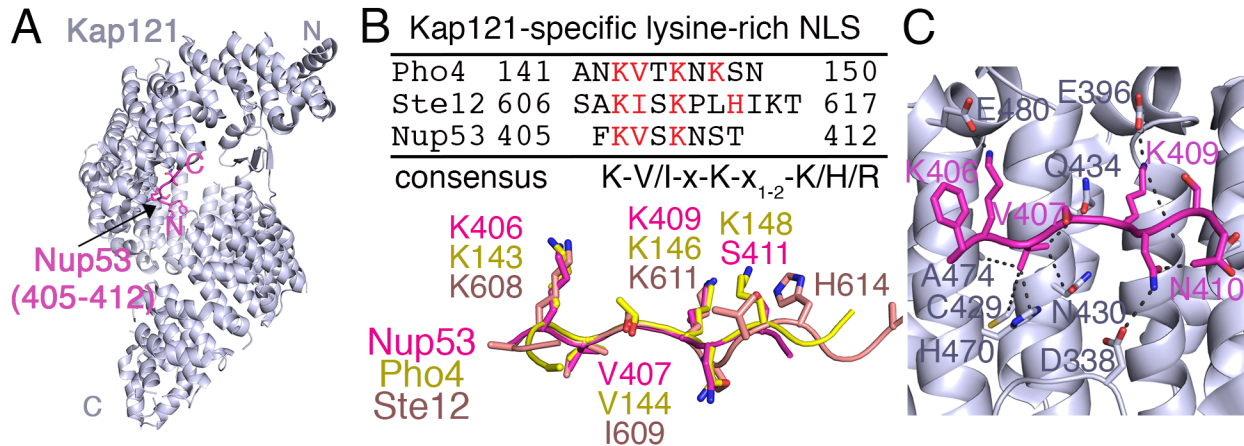


Fig 1-3. Recognition of the lysine-rich Kap121-specific NLS by Kap121. (A) Kap121 (blue) bound to the NLS-like peptide from Nup53 (magenta; PDB:3W3Y). (B) The NLSs of Nup53 (magenta), Pho4 (yellow; PDB:3W3X), and Ste12 (tan; PDB:3W3W) when their Kap121s are superimposed. Alignment of the short NLS fragments revealed a K-V/I-x-K-x₁₋₂-K/H/R consensus motif. (C) Interactions between Kap121 (blue) and Nup53 (magenta).

The RS repeat NLS

Transportin-SR (Trn-SR) and its splice variant Transportin-SR2 (Trn-SR2; also known as Transportin-3, Trn-3 or TNPO3) mediate nuclear import of SR splicing factors, which usually contain one or more RNA Recognition Motif (RRM) domains and a C-terminal arginine-serine (RS) repeat domain (Kataoka et al. 1999; Lai et al. 2000; Lai et al. 2001). Each RS domain may contain up to 50 RS dipeptide repeats. Cargos of Trn-SR proteins include human splicing factors ASF/SF2, SC35, TRA2-alpha, TRA2-beta, and drosophila splicing factors 9G8, Rbp1, and RSf1 (Kataoka et al. 1999; Lai et al. 2000; Lai et al. 2001; Allemand et al. 2002; Yun et al. 2003). Trn-SRs bind the cargo RS repeats, which have been shown to be transferable Trn-SR dependent NLSs (Lai et al. 2000; Lai et al. 2001; Lai et al. 2003). Many but not all cargos need their RS domains to be phosphorylated in order to bind the Trn-SRs. In addition to RS domain containing SR proteins, Trn-SR2 also imports the non-RS splicing regulator RBM4 via its alanine rich C-terminus, which likely binds to a site on Trn-SR2 that overlaps with the RS binding site (Lai et al. 2003). Trn-SR2 has also been suggested to import the HIV-1 preintegration complex (PIC)

(Senger et al. 1998; Allemand et al. 2002; Christ et al. 2008; Chook and Suel 2011; Xu et al. 2011).

The recently reported structure of Trn-SR2 (or TNPO3) bound to phosphorylated splicing factor ASF/SF2 revealed how the Importin recognizes ASF/SF2 and the physical nature of its RS repeat NLS (Figures 1-4A-C) (Maertens et al. 2014). ASF/SF2 has two RRM domains followed by a C-terminal RS repeat region. The optimal Trn-SR2 binding fragment of the cargo was biochemically mapped to a segment that spans the second RRM domain (RRM2) and the phosphorylated RS repeats (Maertens et al. 2014). This RRM2-phosphoRS fragment of ASF/SF2 binds Trn-SR2 in a bipartite manner (Figure 1-4A). The N- and C-termini of Trn-SR2 are close to each other, and together enclose the ASF/SF2 RRM2, which interacts with N-terminal HEAT repeats 4-7 and C-terminal HEAT repeats 19-20. The phosphoRS segment (residues 198-211), which follows RRM2, binds as a horseshoe-shaped loop to the inner concave surface of Trn-SR2 at HEAT repeats 14-18, which is adjacent to the RRM2 binding site (Figures 1-4A and 1-4B). Mutations in the RS repeats but not in the RRM2 disrupted Trn-SR2 binding, suggesting that the phosphoRS is the major Kap binding determinant (Maertens et al. 2014). Proteomic data also showed that 22 of 68 identified Trn-SR cargos contain RS repeats but lack recognizable RRM domains, further supporting the notion that RS repeats are the major transferable Trn-SR-specific NLSs in the cargos (Maertens et al. 2014).

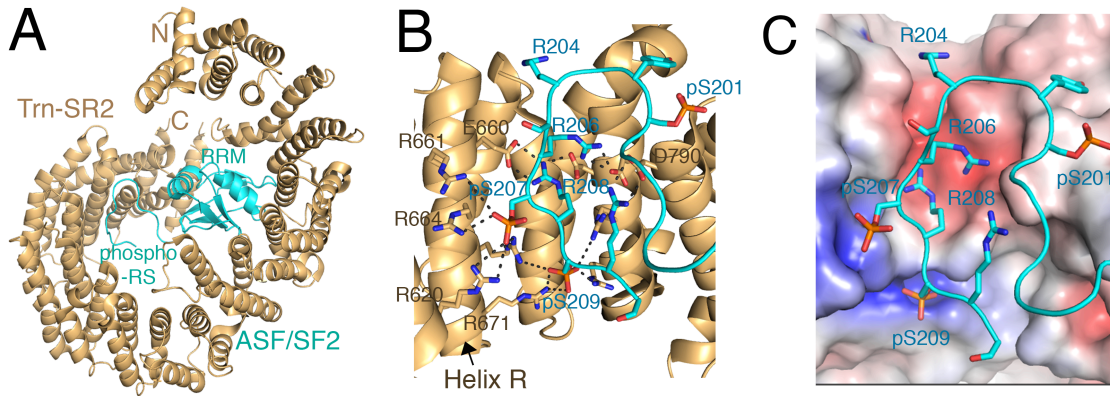


Fig 1-4. Recognition of the RS repeat NLS by Trn-SR2. (A) Trn-SR2 (tan) in complex with RRM2-RS repeat fragment of phosphorylated ASF/SF2 (cyan; PDB:4C0O). (B) Interactions of the phosphoRS of ASF/SF2 (cyan) with Trn-SR2 (tan). Phosphorylated Ser207 and Ser209 make multiple salt bridges with arginines on the R-helix, which is the inner helix of Trn-SR2 HEAT repeat 15. (C) Electrostatic surface potential of the phosphoRS-binding site of Trn-SR2. Red indicates negative electrostatic potential, white neutral, and blue positive. Adjacent basic-acidic patches on Trn-SR2 interact with the alternating phosphoRS arginine and phosphoserine sidechains, respectively.

TrnSR2-phosphoRS interactions are mostly electrostatic and polar (Maertens et al. 2014). Within the horseshoe-shaped phosphoRS loop ($^{198}\text{R-S-P-pS-Y-G-R-S-R-pS-R-pS-R-S}^{211}$) that binds a highly curved concave surface of Trn-SR2, serine and neighboring arginine sidechains project from the backbone of the phosphoRS loop in alternating directions (Figure 1-4B). Three serine residues (Ser201, Ser207 and Ser209) in the phosphoRS are phosphorylated. Phosphate groups of phospho-Ser207 and phospho-Ser209 both point into a basic patch on Trn-SR2, forming multiple salt bridges with arginines on the inner helix of Trn-SR2 HEAT repeat 15, which is also called the R-helix. The series of alternating arginine sidechains of the phosphoRS all point in the opposite direction from the phosphoserines, into an adjacent acidic patch on Trn-SR2 that contains aspartate sidechains from HEAT repeats 17 and 18 (Figure 1-4C) (Maertens et al. 2014). Adjacent basic-acidic patches on the karyopherin may be a signature feature for

recognition of phosphorylated RS repeats or the homologous alternating RE motifs found in other Trn-SR2 cargos like CPSF6 (Figure 1-4C).

The structure suggested that Trn-SR2 recognizes phosphoRS domain by using charged (basic and acidic) residues on and around its R-helix (Figures 1-4B and 1-4C) (Maertens et al. 2014). However, it remains unclear how many Trn-SR or Trn-SR2 cargos need their RS domains phosphorylated in order to be imported into the nucleus. The only other Trn-SR or Trn-SR2 cargo that is known to be imported as a phospho-protein is TRA2-beta. Trn-SR2 imports TRA2-beta only when it is phosphorylated, but splice variant Trn-SR can import both unphosphorylated and phosphorylated TRA2-beta ((Yun et al. 2003). The only difference between splice variant Trn-SR and Trn-SR2 is a 33-residue insertion in a Trn-SR loop that is distant from the phosphoRS binding site of Trn-SR2, suggesting that both Kaps likely bind phosphoRS very similarly (Kataoka et al. 1999). Quantitative biochemical studies and structures of both Trn-SRs with phosphorylated and unphosphorylate RS repeats will be useful in understanding bound structures of both versions of the RS repeats and how they are recognized by the same Kaps.

Other Trn-SR2 cargos such as CPSF6 contain homologous RE or RD motifs, which may mimic phosphorylated RS repeats (De Iaco and Luban 2011; De Iaco et al. 2013). CFSP6 has a few RS repeats in addition to its RE repeats, and both phosphorylated and unphosphorylated CPSF6 can bind Trn-SR2 (Maertens et al. 2014). Mutations in the Trn-SR2 phosphoRS binding site disrupted CPSF6 binding, suggesting a similar mode of binding as the phosphoRS of ASF/SF2 (Maertens et al. 2014). It is not known if the RE or the RS repeats or both motifs in CPSF6 are used for Trn-SR2 binding. Other than RS/RE repeats containing SR proteins, Trn-SR2 also imports splicing regulator RBM4 by binding its disordered C-terminal alanine-rich (CAD) region. RBM4 competes with RS repeats for nuclear import by Trn-SR2, suggesting that

the RBM4 CAD likely binds a Trn-SR2 site that overlaps with the phosphoRS binding site (Lai et al. 2003). Structures of Trn-SR and Trn-SR2 in complex with cargos with unusual RS/RE repeat region such as in CPSF6, and with cargos without RS repeats such as RBM4, will be important in understanding how the Trn-SRs recognize diverse cargos for nuclear import.

Summary

Of the eleven human Kaps that import protein cargos into the nucleus, only two well-characterized classes of NLSs were previously known: the classical-NLS is recognized by the Imp α/β heterodimer and the PY-NLS recognized by Kap β 2. The classical-NLS is made up of compact and well-defined basic sequences whereas the larger PY-NLS is much more diverse and needs to be defined by a set of physical criteria which includes a set of loose consensus motifs. Recent published work points to additional diverse elements within the PYNLS as Kap β 2 recognizes variants of the namesake PY dipeptide motif such as the PL motif of Nab2, and other structural elements such as the short central helix within the FUS PY-NLS. Furthermore, of the 17 new cargos reported recently for Kap β 2, about half have no recognizable PY-NLS, again suggesting diverse modes of cargo recognition by Kap β 2 including the possibility that the PY-NLS may diverge to incognito status.

Recent structures of Kap-cargo complexes have revealed physical characteristics of two new classes of NLSs: the lysine-rich Kap121- or Imp5-specific NLS and the RS repeats NLS recognized by Transportin-SR2. The former is described by a compact K-V/I-x-K-x₁₋₂-K/H/R consensus, which was used to predict new NLSs in eleven known Kap121 cargos. The structure of Trn-SR2 or TNPO3 in complex with cargo ASF/SF2 revealed how phosphorylated RS repeats are recognized by the Importin. Phosphorylated RS repeats are specifically recognized through a highly basic surface on Transportin-SR2 formed by the R-helix, and an acidic surface formed by

adjacent HEAT repeats. The phosphoRS binding site is highly conserved in the splice variant Trn-SR, which likely recognizes phosphoRS repeats similarly.

Structural studies of Imp α , Kap β 2, Kap121, and Transportin-SR2 in complex with their import cargos have revealed both sequence and structural requirements of recognition for four distinct classes of NLS: the classical-NLS, the PY-NLS, the Kap121-specific lysine-rich NLS, and the RS repeat NLS. Structures are now needed for the remaining Importins (Imp4, Imp7, Imp8, Imp9, Imp11 and Exp4) bound to their respective cargos to reveal the physical and chemical nature of the NLSs that they each recognize, and to understand the versatility and diversity of signal recognition by this family of nuclear transport receptors.

NLSs and Nuclear Import by other Kap β s

Many of the import-Kap β s (or Importins), such as Importin-4, Importin-7, and Importin-9, are less studied and have many fewer known cargoes. Furthermore, NLSs that have been mapped within these cargoes are usually large fragments of the cargoes and alignment of these regions shows no consensus sequence.

Importin-4

Importin-4 (Imp4) was shown to mediate nuclear import of the core histones (H3 and H4), the vitamin D receptor, transition protein 2 (TP2), HIF1- α and the ribosomal protein rPS3a (Chook and Suel 2011). The core histones, HIF1- α and rPS3a were also shown to be imported by other Importins. The NLSs that have been mapped for Imp4 cargoes are enriched in basic amino acids especially lysines and secondary structure/disorder predictions suggest that they are structurally disordered or contain single helical elements which make up a linear or quasi-linear NLS.

The yeast homolog of Imp4, Kap123p, was also shown to be the major importer of histones and many ribosomal proteins (Rout et al. 1997; Mosammaparast et al. 2002b; Blackwell et al. 2007). Kap123p shows functional redundancy with Kap121p and is a secondary import factor for many Kap121p cargoes. However unlike Kap121p, Kap123p is not an essential protein. Additionally, previous studies of nuclear import rates in yeast suggest that Kap123p rapidly imports abundant cargoes such as ribosomal proteins and histones, while Kap121p is more specialized for recognition of cargoes whose import needs to be regulated. Examples of such cargoes include the phosphate-regulated transcription factor Pho4p and transcription factor Ste12p, which is required for mating and cell differentiation in yeast (Kaffman et al. 1998; Leslie et al. 2002; Timney et al. 2006).

Importin-7

Importin-7 (Imp7) imports many cargoes that are also imported by other Importins such as core histones (H2A, H2B, H3, and H4), many ribosomal proteins, CDK5 activator p35, HIF1- α , c-Jun, and the glucocorticoid receptor. Cargoes specific to Imp7 include the proline-rich homeodomain, zinc finger protein EZI, signal transducer Smad3, and protein kinases ERK-2 and MEK1 (Chook and Suel 2011). Imp7 can also import some cargoes such as linker histone H1, HIV-I REV, and adenovirus core protein pVII, as an Imp β •Imp7 heterodimer (Bauerle et al. 2002; Jakel et al. 2002; Arnold et al. 2006; Wodrich et al. 2006). Mapped NLS regions of several Imp7 cargoes show that Imp7 can bind NLSs that are very structurally diverse. These include folded domains like the proline-rich homeodomain, the zinc fingers of EZI, the PAS domain of HIF1- α , and the leucine-zipper domain of c-Jun. Imp7 also recognizes linear disordered NLSs such as the 10-residue Ser-Pro-Ser (SPS) region of ERK-2.

Importin-9

Importin-9 (Imp9) cargoes include the core histones (H2A, H2B, H3, and H4), ribosomal proteins, actin, the A subunit of protein phosphatase 2A (PP2A), c-Jun, aristaless (Arx) and the hepatocellular carcinoma-associated protein (Chook and Suel 2011). The mapped NLS sequences in Arx, PP2A, c-Jun and rpS7 are quite diverse but are all highly positively charged. Furthermore like Imp7, Imp9 can recognize structurally diverse NLSs including folded domains like the homeodomains of Arx, the HEAT repeats of PP2A, the leucine-zipper domains of c-Jun, and the disordered NLS of rpS7.

Histones: Introduction

Chromatin

Chromosomes are made up of a complex known as chromatin, which consists of a fundamental repeating unit, known as the nucleosome, which is made up DNA and histone proteins (Luger et al. 2012). Chromatin can be divided into two structurally and functionally distinct regions: heterochromatin and euchromatin (Campos and Reinberg 2009). Heterochromatin is the condensed form of chromatin (Trojer and Reinberg 2007). The DNA in this region is usually silenced and contains hypoacetylated histones and high levels of DNA methylation. Generally, heterochromatin is found at the telomeres and domains near the centromeres in different organisms. Heterochromatin can be further divided into two major subtypes: constitutive and facultative (Trojer and Reinberg 2007). Constitutive heterochromatin contains a high density of repetitive DNA elements and transposable elements and is irreversibly silenced and remains so during cell division. Unlike constitutive heterochromatin, facultative heterochromatin has the ability to become transcriptionally active through regulation of DNA methylation. Euchromatin includes both repressed and active genes and is less condensed than heterochromatin and actively transcribed (Schones et al. 2008). Unlike heterochromatin, this region contains hyperacetylated histones.

Nucleosomes and Histones

Nucleosomes are made up of ~147 bp DNA wrapped around a histone octamer, that is comprised of two copies of four core histones: H2A, H2B, H3, and H4 (Eickbush and Moudrianakis 1978; Luger et al. 1997). An additional linker, histone H1, completes the nucleosome by protecting the linker DNA between histone octamers (Venkatesh and Workman 2015). The histones sequences are highly conserved in eukaryotes. . The histones are also

structurally similar and are made up of two domains: a N-terminal disordered tail region followed by a globular histone fold domain (Luger et al. 1997; White et al. 2001). The histone fold domain consists of three α -helices separated by loops. The N-terminal tails are rich in basic residues and are subject to multiple posttranslational modifications, which is important for epigenetic regulation (Portela and Esteller 2010). Two H3/H4 dimers come together to form a tetramer through the formation of a four-helix bundle made up from α -helices 2 and 3 from each H3/H4 dimer. Two H2A/H2B heterodimer bind on opposite sides of the H3/H4 tetramers interacting with the H3/H4 tetramer through a second four-helix bundle between α -helices 2 and 3 from H2B and H4 histone fold domains to form the histone octamer. Both the N-terminal tails and histone fold domains contribute to nucleosome-DNA interactions through hydrogen bonds with the phosphodiester backbone of DNA.

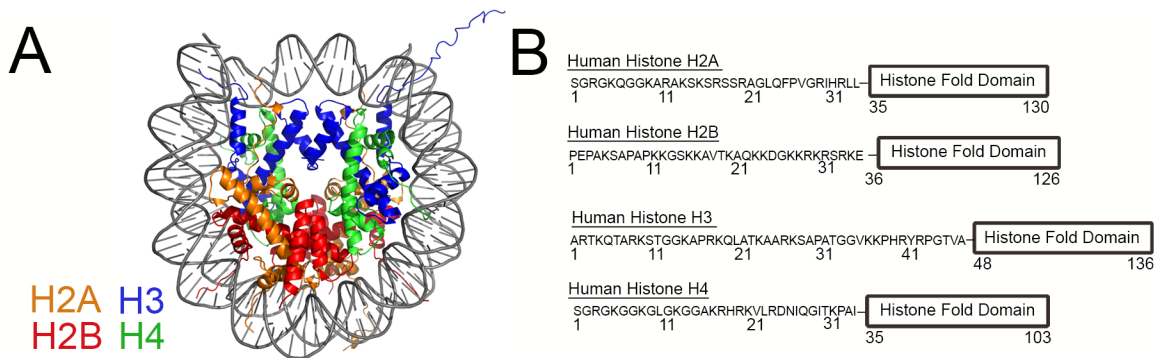


Fig 1-5. Nucleosome structure and the core histones. A) Crystal structure of the nucleosome octamer at 2.8 Å resolution (Luger et al. 1997). B) Domain organization of human histone H2A, H2B, H3, and H4 (Adapted from (Das et al. 2010))

Histone Variants

Whereas the canonical core histones package newly synthesized nucleosome, they can be replaced with histone variants that alter nucleosome structure, stability, dynamics, and accessibility (Sarma and Reinberg 2005). There are four known isoforms of H3: H3.1, H3.2, H3.3, and centromeric histone H3 (CENPA). H3.1 is the canonical H3 and H3.2 is similar

differing by only one amino acid (Sarma and Reinberg 2005). The variant H3.3, which differs from H3.1 by four amino acids, is incorporated into nucleosome in both a replication-dependent and replication-independent manner and present at transcriptional active loci (Tagami et al. 2004). H3.3 expression is lower than H3.1 during cell division but increases significantly after cell division and makes up more than half of the total amount of H3 in the cell (Ahmad and Henikoff 2002). The other H3 variant, CENPA binds to centromeres and aids in kinetochore assembly (Palmer et al. 1987).

Histone H2A has the largest number of variants, which includes H2A.X, H2A.Z, MacroH2A, and H2A-bar-body deficient (H2ABBD) (Sarma and Reinberg 2005). H2A.X, the major core histone in yeast, is important in DNA repair and DNA recombination (Downs et al. 2000). H2A.Z had been shown to be involved in regulation of gene expression and chromosome segregation (Faast et al. 2001). The MacroH2A variant localizes predominantly to the inactive X-chromosome and involved in X-chromosome inactivation and transcriptional repression (Pehrson and Fried 1992). Little is known about the H2A variant H2ABBD except that is excluded from the X-chromosome and may be important for transcriptional activation (Chadwick et al. 2001).

No variants have found for the core histone H2B and H4 (Sarma and Reinberg 2005). However, linker histone H1 has numerous sequence variants including H1⁰, H5, and the sperm and testis-specific variants (Kimmins and Sassone-Corsi 2005). The abundance of these variants fluctuates in different cell types as well as during the cell cycle, differentiation, and development.

Post-Translational Modifications and Histone Modifying Enzymes

Histones are key players in epigenetics and many post-translational modifications have been shown to occur in the N-terminal tails of the histones including acetylation, methylation, phosphorylation, ubiquitination, SUMOylation, and ADP-ribosylation, among others (Portela and Esteller 2010). These modifications function either to disrupt chromatin contacts or aid in recruitment of non-histone proteins to the chromatin. Thus post-translational modifications have important roles in gene transcriptional regulation, DNA repair, DNA replication, alternative splicing, and chromosome condensation (Kouzarides 2007). Histone acetylation, methylation, and phosphorylation are added by histone acetyltransferases (HATs), histone methyltransferases (HMTs), and serine/threonine kinases, respectively (Bhaumik et al. 2007). Lysine acetylation can occur by adding single acetyl groups to the ϵ -amino group, whereas mono-, di- and trimethylation occur by adding up to three methyl groups to the lysine residue. These modifications can be removed by histone deacetylases (HDACs), histone demethylases (HDMs), and phosphatases (Bhaumik et al. 2007).

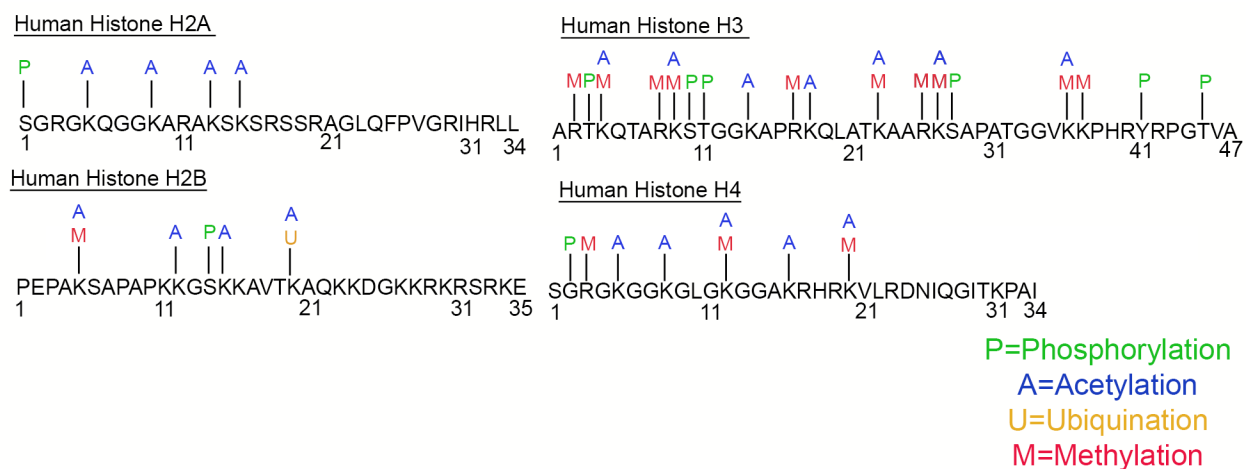


Fig 1-6. Known post-translational modification found in the N-terminal histone tails. Adapted from (Portela and Esteller 2010)

Histone Chaperones

Along with post-translational modifications and histone variant, many histone chaperones have been shown to be important in regulation of gene transcription, chromosome structure, and nucleosome biogenesis (Burgess and Zhang 2013). For H3/H4, histone chaperones Nuclear autoantigenic sperm protein (NASP) and Anti-silencing factor 1 (Asf1) are involved in H3/H4 biogenesis in the cytoplasm (English et al. 2006; Li et al. 2008; Cook et al. 2011). Once in the nucleus, Asf1 is important in transfer H3/H4 dimers in nucleus to Chromatin assembly factor 1 (CAF-1) and Regulator of Ty transposition (Rtt106) (Tyler et al. 1999; Su et al. 2012). CAF-1 and Rtt106 aid in formation and deposition of H3/H4 tetramer onto DNA on newly synthesized nucleosomes.

For the H3 variants, different chaperones are used during replication-independent nucleosome assembly. The chaperone Death domain-associated protein (Daxx) recognizes H3.3/H4 and is involved in deposition at telomeric heterochromatin and the chaperone histone cell cycle regulation defective homolog A (HIRA) is important for H3.3/H4 deposition at genic regions (Ray-Gallet et al. 2002; Goldberg et al. 2010). Furthermore, histone chaperone DEK regulates H3.3/H4 incorporation and maintenance of heterochromatin (Sawatsubashi et al. 2010). The histone variant CENP is regulated and incorporated by the Holliday junction recognition protein (HJURP) (Foltz et al. 2009).

For H2A/H2B, the histone chaperone nucleosome assembly protein (Nap1) has been shown to make a complex with H2A/H2B, along with the yeast Importin Kap114, in the cytoplasm for nuclear import (Mosammaparast et al. 2002a; Andrews et al. 2010). Furthermore, it has been shown that Nap1 is important for deposition of H2A/H2B dimers onto H3/H4 tetramers already deposited on DNA. For H2A variants, chaperone for H2A.Z/H2B (Chz1) is

important for H2A.Z/H2B deposition (Luk et al. 2007). Whereas, Aprataxin-PNK-like factor (APLF) is important deposition of the H2A variant macro2A.1 during DNA damage (Mehrotra et al. 2011).

Some chaperones are able to recognize all core histones. This includes the chaperone FACT (facilitates chromatin transcription) that can bind and exchange H3/H4, H2A/H2B, and H2A.X/H2B within the nucleosome (Belotserkovskaya et al. 2003). FACT can also regulate DNA availability without dispersing the histones by binding a reorganized nucleosome in which the histones are dissociated from one another and also from the DNA, but remain tethered together. These destabilize nucleosomes aid in promotion of polymerase progression on chromatin templates.

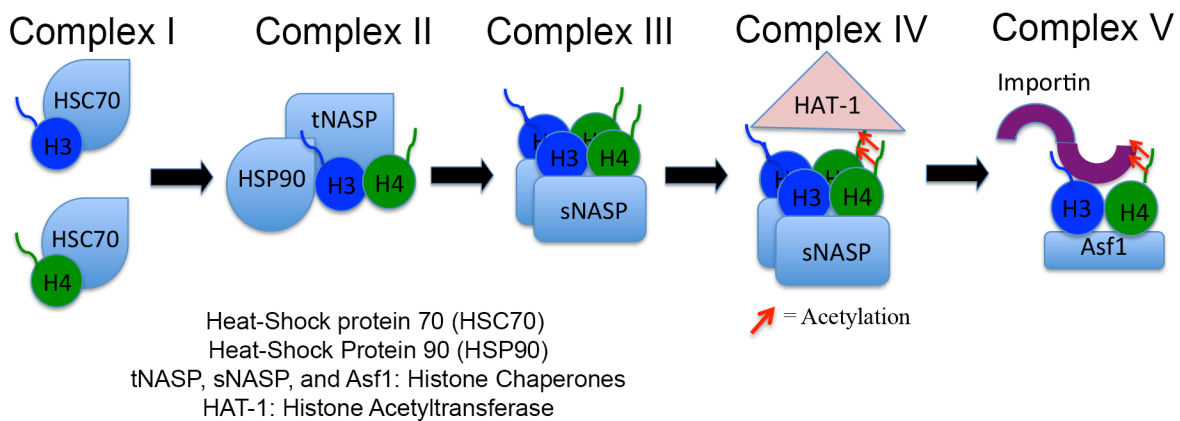


Fig 1-7. Steps in histone biogenesis after translation for H3 and H4 before nuclear import. Adapted from (Campos et al. 2010)

Nucleosome Biogenesis

Nucleosome biogenesis can be classified into either replication-dependent or replication-independent nucleosome assembly. H3.3 is mainly assembled in by HIRA nucleosomes in replication-independent manners while other the histones (H2A, H2B, H3 and H4) and variants are synthesized in the cytoplasm and assembled into new nucleosomes in the nucleus during S-

phase in a replication-dependent manner (Eickbush and Moudrianakis 1978; Smith and Stillman 1991; Luger et al. 1997; Nakagawa et al. 2001; White et al. 2001; Campos and Reinberg 2009; Keck and Pemberton 2012; Annunziato 2013; Burgess and Zhang 2013; Elsasser and D'Arcy 2013). Little is known about the early stages of biogenesis of H2A and H2B before nuclear import, however a lot of work has been done to understand these stages for H3 and H4 (Campos et al. 2010). For example it has been shown that after translation, heat-shock cognate 70 proteins (HSC70) bind newly synthesized H3 and H4 monomers as they exit the ribosome, which aids in folding and prevention of aggregation of monomeric histones H3 and H4 (Alekseev et al. 2005; Hartl and Hayer-Hartl 2009; Campos et al. 2010). Furthermore, methylation of Lys9 in H3 occurs soon after translation, however the role of this modification in nucleosome assembly is unknown but it can be further modified to trimethylated Lys9 (H3K9me3) in the nucleus, mark of heterochromatin (Loyola et al. 2006). Monomeric H3 and H4 are transferred to the chaperones heat-shock protein 90 (HSP90) and testicular nuclear autoantigenic sperm protein (tNASP), which aid in further folding and assembly of H3/H4 dimers (Campos et al. 2010). H3/H4 dimers are then transferred to somatic NASP (sNASP), which recruits the histone acetyltransferase complex HAT-1-RbAp46 to acetylate the N-terminal histone tails (Verreault et al. 1998; Murzina et al. 2008; Campos et al. 2010; Jasencakova et al. 2010; Ejlassi-Lassalette et al. 2011; Li et al. 2014). Mass spectrometry studies have shown that 20-30% of histones H3 in the cytoplasm are acetylated at Lys14 and/or Lys18 while all cytoplasmic histones H4 are acetylated at Lys5 and Lys12 (Muhlhauser et al. 2001; Blackwell et al. 2007; Campos et al. 2010; Jasencakova et al. 2010).

It remains unclear and controversial if and what effect acetylation has on nuclear import of the histones. Previous studies in yeast showed that glutamine mutations of lysines (a means of

mimicking acetylation) in the histone H3 and H4 tails resulted in loss of nuclear accumulation (Blackwell et al. 2007). Additionally, in the absence of the H4 tail, H3 acetylation as observed with lysine to glutamine mutations led to inviability but it is unclear if this loss of function was a result of nuclear import defect or of defective chromatin assembly in the nucleus (Blackwell et al. 2007). Finally, acetylation mutants of both H3 and H4 tails were viable in yeast and only resulted slower growth (Blackwell et al. 2007). These results suggest that acetylation of histones H3 and H4 may inhibit their nuclear import. However, in contrast studies in *P. polycephalum* showed that acetylation led to a greater degree of nuclear accumulation (Ejlassi-Lassalette et al. 2011).

After acetylation, H3/H4 dimers are transferred to the histone chaperone anti-silencing function protein 1 (Asf1) and bound by Importins for transport into the nucleus (Baake et al. 2001; Muhlhauser et al. 2001; Mosammaparast et al. 2002b; Greiner et al. 2004; Mousson et al. 2005; English et al. 2006; Blackwell et al. 2007; Natsume et al. 2007; Alvarez et al. 2011; Zhang et al. 2013). The crystal structure of the Asf1-H3/H4 complex showed that Asf1 interacts with the histone-fold domains of the H3/H4 dimer (English et al. 2006; Natsume et al. 2007). Once in nucleus, Asf1-H3/H4 is dissociated from the Importins and H3/H4 is transferred from Asf1 to CAF-1 and Rtt106 (Li et al. 2012). Acetylation of H3 at Lys56 is required for efficient association of H3/H4 with CAF-1 and Rtt106 (Adkins et al. 2007). CAF-1 and Rtt106 are important in tetramerization of H3/H4 dimers and depositing of H3/H4 tetramers on the DNA first (Liu et al. 2012; Winkler et al. 2012). Assembly of nucleosome occur in a stepwise manner with H3/H4 tetramer, which have a greater affinity for DNA, are deposited first (Li et al. 2012).

Less is known about the early stages of histone biogenesis of H2A/H2B. It has been shown in yeast that H2A/H2B are bound to Nap1 in the cytoplasm (Mosammaparast et al. 2001).

Then the Nap1-H2A/H2B complex associates with Kap114p, yeast homolog of Imp9. Nap1 increases the affinity of Kap114p for H2A/H2B (Mosammaparast et al. 2001; Mosammaparast et al. 2002a). The Kap114p-Nap1-H2A/H2B complex is Ran-GTP insensitive suggesting role of other factors to aid in complex dissociation (Mosammaparast et al. 2001). Unlike with H3/H4, no post-translational modifications for H2A/H2B, prior to nuclear import, have been determined. After nuclear import, H2A/H2B are directed toward nucleosome assembly where H2A/H2B, which has a high affinity for H3/H4 bound to DNA, is added to complete the nucleosome particle (English et al. 2005; Burgess and Zhang 2013).

Nuclear Import of Histones

Newly translated histone H2A/H2B dimers and H3/H4 dimers are imported into the nucleus for deposition onto the replicating chromatin ((Eickbush and Moudrianakis 1978; Smith and Stillman 1991; Luger et al. 1997; Nakagawa et al. 2001; White et al. 2001; Campos and Reinberg 2009; Keck and Pemberton 2012; Annunziato 2013; Burgess and Zhang 2013; Elsasser and D'Arcy 2013). Previously it has been shown that the N-terminal tails of H2A, H2B, H3, and H4 all contain contains an NLS (Mosammaparast et al. 2001; Mosammaparast et al. 2002b). Furthermore, a combination of co-immunoprecipitation experiments, *in vitro* binding assays with recombinant proteins, and nuclear localization studies in yeast and permeabilized HeLa cells have shown that several Importins can bind and import the histones (Johnson-Saliba et al. 2000; Baake et al. 2001; Mosammaparast et al. 2001; Muhlhauser et al. 2001; Mosammaparast et al. 2002b; Greiner et al. 2004; Blackwell et al. 2007; Campos et al. 2010). For H2A and H2B, these include the yeast Importins Kap95, Kap104, Kap123, Kap121, and Kap114 and human Importins Imp β , Kap β 2, Imp5, Imp7, and Imp9. For H3 and H4, these include the yeast Importins Kap95,

Kap104, Kap123, and Kap121 and their human homologs Imp β , Kap β 2, Imp4, and Imp5 respectively, along with three additional human Importins Imp7, Imp9 and the Importin adaptor Imp α .

Previous studies in yeast showed that N-terminal tails of histones H3 and H4 are necessary and sufficient for nuclear import whereas removal of either the H3 or H4 tail does not prevent nuclear import but simultaneous removal of both H3 and H4 tails produced non-viable yeast (Mosammaparast et al. 2002b; Blackwell et al. 2007). Furthermore For H3 and H4, studies in *P. polycephalum* also showed that removal of both H3 and H4 tails resulted in the loss of nuclear H3/H4 (Ejlassi-Lassalette et al. 2011). However, for the H2A/H2B dimer, it has been shown that the N-terminal tails are dispensable for nuclear import but at least one tail is required for replication-dependent active assembly of H2A/H2B dimers into chromatin (Thiriet and Hayes 2001).

Although multiple Importins have been shown to bind and mediate nuclear import of histones, Imp4 and Kap114 (yeast homolog of Imp9) are considered the major importers for H3/H4 and H2A/H2B, respectively. Imp4 is consistently the most abundant Importin that co-purifies with H3 and H4 along with histone chaperone Asf1 in immunoprecipitation experiments and Kap114 (yeast homolog of Imp9) co-purifies with H2A and H2B along with histone chaperone Nap1 (Mosammaparast et al. 2001; Muhlhausser et al. 2001; Campos et al. 2010; Jasencakova et al. 2010; Alvarez et al. 2011).

CHAPTER 2

KARYOPHERIN- β 2 RECOGNITION OF A PY-NLS VARIANT THAT LACKS THE PROLINE-TYROSINE MOTIF

Abstract

Karyopherin- β 2 or Transportin-1 binds proline-tyrosine nuclear localization signals (PY-NLSs) in its cargos. PY-NLSs are described by structural disorder, overall positive charge, and binding epitopes composed of an N-terminal hydrophobic or basic motif and a C-terminal R-X₂₋₅P-Y motif. The N-terminal tail of histone H3 binds Kap β 2 with high affinity but does not contain a recognizable PY-NLS. Crystal structure of Kap β 2-H3 tail shows residues 11-27 of H3 binding to the PY-NLS site of Kap β 2. Residues ¹¹TGGKAPRK¹⁸ of H3 bind the site for PY-NLS Epitope 1 (N-terminal hydrophobic/basic motif) and is most important for Kap β 2-binding. Residue Arg26 of H3 occupies the PY-NLS Epitope 2 position (usually arginine of R-X₂₋₅P-Y) but Epitope 3 (proline-tyrosine motif) is missing in the H3 tail. This is the first example of a PY-NLS variant with no proline-tyrosine or homologous proline-hydrophobic motif. The H3 tail uses a very strong Epitope 1 to compensate loss of the often-conserved proline-tyrosine epitope.

Introduction

Karyopherinβs (Kaps; Importins and Exportins) are responsible for the majority of nuclear-cytoplasmic transport in eukaryotic cells (Gorlich and Kutay 1999; Chook and Blobel 2001; Weis 2003; Cook et al. 2007). Each of the 20 human Kaps transports a different set of cargos by binding a nuclear localization signal (NLS) or nuclear export signal (NES) within the cargo proteins (Chook and Suel 2011)(Xu et al. 2010; Chook and Suel 2011; Fung and Chook 2014; Soniat and Chook 2015). Karyopherinβ2 (Kapβ2 or Transportin-1) is an Importin that transports many protein cargos including numerous RNA binding proteins into the nucleus (Xu et al. 2010; Chook and Suel 2011; Twyffels et al. 2014; Soniat and Chook 2015). Kapβ2 recognizes an NLS termed the PY-NLS, which can be 15-100 residue long, very diverse in sequence and thus cannot be sufficiently described by a traditional consensus sequence. PY-NLSs are instead described by a collection of physical criteria including 1) structural disorder, 2) overall positive charge, and 3) weakly conserved sequence motifs composed of a loose N-terminal hydrophobic or basic motif and a C-terminal R-X₂₋₅P-Y motif (Lee et al. 2006).

Sequence motifs of the PY-NLS contain three energetically important epitopes that bind Kapβ2. The N-terminal hydrophobic/basic motif is Epitope 1, the arginine of the R-X₂₋₅P-Y motif is Epitope 2, and the proline-tyrosine (P-Y) or homologous P-Φ (Φ is hydrophobic residue) motif is Epitope 3. These binding epitopes appear structurally independent as they connected by flexible and sequence-diverse linkers, and they are considered energetically quasi-independent as there appears to be little cooperativity between them when binding Kapβ2 (Suel et al. 2008). Very importantly, Epitopes 1, 2 and 3 contribute differently to overall binding energy in different PY-NLS peptides (Suel et al. 2008).

Most known Kapβ2 cargos contain PY-NLSs but a few cargos do not seem to have

recognizable PY-NLSs (Chook and Suel 2011; Twyffels et al. 2014; Soniat and Chook 2015). The non-PY-NLS containing proteins that bind Kap β 2 include the core histones (H2A, H2B, H3, and H4), ribosomal proteins (rpL23A, rpS7, rpL5, rpL7), RNA-editing enzyme ADAR1, transcription factor FOXO4, and viral proteins (HIV-1 REV, HPV E6). Several groups have shown that N-terminal tails of H3 and H4 are important for Kap β 2 recognition and nuclear import but their NLSs have not been characterized biochemically or structurally (Johnson-Saliba et al. 2000; Baake et al. 2001; Muhlhauser et al. 2001; Mosammaparast et al. 2002b; Greiner et al. 2004; Blackwell et al. 2007; Campos et al. 2010). It is currently not known how non-PY-NLS cargos like the histone tails bind Kap β 2. It is unclear if they carry a different NLS that binds Kap β 2 at a site distinct from the PY-NLS binding site or if they bind to PY-NLS site and are unrecognized variants of the PY-NLS .

We performed structural and biochemical analysis of Kap β 2 bound to the histone H3 tail to reveal Kap β 2 binding elements in the H3 tail. The H3 tail binds to the PY-NLS binding site of Kap β 2 with similar high affinity as known PY-NLSs. The H3 tail uses a basic N-terminal segment that binds like PY-NLS Epitope 1 (N-terminal basic motif) of basic PY-NLSs and an arginine residue that is equivalent to Epitope 2 (usually arginine of the C-terminal R-X₂₋₃-P-Y motif), to bind Kap β 2. The H3 tail does not have a P-Y or homologous P- ϕ motif, and the binding site on Kap β 2 for the P-Y motif remains unoccupied. The structure reveals the first PY-less variant of the PY-NLS.

Materials and Methods

Cloning, Expression, and Purification of H3 tail and Kap β 2.

GST-fusion constructs were generated by inserting PCR fragments corresponding to the regions

of the genes of interest into the pGEX-TEV plasmid, which is a pGEX4T3 vector (GE Healthcare, UK) modified to include a TEV cleavage site (Chook and Blobel 1999). Kap β 2 with a truncated loop, which does not interfere with NLS binding, was used for crystallization (residues 337– 367 of Kap β 2 were replaced with a GGSGGSG linker) (Lee et al. 2006; Cansizoglu et al. 2007). GST-fusion construct of the Histone H3 tail (1-47) was kindly provided by B. Li (UT Southwestern, TX). MBP-fusion constructs of the H3 tail (1-47) and shorter fragments were subcloned into the pMALTEV vector (pMAL (New England BioLabs, Ipswich, MA) with TEV cleavage site) (Chook et al. 2002). H3 tail mutations were made by site-directed mutagenesis using a Quik-Change Site-Directed Mutagenesis Kit (Stratagene, La Jolla, CA), and all constructs were sequenced.

Human Kap β 2 was expressed as a GST-fusion protein. Human H3 tail (residues 1-47) was also expressed as GST-fusion and MBP-fusion proteins. All recombinant proteins were expressed separately in BL21 (DE3) *E. coli* cells (induced with 0.4 mM isopropyl- β -d-1-thiogalactoside (IPTG) for 12 hours at 25°C). Bacteria were lysed with the EmulsiFlex-C5 cell homogenizer (Avestin, Ottawa, Canada) in buffer containing 50 mM Tris pH 7.5, 200 mM NaCl, 20% glycerol, 2 mM DTT, 1mM EDTA, and protease inhibitors.

GST- Kap β 2 proteins were purified by affinity chromatography on GSH sepharose (GE Healthcare, UK), eluted with buffer containing 50 mM Tris pH 7.5, 75 mM NaCl, 20% glycerol, 2 mM DTT and 20 mM L-Glutathione. GST- Kap β 2 were cleaved with TEV protease, and Kap β 2 was further purified using ion-exchange and gel filtration chromatography in TB buffer (20 mM HEPES pH 7.3, 200 mM sodium chloride, 2 mM DTT, 2 mM magnesium acetate, 10% glycerol, 1 mM EGTA).

To purify MBP-H3 tail proteins, bacterial lysates were incubated with amylose beads (New

England BioLabs, Ipswich, MA) and the fusion proteins eluted with buffer containing 20 mM Tris pH 7.5, 50 mM NaCl, 2 mM EDTA, 2 mM DTT, 10% glycerol, and 10 mM maltose. Eluted proteins were further purified by ion-exchange chromatography.

Structure determination of the Kap β 2 bound to the H3 Tail

GST-H3 tail (residues 1-47) and Kap β 2 (residues 337–367 replaced with a GGSGGSG linker) were mixed at molar ratio of 5:1. GST was removed with TEV protease and the Kap β 2-H3 tail complex further purified by gel filtration in buffer containing 20 mM HEPES, pH 7.3, 110 mM potassium acetate, 2 mM DTT, 2 mM magnesium acetate, and 1 mM EGTA with 20% (v/v) glycerol. The Kap β 2-H3 tail complex was concentrated to 15 mg/mL for crystallization.

Kap β 2-H3 tail crystals were obtained by sitting drop vapor diffusion at 20°C (0.4 μ L protein + 0.4 μ L reservoir solution) with reservoir solution of 200 mM NaF, 20% PEG3350. Crystals were cryo-protected by addition of ~20% (v/v) ethylene glycol, and flash-cooled by immersion in liquid nitrogen. Many crystals did not yield useful diffraction, but few diffracted to 3.05-Å resolution. X-ray 0.9795 Å wavelength diffraction data was collected at the Advance Photon Source 19ID beamline in the Structural Biology Center at Argonne National Laboratory. Data was indexed, integrated, and scaled using HKL3000 (Minor et al. 2006). The structure was determined by molecular replacement using PHASER with a search model of human Kap β 2 (A chain of PDB Code 2QMR) (Cansizoglu and Chook 2007). Several rounds of refinement using PHENIX and manual model building with Coot were performed (Adams et al. 2010; Emsley et al. 2010). Residues 11-27 of H3 tail were built into the electron density maps at the last stages of the refinement. The final model of the Kap β 2-H3 tail complex shows excellent stereochemical parameters based on Molprobity suite in PHENIX (Chen et al. 2010) (Table 3). Illustrations were prepared with PyMOL (Schrodinger).

Measuring dissociation constants with isothermal titration calorimetry

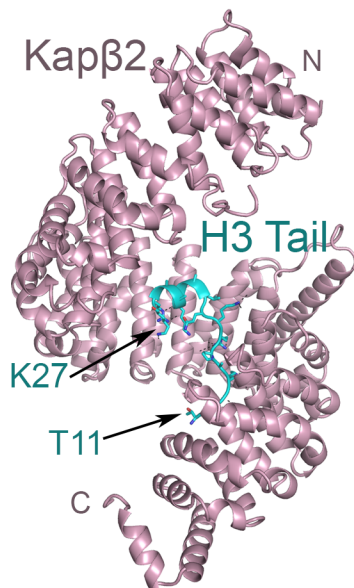
Binding affinities of MBP-H3 tail proteins to Kap β 2 were measured using isothermal titration calorimetry (ITC). ITC experiments were performed with a Malvern ITC200 calorimeter (Malvern Instruments, Worcestershire, UK). Proteins were dialyzed against buffer containing 20 mM Tris, pH 7.5, 100 mM NaCl, 10% glycerol, and 2 mM β -mercaptoethanol. 200-400 μ M MBP-H3 tail proteins were titrated into a sample cell containing 20–40 μ M recombinant Kap β 2. ITC experiments were performed at 20°C with 19 rounds of 4- μ l injections. Data were plotted and analyzed using NITPIC and Sedphat and the data visualized using GUSSE. Averages of three ITC runs were plotted with standard errors in histograms generated by GraphPad Prism.

Results

A



B



C

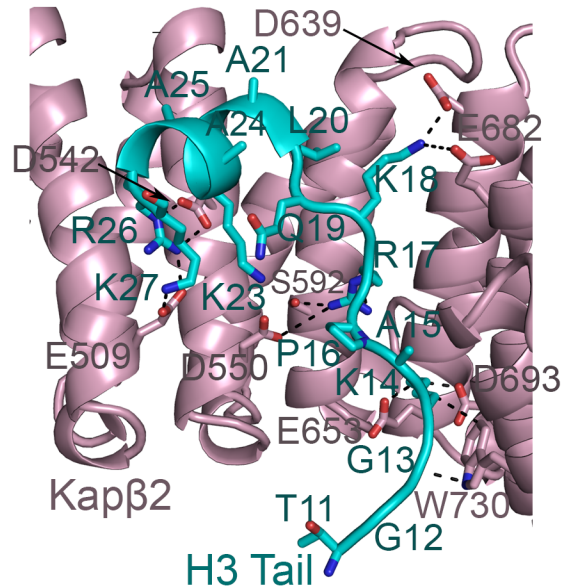


Fig. 2-1. Sequence of the histone H3 tail and structure of the Kap β 2-H3 tail complex.

A) Domain organization of human histone H3 **B)** The 3.05 Å resolution crystal structure of Kap β 2 (pink) bound to histone H3 tail (cyan). **C)** The Kap β 2-H3 tail interface. Contacts between the two proteins (4.0 Å or shorter) are shown with dashed lines.

Structure of the Kap β 2-Histone H3 Tail complex

We solved the 3.05 Å resolution structure of the H3 tail-Kap β 2 complex by molecular replacement. Crystallographic data and refinement statistics are shown in Table 1 and the overall structure of the complex is shown in Figure 2-1A. H3 tail-bound Kap β 2 is very similar to other PY-NLS-bound Kap β 2 proteins. Alignment of Kap β 2 residues 200-800 with Kap β 2 bound to FUS^{PY-NLS} (**4FDD**), hnRNP M^{PY-NLS} (**2OT8**), Nab2^{PY-NLS} (**4JLQ**), hnRNP D^{PY-NLS} (**2Z5N**), JKTBP^{PY-NLS} (**2Z5O**), TAP^{PY-NLS} (**2Z5K**) and hnRNP A1^{PY-NLS} (**2H4M**) gave C α rmsds of 1.25 - 1.74 Å (Lee et al. 2006; Cansizoglu and Chook 2007; Cansizoglu et al. 2007; Imasaki et al. 2007; Niu et al. 2012; Zhang and Chook 2012; Soniat et al. 2013). The superhelical Kap β 2, which is composed of 20 HEAT repeats, uses its PY-NLS binding site on the concave surface of the C-terminal half of the Importin to bind residues 11-27 of the H3 tail (Figure 2-1A).

Residues 11-19 of the H3 tail adopt an extended conformation while residues 20-27 form a 2-turn α -helix (Figure 2-1B). The H3 tail traces a path on Kap β 2 similar to all nine structurally characterized PY-NLSs (Lee et al. 2006; Cansizoglu and Chook 2007; Cansizoglu et al. 2007; Imasaki et al. 2007; Niu et al. 2012; Zhang and Chook 2012; Soniat et al. 2013). Figures 2-1C and 2-1D show the PY-NLSs of hnRNP A1 (also known as the M9 sequence) and hnRNP M, respectively, upon superimposition of the Kap β 2s onto the Kap β 2-H3 tail structure (Lee et al. 2006; Cansizoglu et al. 2007). Residues ¹¹TGGKAPRK¹⁸ of H3 occupy the position of the PY-NLS epitope 1, which is usually the N-terminal hydrophobic or basic motif of a PY-NLS. Hydrophobic motif ²⁷³FGPM²⁷⁶ is Epitope 1 of the hnRNP A1^{PY-NLS} (Figure 2-2A) and the

slightly larger basic segment ⁵⁰KEKNIKR⁵⁶ is Epitope 1 of the hnRNP M^{PY-NLS} (Figure 2-2B). The Arg26 side chain of H3 occupies the position of PY-NLS Epitope 2, which is usually the conserved arginine residue (Arg284 of hnRNP A1, Figure 2-2A; Arg60 of hnRNP M, Figure 2-2B) in the R-X₂₋₅P-Y motif that forms salt bridges with acidic residues in Kapβ2. A striking difference between the H3 tail and conventional PY-NLSs is the former does not contain a PY-NLS Epitope 3, which is usually a P-Y, a homologous P-φ or a P-X (X, any amino acid) motif. In fact, no part of the H3 tail occupies the P-Y binding site on Kapβ2, which remains empty (Figures 2-1B, 2-2A and 2-2B).

Table 2-1. Crystallographic statistics for Kap β 2-Histone H3 tail complex.

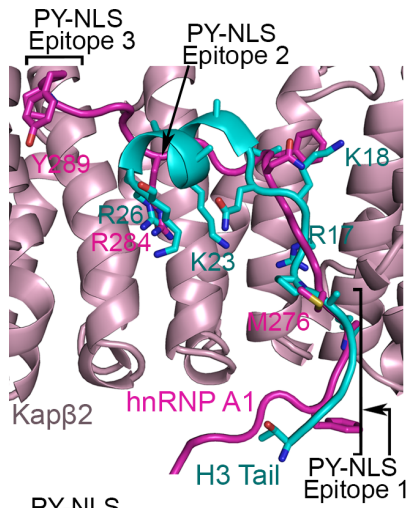
Space group	C222 ₁
Cell dimensions:	
a, b, c (Å)	150.3, 154.2, 192.6
α , β , γ (°)	90, 90, 90
Data Collection	
Wavelength(Å)	0.9795
Resolution (Å)	50.00-3.05 (3.10-3.05) ^a
Completeness (%)	99.9 (100.0) ^a
Redudancy	7.9 (7.5) ^a
R _{merge} (%)	12.3 (100.0) ^a
R _{pim} (%)	4.9 (50.9) ^a
I/ σ I	13.2 (1.7) ^a
Refinement	
Resolution (Å)	47.65-3.05 (3.16-3.05) ^a
No of Reflections	43618 (2172) ^a
R _{work}	20.6 (30.9) ^a
R _{free} (%)	24.9 (37.0) ^a
RMS deviations	
Bond lengths (Å)	0.005
Bond angles (°)	0.935
Average overall B-factor (Å ²)	53.3
Solvent Content (%)	55.9
Ramachandran plot:	
Favored region (%)	94.1
Allowed region (%)	5.2
Outliers (%)	0.7
Model Contents	
Protomers in ASU	
Kap β 2	2
No. of Kap β 2 residues	1651
No. of Kap β 2 atoms	13109
Histone H3 tail	2
No. of Histone H3 tail residues	34
No. of Histone H3 tail atoms	248
No. of water atoms	0
PDB accession code	5J3V

^a Values in parenthesis correspond to the highest-resolution shell

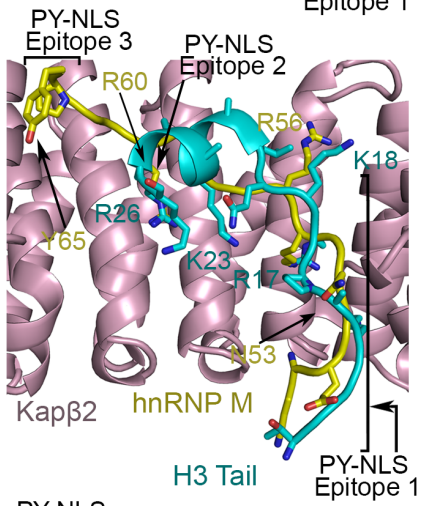
A

		Epitope 1	Epitope 2	Epitope 3	
hnRNP A1	A1	272	NFGPMKGGNFGG---R-SSGPY	289	
hnRNP M	M	49	RKEKNIKR-GNN---R---FEPY	64	
FUS		507	GPGKMSRGEHRQDRR---ERP	526	
Histone H3	H3	11	TGGKAPRKQLATKAARK	27	

B



C



D

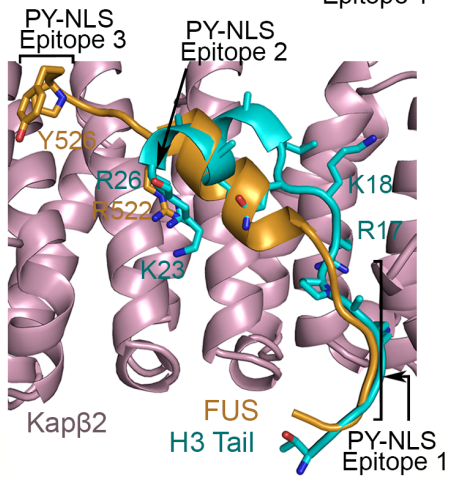


Fig. 2-2. Comparison of the H3 tail with hnRNP A1^{PY-NLS}, hnRNP M^{PY-NLS} and FUS^{PY-NLS}.

A) Sequences of PY-NLSs of histone H3 tail, hnRNP A1, hnRNPA M, and FUS. The N-terminal hydrophobic (yellow) or basic (blue) motifs that form the epitope 1 of the NLS, the central epitope 2 (red), and the C-terminal epitope 3 (green) are shown. **B)** Superposition of Kap β 2s in the Kap β 2-H3 tail and Kap β 2-hnRNP A1^{PY-NLS} (PDB ID 2H4M) complexes. The H3 tail is cyan and the hnRNP A1^{PY-NLS} is magenta. C α rmsd is 1.5 Å for superposition of residues 200-800 of Kap β 2. PY-NLS epitopes 1, 2 and 3 of the hnRNP A1^{PY-NLS} are labeled. **C)** Superposition of Kap β 2s in the Kap β 2-H3 tail and Kap β 2-hnRNP M^{PY-NLS} (PDB ID 2OT8) complexes. The hnRNP M^{PY-NLS} is yellow and the superposition gives a C α rmsd of 1.25 Å. **D)** Superposition of Kap β 2 (pink) bound to H3 tail (cyan) and FUS PY-NLS (Orange; PDB ID 4FDD; C α rmsd 1.74 Å).

Interactions between the H3 Tail and Kap β 2

Like PY-NLSs, the H3 tail makes many electrostatic, polar and hydrophobic interactions with Kap β 2. A list of contacts between the two proteins is shown in Table 2-3. In the N-terminal extended portion of the H3 tail (residues 11-19), Gly13 and Lys14 make hydrophobic interactions with Kap β 2 residue Trp730 (Figure 2-1B and Table 2-3). This is followed by a string of basic residues on H3 that make many contacts with Kap β 2. The Lys14 side chain of H3 forms salt bridges with Kap β 2 residues Glu653 and Asp693. Arg17 of H3 makes salt bridge and polar interactions with Kap β 2 Asp646, Ser591 and Ser592, respectively. Toward the end of the extended part of the H3 tail, Lys18 forms salt bridges with Kap β 2 residue Asp639 (Figure 2-1B). Arg17 and Lys 18 of H3 also make long range electrostatic interactions with several acidic residues of Kap β 2 including Asp550, Glu588, Asp646, Asp653, Glu682 and Asp693 (Table 2-3).

Following the extended portion of H3, residues ²⁰LATKAARK²⁷ of H3 form an α -helix that turns away from the Kap β 2 surface. H3 residues Leu20 and Thr22 make hydrophobic interactions with Kap β 2. H3 Lys23 side chain makes long range electrostatic interactions with Kap β 2 residues Glu509 and Asp550. Arg26 and Lys27 in the H3 helix form salt bridges with Kap β 2 residues Glu509 and Asp543. The H3 tail helix is oriented $\sim 35^\circ$ away from the C-terminal portions of the hnRNP A1 and hnRNP M PY-NLSs. However, despite the different

direction that the H3 tail helix takes, its Arg26 side chain reaches back to make the same salt bridges with Kap β 2 as the conserved Epitope 2 arginines of PY-NLSs (Figures 2-2A and 2-2B). The PY-NLS of the protein Fused in Sarcoma (FUS) also contains a small helix but unlike the H3 helix, which turns away from the Kap β 2 surface, the FUS helix follows the paths of typical PY-NLSs close to the Kap β 2 surface (Figure 2-2C). The NLS in the H3 tail that binds Kap β 2 resembles PY-NLSs structurally and binds Kap β 2 like a PY-NLS even though it does not contain the canonical P-Y or P- Φ dipeptide motif. The H3 NLS for Kap β 2 does not use any binding element in place of the prevalent and often conserved P-Y epitope.

Mutagenic analysis of the Kap β 2-Histone H3 tail interactions

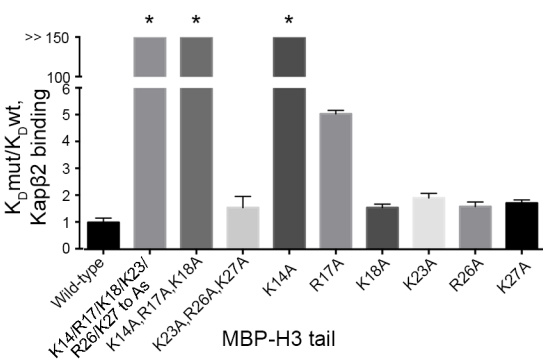


Fig. 2-3. Mutagenesis of the H3 tail and effects of Kap β 2 binding. A histogram showing results of ITC analysis of Kap β 2 binding to a series of H3 tail mutants. $K_D \text{ mut}/K_D \text{ wt}$ values for a series of H3 tail mutants (K_D measurements from triplicate ITC experiments; Table 2) are plotted.

The H3 tail binds Kap β 2 with high affinity (K_D of 77.1 nM, measured by isothermal titration calorimetry (ITC)) comparable with known Kap β 2–PY-NLS interactions (Lee et al. 2006; Cansizoglu et al. 2007; Suel et al. 2008; Suel and Chook 2009; Zhang and Chook 2012) (Table 2). We systematically mutated H3 residues that contact Kap β 2 to examine the distribution of binding energy in the peptide. In the extended portion of H3, only basic side chains (Lys14, Arg17 and Lys18) contact Kap β 2. Similarly, many interactions between the H3 helix involve its

basic side chains. Therefore, we mutated all basic residues in the extended part of H3 (mutant H3 tail(K14A,R17A,K18A)), all basic residues in the helix (mutant H3 tail(K23A,R26A,K27A)) and all basic residues in the H3 NLS (mutant H3 tail(K14/R17/K18/K23/R26/K27 to As)), and measured affinities for Kap β 2 by ITC. The H3 tail(K14A,R17A,K18A) mutant no longer bound Kap β 2 but mutating basic residues in the H3 helix (H3 tail(K23A,R26A,K27A)) decreased affinity by only ~1.5 fold (Table 2-2 and Figure 2-2). Mutation of all basic residues (mutant H3 tail(K14/R17/K18/K23/R26/K27 to As)) resulted no Kap β 2 binding (Table 2-2, Figure 2-2). Mutations of individual basic residues show that Lys14 of H3 contributes the most to Kap β 2 binding as the H3 tail(K14A) mutant shows no Kap β 2 binding (Table 2-2 and Figure 2-2). The H3 tail(R17A) mutant binds Kap β 2 ~5-fold weaker while individual mutations of K18A, K23A, K26A and K27A each shows less than 2-fold decrease in affinity (Table 2-2 and Figure 2-2). In summary, the N-terminal extended segment of the H3 tail (11 TGGKAPRKN 19) is important for binding Kap β 2, and within it H3 residue Lys14 appears to be the binding hotspot.

Table 2-2. Binding affinities of Kap β 2 with H3 tails by ITC.

Ligand	K _D (nM)
MBP-H3 Tail(1-47):	
wild-type	77.1±15.5
K14A, R17A, K18A	ND
K14/R17/K18/K23/R26/K27 to As	ND
K23A, R26A, K27A	119.4±39.7
K14A	ND
R17A	388.9±12.3
K18A	119.6±12.6
K23A	147.5±16.3
R26A	122.5±16.1
K27A	132.7±11.2
MBP-H3 Tail(1-28)	104.5±11.8

Discussion

The crystal structure of Kap β 2 bound to the H3 tail shows H3 residues 11-27 binding to Kap β 2, and biochemical analysis identified the ¹¹TGGKAPRK¹⁸ portion of that segment as the most important for Kap β 2 binding. The H3 tail binds Kap β 2 with similar high affinity as many PY-NLSs and occupies the PY-NLS site of Kap β 2 even though there is no recognizable PY-NLS sequence. PY-NLSs usually use three modular and structurally conserved linear epitopes to bind Kap β 2 (Lee et al. 2006; Cansizoglu et al. 2007; Suel et al. 2008; Xu et al. 2010). Our structure suggests that the H3 tail is a PY-NLS variant that contains only two of the usual three PY-NLS epitopes: Epitope 1, which is the N-terminal basic motif and Epitope 2, which is the helix with an arginine residue equivalent to the arginine of the R-X₂₋₃-P-Y motif. The H3 tail notably lacks the canonical P-Y or P- ϕ motif of the PY-NLS, and no binding element in H3 is used in place of the P-Y epitope.

Süel et al explained how combinatorial mixing of energetically weak and strong motifs amongst the three PY-NLS epitopes is used to maintain a range of affinities for Kap β 2 that are appropriate for nuclear import (Suel et al. 2008). Combinatorial use of the 3 epitopes also accommodates large sequence diversity within PY-NLSs. The H3 tail presents an extreme example, where the sequence is so different that it is not recognizable as a PY-NLS. It is the most conserved motif of the PY-NLS is its C-terminal P-Y, P- ϕ or a marginally homologous P-X motif, which is missing in the H3 tail (Soniata and Chook 2015). The P-Y motif or Epitope 3 is also often, though not always, the epitope that contributes the most to total binding energy of the PY-NLS. In the H3 tail, the use of a strong N-terminal basic motif ¹¹TGGKAPRK¹⁸ and a potentially moderate-strength helical epitope 2 appear to have obviated the need for the third epitope, the canonical C-terminal P-Y epitope.

There are other Kap β 2 cargos that do not have recognizable PY-NLSs (reviewed in (Soniata and Chook 2015)). We envision three scenarios for how these unrecognizable PY-NLSs may bind Kap β 2. In the first scenario, some cargos may contain entirely distinct signals that bind to a different site on Kap β 2. Second, other cargos may have motifs related to P-Y that have diverged to other amino acids but can still bind the P-Y binding site of Kap β 2. For example, the human RNA-editing enzyme ADAR1 (adenosine deaminase acting on RNA 1) does not have a recognizable PY-NLS but is imported specifically by Kap β 2 (Barraud et al. 2014). The NLS in ADAR1 was mapped using NMR and biochemical studies to two disordered segments that flank the second dsRNA-binding domain (dsRBD1). Neither of flanking segments have a P-Y or P- ϕ motif but it was suggested that these fragments are positioned by the dsRBD1 domain to bind Kap β 2 like other PY-NLSs. Structural modeling and sequence alignment suggested that ⁷⁰⁸MMPN⁷¹¹ in the first flanking segment is the hydrophobic motif of PY-NLS Epitope 1 and a conserved positively charged residue in the second segment is Epitope 2. ADAR1 does not contain a P-Y motif but it was suggested that an ⁸⁰⁰ER⁸⁰¹ dipeptide in the second segment might be Epitope 3 and occupy the P-Y binding site. The third scenario is the true PY-less PY-NLS, like the H3 tail, that uses only Epitopes 1 and 2 to bind Kap β 2. Our results currently suggest that sequences with only two PY-NLS epitopes can be functional Kap β 2 NLSs. It remains to be seen if there may be unusually strong PY-NLS Epitopes 1, 2 or 3 that can be used alone as a Kap β 2 NLS.

In addition to Kap β 2, the H3 tail also binds Imp β , Imp4, Imp5, Imp7, Imp9 and Imp α (Soniata and Chook 2015; Soniata and Chook 2016). Other core histone tails and sequences in several ribosomal proteins were also reported to bind multiple Importins (Jakel and Gorlich 1998; Johnson-Saliba et al. 2000; Baake et al. 2001; Muhlhausser et al. 2001; Mosammaparast et

al. 2002b; Greiner et al. 2004; Blackwell et al. 2007). For example, ribosomal protein L23A (rpL23A) binds Imp α , Kap β 2, Imp5, and Imp7 through a 43-residue segment termed the β -like import receptor binding (BIB) sequence (Jakel and Gorlich 1998). Other ribosomal proteins like rpS7 and rpL5 may also contain BIB-like sequences (Jakel and Gorlich 1998). Jäkel and Görlich suggested that BIB sequences are ancestral nuclear import signals that existed before Importins diverged to have specialized/distinct NLS binding sites (Jakel and Gorlich 1998). Even though an Importin like Kap β 2 has evolved to bind a specific class of signal like the PY-NLS, Kap β 2 probably still retains the ability to bind the putative ancestral BIB that had not evolved a P-Y motif. Alignment of the H3 tail with the rpL23A BIB (residues 32-74) shows sequence similarity of rpL23A residues ⁵⁹KYPRKSAPRRNK⁷⁰ with the H3 ¹⁴KAPRKQLATKAAR²⁶. It remains to be determined if parts of the BIB of rpL23A or other ribosomal proteins bind Kap β 2 like the PY-less PY-NLS of the histone H3 tail.

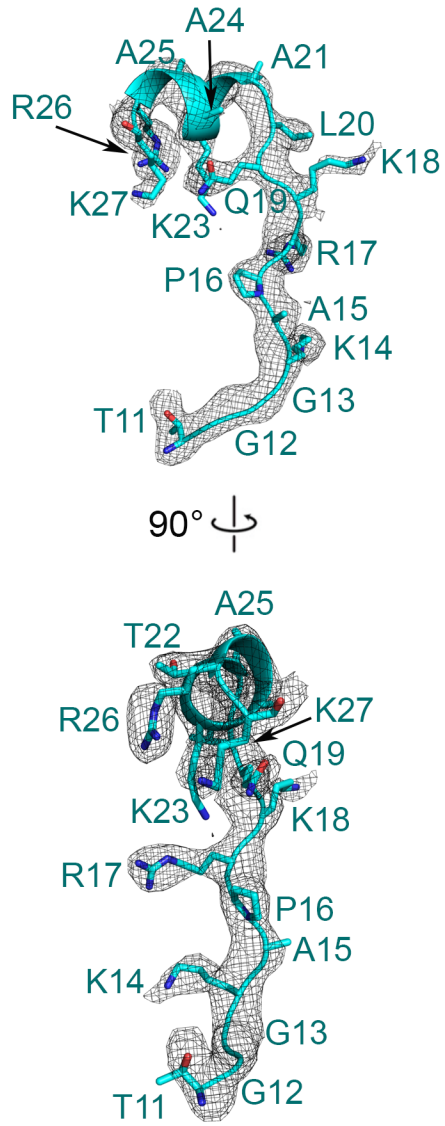


Fig. 2-4. mFo-DFc difference map, contoured at 2σ (grey mesh), at the H3 tail binding site of Kap β 2 before the H3 tail was modeled, shown with a later model of the H3 tail

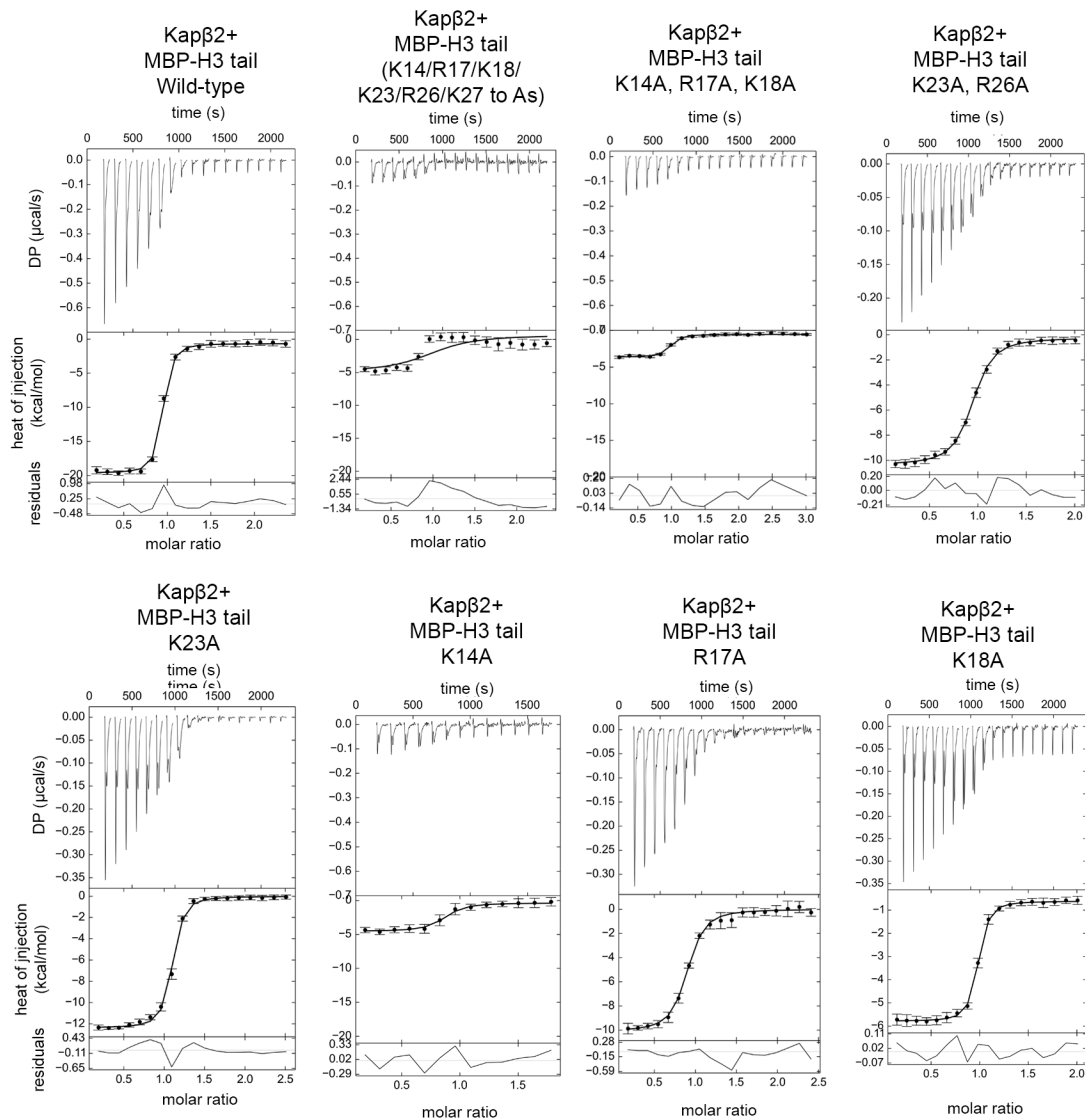


Fig. 2-5. Representative ITC measurements of MBP-H3 tail proteins binding to Kap β 2. After dialyzed against the same buffer, 200-400 μ M H3 proteins were titrated into a sample cell containing 20–40 μ M recombinant Kap β 2. ITC experiments were performed at 20°C with 19 rounds of 4- μ l injections. Data were plotted and analyzed using NITPIC and Sedphat. Data was visualized by GUSI.

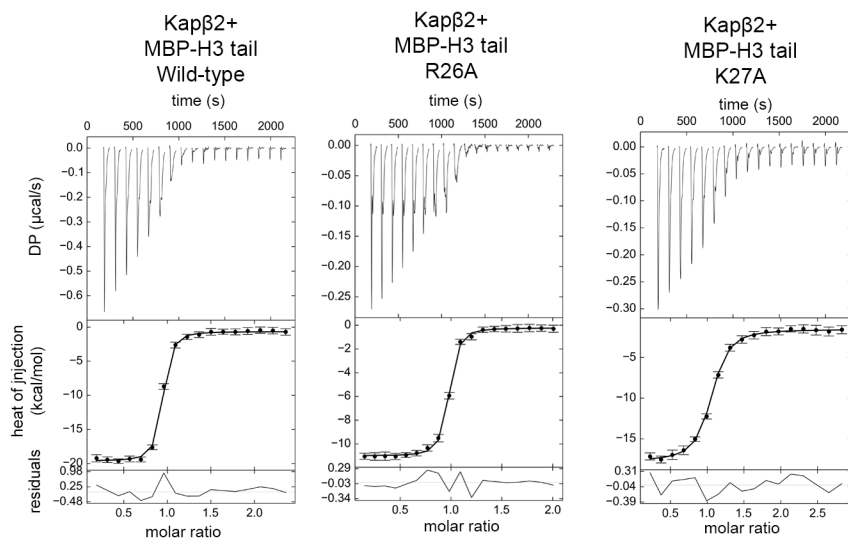


Fig. 2-6. Representative ITC measurements of MBP-H3 tail proteins binding to Kapβ2. After dialyzed against the same buffer, 200-400 µM MBP-H3 and H4 tail proteins were titrated into a sample cell containing 20–40 µM recombinant Kapβ2. ITC experiments were performed at 20°C with 19 rounds of 4-µl injections. Data were plotted and analyzed using NITPIC and Sedphat. Data was visualized by GUSI.

Table 2-3. A list of electrostatic, polar and hydrophobic interactions between Kap β 2 and the H3 Tail^a

<u>H3 Tail</u>	<u>Kapβ2</u>	<u>Interactions</u>
Thr11	Asn807	mc-sc polar
	Glu769	mc-sc polar
Gly13	Asn770	mc-sc polar
	Trp730	mc-sc hydrophobic
Lys14	Asn726	mc-sc polar
	Trp730	sc-sc hydrophobic
	Ala698	sc-sc hydrophobic
	Asp693	Salt bridge
Ala15	Glu653	Salt bridge
	Asn727	mc-sc polar
	Asn726	mc-sc polar
Arg17	Ser723	sc-sc hydrophobic
	Asp646	sc-sc hydrophobic
	Asp646	Long range electrostatic
	Asp550	Long range electrostatic
	Asp693	Long range electrostatic
	Asp653	Long range electrostatic
	Glu588	Salt bridge
	Ser591	sc-sc polar
	Ser591	sc-sc hydrophobic
	Ser592	sc-sc polar
Lys18	Asp639	Salt bridge
	Glu682	Long range electrostatic
	Asp646	Long range electrostatic
	Phe584	sc-mc polar
Leu20	Pro585	sc-mc hydrophobic
	Glu588	sc-sc hydrophobic
	Leu539	sc-sc hydrophobic
Thr22	Ile540	sc-mc hydrophobic
	Ile540	sc-sc hydrophobic
Lys23	Asp543	sc-sc hydrophobic
	Asp543	mc-sc polar
	Asp550	Long range electrostatic
	Glu509	Long range electrostatic
Arg26	Ala505	sc-sc hydrophobic
	Asp543	Salt bridge
	Glu509	Salt bridge
	Thr547	sc-sc polar
	Glu508	Long range electrostatic
	Glu550	Long range electrostatic

Lys27	Glu509	sc-sc hydrophobic
	Glu509	Salt bridge
	Glu510	Long range electrostatic

^a Only contacts < 4Å are listed for polar and hydrophobic interactions but charged contacts < 8Å are listed as long range electrostatic interactions

CHAPTER 3

RECOGNITION ELEMENTS IN THE HISTONE H3 AND H4 TAILS FOR SEVEN DIFFERENT IMPORTINS

Abstract

Multiple Importins can bind the N-terminal tails of histones H3 and H4, and import histones into the nucleus to be assembled into nucleosomes. However, it is not known what binding elements in the histone tails are recognized by the different Importins. We have identified binding elements in the H3 and H4 tails for each of seven Importins: Imp α , Imp β , Kap β 2, Imp4, Imp5, Imp7 and Imp9. For the H3 tail, we found that residues 11-27 are the sole binding element for Imp β , Kap β 2, and for Imp4. The N-terminal basic segment of H3 and a C-terminal IK-NLS motif at residues 35-40 are used together to bind Imp5, Imp7, Imp9 and Imp α . Interactions of the H4 tail with the same Importins show a similar trend of relative affinities as the H3 tail, albeit at least 10-fold weaker, and a similar use of one or two basic regions in the H4 tail. Finally, we show that of all the lysine residues in the H3 and H4 tails, only acetylation of the H3 Lys14, which is the binding hotspot for Imp β , Kap β 2 and Imp4, abolished or substantially decreased binding to several Importins. Overall, we have revealed recognition elements in the H3 and H4 tail for seven different Importins and showed that acetylation of the H3 Lys14 affects Importin

binding and may compromise nuclear import.

Introduction

New nucleosomes are assembled in the nucleus during S-phase as new core histones H2A, H2B, H3 and H4 are synthesized in the cytoplasm. Newly translated histone proteins are assembled into H2A/H2B dimers and H3/H4 dimers and then imported into the nucleus for deposition onto the replicating chromatin (Eickbush and Moudrianakis 1978; Smith and Stillman 1991; Luger et al. 1997; Nakagawa et al. 2001; White et al. 2001; Campos and Reinberg 2009; Keck and Pemberton 2012; Annunziato 2013; Burgess and Zhang 2013; Elsasser and D'Arcy 2013). During translation, heat-shock cognate 70 proteins (HSC70) are recruited to the ribosomal exit to aid the folding of monomeric histones H3 and H4, which are then transferred to the chaperones heat-shock protein 90 (HSP90) and testicular nuclear autoantigenic sperm protein (tNASP), which assemble them into H3/H4 dimers (Alekseev et al. 2005; Hartl and Hayer-Hartl 2009; Campos et al. 2010). H3-H4 dimers are then transferred to somatic NASP or sNASP, which recruits the histone acetyltransferase complex HAT-1-RbAp46 to acetylate the N-terminal H3 and H4 tails (Verreault et al. 1998; Murzina et al. 2008; Campos et al. 2010; Jasencakova et al. 2010; Ejlassi-Lassalette et al. 2011; Li et al. 2014). After acetylation, H3/H4 dimers are transferred to the histone chaperone anti-silencing function protein 1 (Asf1) and bound by Importins for transport into the nucleus (Baake et al. 2001; Muhlhauser et al. 2001; Mosammamarast et al. 2002b; Greiner et al. 2004; Mousson et al. 2005; English et al. 2006; Blackwell et al. 2007; Natsume et al. 2007; Alvarez et al. 2011; Zhang et al. 2013). Histones H3 and H4 each consists of an N-terminal disordered tail region followed by a globular histone fold domain (Luger et al. 1997; White et al. 2001) (Figure 3-1A). The crystal structure of the Asf1-H3/H4 complex showed that Asf1 interacts with the histone-fold domains of the H3/H4 dimer

but does not interact with N-terminal tails of H3 and H4 and has not been shown to interact with Importins (English et al. 2006; Natsume et al. 2007). Upon entry into the nucleus, two H3/H4 dimers are assembled into a tetramer and deposited onto DNA, followed by addition of two H2A/H2B dimers to form the nucleosome particle (English et al. 2005; Burgess and Zhang 2013).

Nuclear import of core histones is mediated by Importins, which are members of the Karyopherin- β family of proteins. Karyopherin- β s (Importins and Exportins) are responsible for the majority of protein traffic between the nucleus and the cytoplasm of eukaryotic cells (Gorlich and Kutay 1999; Chook and Blobel 2001; Weis 2003; Mosammaparast and Pemberton 2004; Cook et al. 2007; Xu et al. 2010). There are at least 10 different Importins in human cells that bind distinct nuclear localization signals (NLSs) in their cargos to target them to the nuclear pore complex (Chook and Suel 2011; Soniat and Chook 2015). Previous studies in yeast showed that N-terminal tails of histones H3 and H4 are necessary and sufficient for nuclear import. Removal of either the H3 or H4 tail does not prevent nuclear import but simultaneous removal of both H3 and H4 tails produced non-viable yeast (Mosammaparast et al. 2002b; Blackwell et al. 2007). Studies in *P. polycephalum* also showed that removal of both H3 and H4 tails resulted in the loss of nuclear H3-H4 (Ejlassi-Lassalette et al. 2011). A combination of co-immunoprecipitation experiments, *in vitro* binding assays with recombinant proteins, and nuclear localization studies in yeast and permeabilized HeLa cells have shown that several Importins can bind and import H3 and H4. These include the yeast Importins Kap95, Kap104, Kap123, and Kap121 and their human homologs Imp β , Kap β 2, Imp4, and Imp5 respectively, along with three additional human Importins Imp7, Imp9 and the Importin adaptor Imp α (Johnson-Saliba et al. 2000; Baake et al. 2001; Muhlhauser et al. 2001; Mosammaparast et al. 2002b; Greiner et al. 2004; Blackwell et

al. 2007; Campos et al. 2010). Although multiple Importins have been shown to bind and mediate nuclear import of histones H3 and H4, Imp4 is consistently the most abundant Importin that co-purifies with H3 and H4 along with histone chaperone Asf1 in immunoprecipitation experiments. These findings suggest that Imp4 may be the major nuclear importer that forms an Importin-histone-chaperone complex composed of Imp4, the H3/H4 dimer and the histone chaperone Asf1 for transport across the nuclear pore complex (Muhlhauser et al. 2001; Campos et al. 2010; Jasencakova et al. 2010; Alvarez et al. 2011).

Additionally, acetylation of the histones H3 and H4 at lysine residues in their N-terminal tails seems to occur in the cytoplasm prior to their import into the nucleus (Muhlhauser et al. 2001; Blackwell et al. 2007; Campos et al. 2010; Jasencakova et al. 2010). However, it remains unclear and controversial if and what effect acetylation has on nuclear import of the histones. Mass spectrometry studies have shown that 20-30% of histones H3 in the cytoplasm are acetylated at Lys14 and/or Lys18 while all cytoplasmic histones H4 are acetylated at Lys5 and Lys12 (Jasencakova et al. 2010). Studies in yeast showed that glutamine mutations of lysines (a means of mimicking acetylation) in the histone H3 and H4 tails resulted in loss of nuclear accumulation. Furthermore, in the absence of the H4 tail, H3 acetylation as observed with lysine to glutamine mutations led to inviability but it is unclear if this loss of function was a result of nuclear import defect or of defective chromatin assembly in the nucleus (Blackwell et al. 2007). Finally, 'acetylation' mutants of both H3 and H4 tails were viable in yeast but slow growing (Blackwell et al. 2007). These previous reports collectively suggest that acetylation of histones H3 and H4 may be inhibitory to their nuclear import. However, there are also contrasting reports where histone acetylation in *P. polycephalum* led to a greater degree of nuclear accumulation (Ejlassi-Lassalette et al. 2011). Additionally, acetylated H4 tail peptides were shown to bind

Imp4 better than the unacetylated peptide suggesting that acetylation may promote nuclear import (Alvarez et al. 2011).

Of the seven Importins and Importin adaptor (Imp β , Kap β 2, Imp4, Imp5, Imp7, Imp9 and Imp α) known to bind and import histones H3 and H4, only classes of NLSs recognized by Imp α /Imp β , Kap β 2 and Imp5 have been characterized. Imp α /Imp β recognizes the classical-NLS (c-NLS) with Imp α binding directly to the signal, Kap β 2 recognizes the PY-NLS, which is entirely distinct from the c-NLS and Imp5 recognizes a short lysine-rich NLS named the IK-NLS (also distinct from the c-NLS) (Xu et al. 2010; Chook and Suel 2011; Soniat and Chook 2015). Classical-NLSs contain either one (monopartite; K-K/R-X-K/R) or two (bipartite; (K/R)(K/R)X₁₀₋₁₂(K/R)_{3/5}) clusters of positively charged amino acids, where X is any amino acid and (K/R)_{3/5} represents three lysine or arginine residues out of five consecutive amino acids (Dingwall et al. 1982; Kalderon et al. 1984a; Lanford and Butel 1984). The PY-NLS is defined by a set of physical criteria, which include loose sequence motifs (N-terminal hydrophobic or basic motifs and a C-terminal R/K/H-X₂₋₅-P-Y motif), structural disorder, and an overall basic charge (Lee et al. 2006). The IK-NLS is defined by the consensus motif K-V/I-X-K-X₁₋₂-K/H/R (Kobayashi and Matsuura 2013). Classes of NLS that specifically bind to Imp4, Imp7 and Imp9 have not yet been characterized. Examination of sequences in the H3 and H4 tails revealed no recognizable c-NLS (predicted using cNLS Mapper) or PY-NLS even though both tails have been shown to bind and be imported by Imp α /Imp β and Kap β 2 (Lee et al. 2006; Kosugi et al. 2009b). A previous report suggested that residues 35-40 at the C-terminal end of the H3 tail resemble an Imp5-specific IK-NLS (Kobayashi and Matsuura 2013).

It is well established that several Importins can import histones H3 and H4 into the nucleus by binding the histone tails. However, it is not known what sequence elements in the

tails are recognized by each of the Importins. Is there a common NLS in each of histone H3 and histone H4 that is recognized by all the Importins or does each Importin recognize a distinct NLS within the histones? Here, we probe the binding determinants in the N-terminal tails of histones H3 and H4 for each of the six different human importins (Imp β , Kap β 2, Imp4, Imp5, Imp7, Imp9) and for the Importin adaptor Imp α , through quantitative biochemical analysis. Previous structural work revealed that Kap β 2 binds the segment of H3 tail between residues 11 and 27, which contains six basic side chains that are important for binding the Importin and resembles a PY-NLS that is missing its P-Y epitope. The same basic segment of H3 is important for binding Imp β , Imp4, Imp5, Imp7, Imp9 and Imp α . In addition, a C-terminal IK-NLS-like motif at residues 35-40 of H3 is also used to bind Imp5, Imp7, Imp9 and Imp α . The first 20 residues of the H4 tail are enriched in basic and glycine residues and that segment is used to bind Imp β , Kap β 2, Imp4 and Imp7, and Imp9. Like the H3 tail, the H4 tail also contains an IK-NLS-like motif at its C-terminus, which is also used to bind Imp5, Imp7, Imp9 and Imp α . As we uncover binding determinants in the histone tails for each of the six Importins and Imp α , we also studied the effects of histone tail acetylation on Importin interactions. We show that acetylation of Lys14 of the H3 tail disrupts binding to all six Importins and Imp α while acetylation of Lys18 of H3 tail had little effect on Importin binding. Acetylation of Lys5 and Lys 12 of the H4 tail also has only mild effects on binding to the Importins. Overall, we have mapped Importin-binding determinants to either one or two basic epitopes in the H3 and H4 tails and revealed differential effects of Importin-binding when individual lysines within these epitopes are acetylated.

Materials and Methods

Plasmids

GST-fusion constructs were generated by inserting PCR fragments corresponding to the regions of the genes of interest into the pGEX-TEV plasmid, which is a pGEX4T3 vector (GE Healthcare, UK) modified to include a TEV cleavage site (Chook and Blobel 1999). The GST-fusion constructs were constructed with full-length human Imp α (Δ IIBB), Imp β , Kap β 2, Imp4, Imp5, Imp7, Imp9, Imp11, Imp8 and TrnSR (Zhang et al. 2011). GST-fusion constructs of the Histone H3 tail (1-47), and the Histone H4 tail(1-34) were kindly provided by B. Li (UT Southwestern, TX). MBP-fusion constructs of the H3 tail (1-47) and H4 tail (1-34) and shorter fragments were subcloned into the pMALTEV vector (pMAL (New England BioLabs, Ipswich, MA) with TEV cleavage site) (Chook et al. 2002). H3 tail and H4 tail mutations were made by site-directed mutagenesis using a Quik-Change Site-Directed Mutagenesis Kit (Stratagene, La Jolla, CA), and all constructs were sequenced. Acetylated-H3 tail (K14Ac and K18Ac) peptides and the acetylated-H4 tail (K5Ac/K12Ac) peptide were purchased from Biomatik.

Expression and purification of histones and importins.

Human Imp α (Δ IIBB), Imp β , Kap β 2, Imp4, Imp5, Imp7, Imp9, Imp11, Imp8, and TrnSR were expressed as a GST-fusion proteins. Human H3 tail (residues 1-47) and H4 tail (residues 1-34) were also expressed as GST-fusion and MBP-fusion proteins. All recombinant proteins were expressed separately in BL21 (DE3) *E. coli* cells (induced with 0.4 mM isopropyl- β -D-thiogalactoside (IPTG) for 12 hours at 25°C). Bacteria were lysed with the EmulsiFlex-C5 cell homogenizer (Avestin, Ottawa, Canada) in buffer containing 50 mM Tris pH 7.5, 200 mM NaCl, 20% glycerol, 2 mM DTT, 1mM EDTA, and protease inhibitors.

GST-Importin proteins were purified by affinity chromatography on GSH sepharose (GE Healthcare, UK), eluted with buffer containing 50 mM Tris pH 7.5, 75 mM NaCl, 20% glycerol, 2 mM DTT and 20 mM L-Glutathione. GST-Importins were cleaved with TEV protease, and the

Importin proteins were further purified using ion-exchange and gel filtration chromatography in TB buffer (20 mM HEPES pH 7.3, 200 mM sodium chloride, 2 mM DTT, 2 mM magnesium acetate, 10% glycerol, 1 mM EGTA).

For pull-down binding assays, bacteria expressing the GST-histone tail proteins were lysed by sonication and centrifuged. The supernatants were incubated with GSH Sepharose (GE Healthcare, UK), followed by extensive washes with TB buffer that contains 10% glycerol. Immobilized GST-histone tail proteins were stored in TB buffer containing 40% glycerol, at -20°C .

To purify MBP-histone tail proteins, bacterial lysates were incubated with amylose beads (New England BioLabs, Ipswich, MA) and the fusion proteins eluted with buffer containing 20 mM Tris pH 7.5, 50 mM NaCl, 2 mM EDTA, 2 mM DTT, 10% glycerol, and 10 mM maltose. Eluted proteins were further purified by ion-exchange chromatography.

Pull-down binding assays

Pull-down binding assays were performed by incubating immobilized GST-H3 and H4 tail proteins with purified Importins in TB buffer for 30 min at 4°C , followed by extensive washing with the same buffer. Approximately 10-20 μg of immobilized GST-H3 and H4 tail proteins were incubated with ~ 60 μg of purified Importins. For RanGTP dissociations assays, ~ 40 μg of purified RanGTP was incubated with immobilized GST-H3 bound to Importins, followed by extensive washing. Activity of Imp β , Kap $\beta 2$, Imp4, Imp5, Imp7, and Imp9 were verified by their binding to RanGTP and activity of Imp α was verified by binding to the classical-NLS of the SV40 T antigen. Bound proteins were visualized using SDS-PAGE and Coomassie blue staining. Gels were subject to densitometry analysis using ImageJ. The density of the Importin band in each gel lane was divided by the density of the GST-histone tail band in the same lane.

The ratios were then normalized to the ratio of the Importin band over the wild-type GST-H3 and H4 tail wild-type bands. Relative band intensities of experiments performed in triplicate are plotted with standard errors in histograms generated with GraphPad Prism.

Qualitative comparison of Importin-histone tail binding were performed by incubating 400 μ L of 500 nM immobilized GST-H3 sepharose beads and H4 tail proteins with 400 μ L of 1 400 μ M purified Importins in TB buffer for 30 min at 4°C, followed by extensive washing with the same buffer. Bound proteins were visualized using SDS-PAGE and Coomassie blue staining. Gels were subject to densitometry analysis using ImageJ. The density of the Importin band in each gel lane was divided by the density of the GST-histone tail band in the same lane. Input of Importins were visualized by SDS-PAGE/Coomassie blue staining to ensure that a similar concentrations of Importins were added, and excess unbound Importins in the flow-through were also monitored.

Measuring dissociation constants with isothermal titration calorimetry

Binding affinities of MBP-H3 tail proteins to Kap β 2 and Imp5 were measured using isothermal titration calorimetry (ITC). ITC experiments were performed with a Malvern ITC200 calorimeter (Malvern Instruments, Worcestershire, UK). Proteins were dialyzed against buffer containing 20 mM Tris, pH 7.5, 100 mM NaCl, 10% glycerol, and 2 mM β -mercaptoethanol. 200-400 μ M MBP-H3 tail proteins were titrated into a sample cell containing 20–40 μ M recombinant Kap β 2 or Imp5. ITC experiments were performed at 20°C with 19 rounds of 4- μ l injections. Data were plotted and analyzed using NITPIC and Sedphat and the data visualized using GUSSE. Averages of three ITC runs were plotted with standard errors in histograms generated by GraphPad Prism.

Results

Seven different human Importins bind the H3 and H4 tails

Six Importins Imp β , Kap β 2, Imp4, Imp5, Imp7, Imp9 and the Importin adaptor Imp α , were previously shown to bind to both histone H3 and histone H4 and transport them into the nucleus (Johnson-Saliba et al. 2000; Baake et al. 2001; Muhlhauser et al. 2001; Campos et al. 2010; Alvarez et al. 2011). The N-terminal tails of histones H3 and H4 were shown to be important for nuclear import of the histones in both yeast and *P. polycephalum* (Mosammaparast et al. 2002b; Ejlassi-Lassalette et al. 2011). To study interactions between Importins and the H3 and H4 tails, we first performed pull-down binding assays using immobilized GST- H3 tail (residues 1-47) and immobilized GST-H4 tail (residues 1-34) with nine different recombinant human Importins - Imp β , Kap β 2, Imp4, Imp5, Imp7, Imp9, Imp11, Imp8, TrnSR and the Importin adaptor Imp α (Figure 3-1). Binding was observed using Coomassie Blue staining, and we saw the same seven transporters Imp β , Kap β 2, Imp4, Imp5, Imp7, Imp9 and Imp α , previously shown to import histones H3 and H4, bind strongly to both H3 and H4 tails here. Imp11, Imp8, and TrnSR did not bind either the H3 or H4 tail. Activities of Imp β , Kap β 2, Imp4, Imp5, Imp7, and Imp9 were verified by binding to RanGTP and activity of Imp α by binding to the classical-NLS from SV40 T antigen (Figure 3-6A-D). Interactions between the Importins (Imp β , Kap β 2, Imp4, Imp5, Imp7, Imp9) and the histone tails are sensitive to RanGTP (Figure 3-6E).

We measured dissociation constants or K_{Ds} of the H3 and H4 tails binding to both Kap β 2 and Imp5 by ITC. The H3 tail binds Kap β 2 with a K_D of 77.1 nM and it binds Imp5 with a K_D of 57 nM (Tables 1). The low nanomolar binding affinity is comparable with known Kap β 2–PY-NLS interactions (Lee et al. 2006; Cansizoglu et al. 2007; Suel et al. 2008; Suel and Chook 2009;

Zhang et al. 2011; Zhang and Chook 2012). The histone H4 tail binds with approximately 10-fold lower affinity to each Kap β 2 and Imp5. The H4 tail binds Kap β 2 with a K_D of 871 \pm 40 nM and it binds Imp5 with a K_D of 619 \pm 53 nM. We were not able to measure the dissociation constants of the histone tails binding to Imp β , Imp4, Imp7, Imp9 and Imp α by either ITC, microscale thermophoresis (MST) or fluorescence anisotropy. Instead, band densities for bound Importins and histone tails in the pull-down binding assays in 3-1C (protein concentrations used were 1/8 those in Figure 3-1B) were measured and their ratios compared in a histogram to estimate relative strengths of H3 tail and H4 tail binding to Imp β , Kap β 2, Imp4, Imp5, Imp7, Imp9 and Imp α . Comparison of the bound Importin bands suggested the binding affinity trend (from high to low affinity) for N-terminal H3 tail is Kap β 2, Imp5 ($K_D < 100$ nM) > Imp β , Imp9, Imp α > Imp4, Imp7. The H4 tail binds Importins at least 10-fold weaker than the H3 tail, and the binding trend for Importins binding to the H4 tail is slightly different with Imp5 > Imp9, Imp α > Imp β , Kap β 2, Imp4, Imp7. The H4 tail binds strongest to Imp5 (K_D 619 \pm 53 nM) and more weakly to the other six Importins.

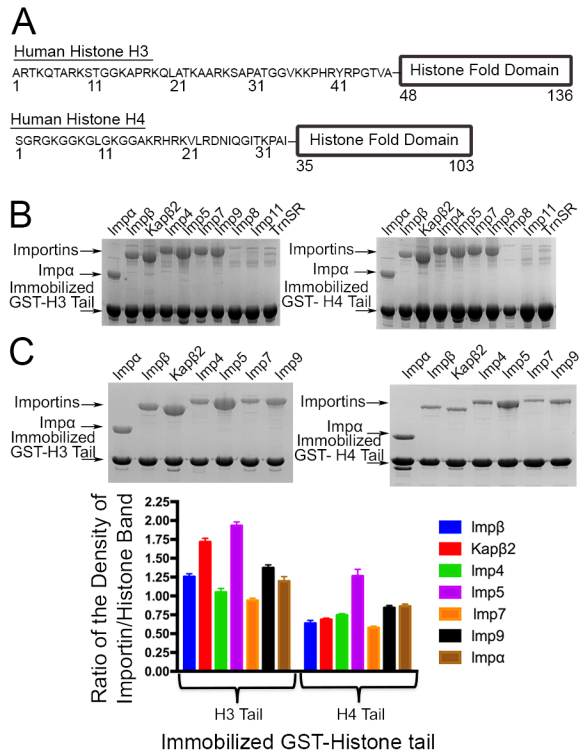


Fig. 3-1. Seven different human Importins bind the H3 and H4 tails.

A) Domain organization of human histone H3 and H4. **B)** Pull-down binding assays of 2 μ M immobilized GST-H3 tail and GST-H4 tail with 4 μ M of each recombinant Importins (SDS-PAGE/Coomassie Blue). **C)** Pull-down binding assays of 250 nM immobilized GST-H3 tail and GST-H4 tail with 500 nM of each recombinant Importins. Relative band intensities from three separate experiments are plotted in histograms.

Interactions of the basic segment within residues 11-27 of H3 tail with other Importins

Structure determination by X-ray crystallography of Importin-H3 complexes (using Imp β , Kap β 2, Imp4, Imp5, Imp7, and Imp9) was attempted to identify binding determinants in the H3 tail for each Importin. Crystals of the histone H3 tail (residues 1-47) in complex with Kap β 2, Imp4, and Imp5, respectively, were obtained but only the H3 tail-Kap β 2 complex produced diffracting crystals. Recently we determined the structure of Kap β 2 in complex with the H3 tail (Fig 2-1B). The structure along with thermodynamic analysis showed that residues 11-27 of the H3 tail is important for Kap β 2 recognition where Lys14 is a hotspot for binding. We performed pull-down binding assays to examine if this same H3 tail segment is also involved in

binding Imp β , Imp4, Imp5, Imp7, Imp9 and Imp α . The GST-H3 tail(K14/K17/K18/K23/R26/K27 to As) mutant is immobilized and its interaction with each of the other six Importins examined (Figure 3-2A). Mutation of all six basic residues within residues 11-27 of H3 appears to abolish binding to Imp β , Imp4, Imp7, Imp9 and Imp α , suggesting that the same region of H3 that binds Kap β 2 is also critical for binding these other Importins. Interestingly, the GST-H3 tail(K14/K17/K18/K23/R26/K27 to As) mutant shows only a small decrease in binding Imp5 in pull-down binding assays (Fig 3-2A). ITC data shows that binding of the MBP-H3 tail(K14/K17/K18/K23/R26/K27 to As) to Imp5 is decreased ~15-fold compared to wild type MBP-H3 tail (K_D of 862 nM for the mutant vs. 57 nM for wild-type H3 tail; Table 3-1). The pull-down and ITC studies with Imp5 suggest that additional binding element(s) beyond residues 11-27 of H3 is likely involved in binding Imp5.

We mutated individual basic residues within residues 11-27 of the H3 tail to further dissect binding determinants for each of Imp β , Imp4, Imp5, Imp7, Imp9 and Imp α . Pull-down binding assays (Coomassie Blue staining) for Imp β , Kap β 2, Imp4, Imp5, Imp7, Imp9 and Imp α are shown in Figure 3-2B. Single site mutant H3 tail(K14A) showed a large decrease in binding to Imp β , Kap β 2, Imp4, Imp7 and Imp9 but had only mild effect on binding Imp α and Imp5. In contrast, single mutations of H3 Arg17 and of H3 Lys18 only mildly affected all the Importins and Imp α . Mutation of the H3 Lys23 decreased the binding of both Imp7 and Imp9 to below 30% of wild-type H3 tail but had much milder effects on the other Importins. Single mutants of Arg26, and of Lys27 showed little or no effect on binding of any of the Importins. Interestingly, although Imp α binding was disrupted when all basic residues between H3 residues 11-27 were mutated to alanine (Figure 3-2B) no single mutation affected Imp α binding, suggesting that binding energy is distributed across the entire H3 residues 11-23 segment for Imp α binding,

possibly through interactions involving both side chain and main chain atoms of H3 that are reminiscent of c-NLS interactions.

In summary, the basic segment that spans H3 residues 11-27 is important for binding Imp β , Kap β 2, Imp4, Imp5, Imp7, Imp9 and Imp α . Here, residue Lys14 seems to be a hotspot for binding all the Importins except for Imp5 and Imp α . The basic segment that spans H3 residues 11-27 appears not to be the sole binding element for Imp5, consistent with a previous report that suggested an Imp5-binding epitope further C-terminus at residues 35-40 (Kobayashi and Matsuura 2013).

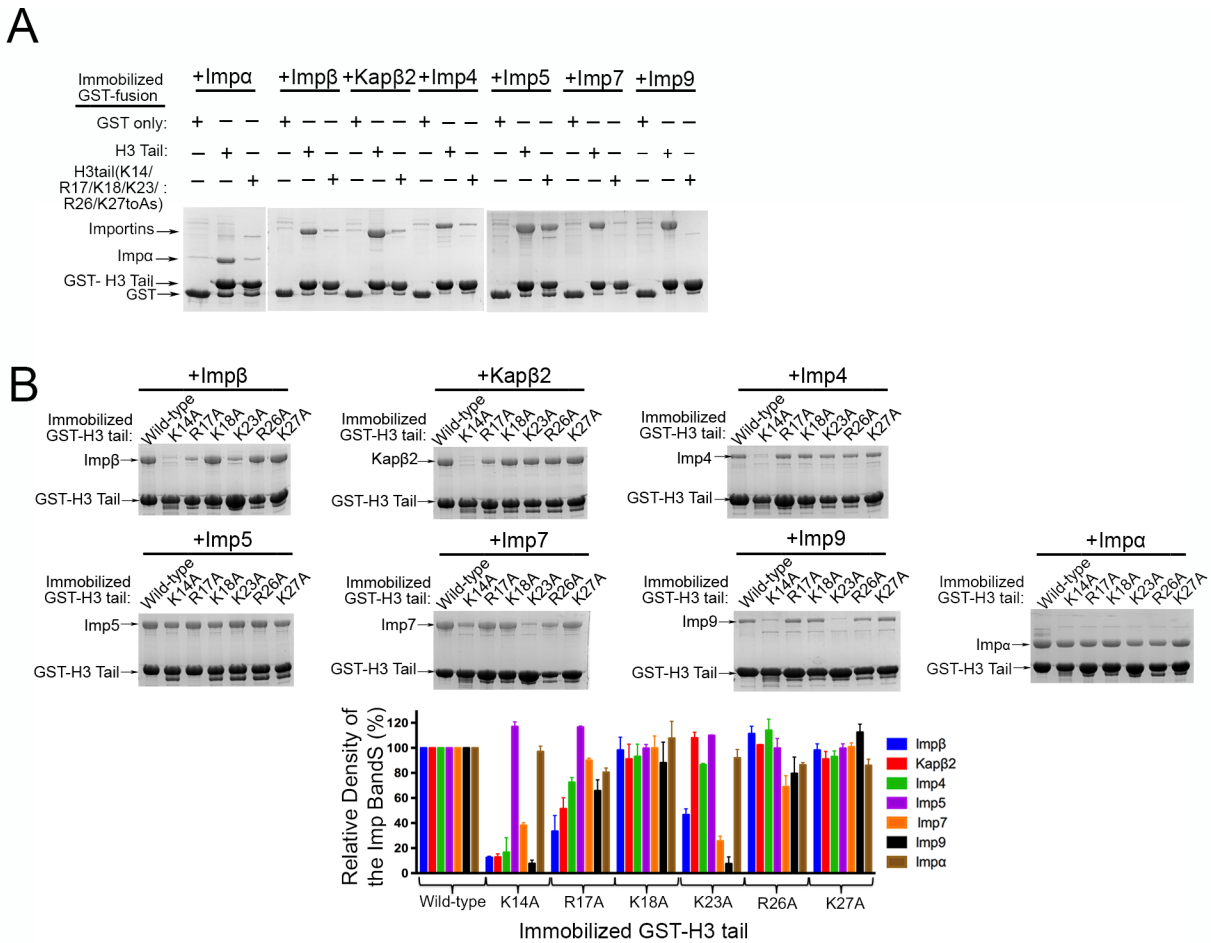


Fig. 3-2. The N-terminal basic segment at residues 11-27 of the H3 tail is important for binding Importins.

A) Pull-down binding assay of immobilized GST-H3 tail proteins (wild-type H3 tail and the H3 tail(K14/R17/K18/K23/R26/K27 to As) mutant) with Imp β , Kap β 2, Imp4, Imp5, Imp7, Imp9 and Imp α (SDS-PAGE/Coomassie staining). **C)** Pull-down binding assay of immobilized GST-H3 tail proteins (wild-type H3 tail and single site alanine mutants for K14, R17, K18, K23, R26 and K27) with Imp β , Kap β 2, Imp4, Imp5, Imp7, Imp9 and Imp α (SDS-PAGE/Coomassie staining). Relative intensities of the gel bands from three separate experiments are plotted in histograms.

Table 3-1. Binding affinities of Imp5 with H3 tails by ITC.

MBP-H3 Tail(1-47):	K_D (nM) determined by ITC
wild-type	57.2±5.0
K14/R17/K18/K23/R26/K27 to As	861.6±37.1
K14A, R17A, K18A	26.1±6.1
K23A, R26A, K27A	119.1±9.3
³⁵ VKKPHR ⁴⁰ to As	198.1±35.2
K14/R17/K18/K23/R26/K27/ ³⁵ VKKPHR ⁴⁰ to As	ND
H3 tail (aa 1-28)	811.5±43.1

A C-terminal IK-NLS-like epitope in the H3 tail

Like Kap β 2, Imp5 also binds the H3 tail with high affinity ($K_D=57$ nM; Table 3-1). However, unlike the binding to other Importins where mutation of all basic side chains between H3 residues 11-27 abolished binding, the MBP-H3 tail(K14/K17/K18/K23/R26/K27 to As) mutant shows substantial binding to Imp5 (Figure 3-2A and Table 3-1), suggesting the presence of additional Imp5-binding epitope(s). Matsuura and colleagues had previously reported that the C-terminal sequence ³⁵VKKPHR⁴⁰ in the H3 tail match the consensus sequence K-V/I-X-K-X₁₋₂-K/H/R for the Kap121- or Imp5-specific IK-NLS motif (Kobayashi and Matsuura 2013) (Figure 3-3A). To determine if the IK-NLS-like motif is indeed important for Imp5 binding, we mutated the ³⁵VKKPHR⁴⁰ segment to alanines and analyzed binding to Imp5 by ITC and pull-down assays (Table 3-1, Figures 3-3B and 3-3C). The MBP-H3 tail(³⁵VKKPHR⁴⁰ to As) mutant showed ~4-fold weaker binding to Imp5 compared to the wild type H3 tail, suggesting that the

IK-NLS motif does indeed contribute to Imp5 binding. Interestingly, energetic contribution of the IK-NLS motif to Imp5 binding is less than that of all basic residues within residues 11-27 as the MBP-H3 tail(K14/K17/K18/K23/R26/K27 to As) mutant shows a 15-fold decrease in Imp5 affinity (Table 3-1 and Figure 3-3B). Mutation of both the basic segment within residues 11-27 and the IK-NLS epitope (MBP-H3 tail(K14/K17/K18/K23/R26/K27/³⁵VKKPHR⁴⁰ to As) mutant) completely abolished Imp5 binding (Table 3-1 and Figure 3-3B). A truncated H3 tail containing only residues 1-28, which lacks the IK-NLS motif and the intervening ²⁹APATGG³⁴, binds Imp5 with lower affinity than the H3 tail(³⁵VKKPHR⁴⁰ to As) mutant ($K_D=811\text{nM}$ for MBP-H3 tail(1-28) vs. $K_D=198\text{nM}$ for MBP-H3 tail(³⁵VKKPHR⁴⁰ to As); Table 3-1 and Figure 3-3B), suggesting either contributions from the intervening ²⁹APATGG³⁴ segment and/or cooperativity between residues 11-27 and the IK-NLS epitope.

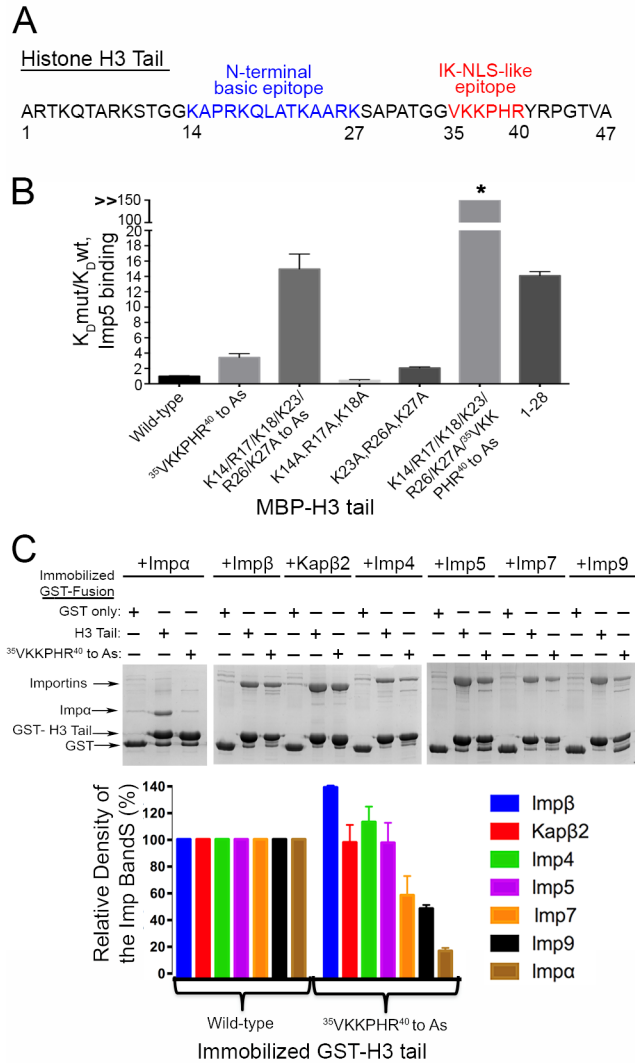


Fig. 3-3. $^{35}\text{VKKPHR}^{40}$ of the H3 tail contributes to binding Imp5, Imp7, Imp9 and Imp α .

A) A proposed Imp5-specific IK-NLS motif in H3 tail. **B)** ITC analysis of Imp5 and H3 tail showing that basic epitope in $^{35}\text{VKKPHR}^{40}$ is also important for Imp5 binding. $K_D \text{ mut}/K_D \text{ wt}$ values for a series of H3 tail mutants (K_D measurements from triplicate ITC experiments) are shown in a histogram. **C)** Pull-down binding assay of immobilized GST-H3 tail proteins (wild-type H3 tail and the H3 tail($^{35}\text{VKKPHR}^{40}$ to As) mutant) with Imp β , Kap β 2, Imp4, Imp5, Imp7, Imp9 and Imp α (SDS-PAGE/Coomassie staining). Relative intensities of the gel bands from experiments performed in triplicate are plotted in histograms.

Truncation of the H3 tail to residues 1-28 had no effect on Kap β 2 binding consistent with structural observations that binding elements for this Importin resides within residues 11-27 of the H3 tail. Pull down binding assays of the H3 tail($^{35}\text{VKKPHR}^{40}$ to As) mutant also showed no

obvious decrease in the binding to Imp β , Kap β 2 and Imp4 (Figure 3-3C). However, binding to Imp α is significantly decreased, and binding to Imp7 and to Imp9 are also both slightly decreased. In summary, Imp β , Kap β 2 and Imp4 appear to mostly bind the basic region in residues 11-27 of H3. Imp5, Imp7, Imp9 and Imp α appear to bind at least two regions of the H3 tail: 1) the basic region from residues 11-27, and 2) the C-terminal IK-NLS epitope.

The Histone H4 tail also contains basic epitope(s) for binding multiple Importins

As shown in Figure 3-1, the same Importins and Imp α that bind the H3 tail also bind the H4 tail. To understand how the individual Importins recognize the H4 tail, we went on to map binding determinants in the H4 tail for each of Imp β , Kap β 2, Imp4, Imp5, Imp7, Imp9 and Imp α . We attempted to crystallize H4 tail bound to Imp β , Kap β 2, Imp4, Imp5, Imp7, and Imp9, respectively, but obtained only crystals of the Kap β 2-H4 tail complex, which did not diffract X-rays. The unfortunate crystallographic results are consistent with the ~10-fold lower affinities of the H4 tail (compared to the H3 tail) for Kap β 2 and for Imp5 ($K_D=871\pm 40$ nM for Kap β 2; $K_D=619\pm 53$ nM for Imp5; compare with K_{DS} for H3 in Table 3-1).

In the absence of structural information for the H4 tail, we focused on biochemically analyzing Importin interactions with H4 tail mutants. The first 20 residues of H4 are rich in glycine and basic residues (Figure 3-4A). When all basic residues in this N-terminal region are mutated to alanines, the resulting GST-H4 tail(K5/K8/K12/K16/R17/R19/K20 to As) mutant is no longer able to bind Imp β , Kap β 2, Imp4, Imp7, Imp9 and Imp α (Figure 3-4B). We generated single site mutants of individual basic residues Lys5, Lys8, Lys12, Lys16, Arg17, Arg19, and Lys20 and immobilized them for pull-down binding assays (Figure 3-4C). The H4 tail(K5A) mutant has little or no effect on binding any of the Importins. Both the H4 tail(K8A) and the H4 tail(K12A) mutants show decreased binding (>50% decreases) to Imp β , Kap β 2, and Imp7

(Figure 3-4C). The H4 tail(K12A) mutant also shows decreased binding to Imp4 and Imp9. The H4 tail(K16A) mutant seems to have an effect only on Kap β 2 binding while the R17A, the R19A and the K20A mutants all have little or no effect on binding any of the Importins. These results suggest that the H4 tail uses basic side chains within residues 5-20 to bind Imp β , Kap β 2, Imp4, Imp7, Imp9, and Imp α .

Binding to Imp5 was not affected by mutations of all the basic residues within the first 20 amino acids of the H4 tail or by mutations of any individual basic side chains within that segment (Figure 3-4B and 4D). No IK-NLS had been reported or predicted within the H4 tail but we aligned the IK-NLS of the H3 tail (³⁵VKKPHR⁴⁰) to the H4 tail sequence and found that residues ²⁹ITKP³² is a close but not perfect match for the IK-NLS consensus sequence of K-V/I-X-K-X₁₋₂-K/H/R (Figure 3-4A). We mutated H4 tail ²⁹ITKP³² to alanines to determine if this IK-NLS-like motif is important for Imp5 binding. The GST-H4 tail(²⁹ITKP³² to As) mutant shows little to no decrease in Imp5 binding (Figure 3-4C). However, when combined with mutations of basic residues between residues 5-20, the mutant GST-H4 tail(K8/K12/K16/R17/R19/K20/²⁹ITKP³² to As) no longer binds Imp5 (Figure 3-4C). As expected from results in Figure 3-4B, the GST-H4 tail(K8/K12/K16/R17/R19/K20/²⁹ITKP³² to As) mutant does not bind Imp β , Kap β 2, Imp4, Imp7 and Imp9.

In summary, the H4 tail contains a basic region from residues 5-20 that is important for binding Imp β , Kap β 2, Imp4, Imp7, Imp9, and Imp α . Within this N-terminal basic region, residue Lys12 seems to be a binding hotspot for most of the Importins. The H4 tail uses at least two basic segments to bind Imp5: 1) a basic epitope within residues 5-20 that is important for Imp β , Kap β 2, Imp4, Imp7 and Imp9 binding, and 2) a C-terminal IK-NLS-like motif (²⁹ITKP³²).

tail(K5/K8/K12/K16/R17/R19/K20 to As) mutant) with Imp β , Kap β 2, Imp4, Imp5, Imp7, Imp9 and Imp α (SDS-PAGE/Coomassie staining).

Acetylation of H3 and H4 tails affects Importin binding

Previous mass spectrometry studies showed that 20-30% of the histone H3 in the cytoplasm is acetylated at Lys14 and/or Lys18 while all cytoplasmic histones H4 is acetylated at Lys5 and Lys12 (Jasencakova et al. 2010). We have shown that the H3 Lys14 is especially important for the H3 tail binding to Imp β , Kap β 2, Imp4, Imp7, and Imp9 (Figure 3-2C). Similarly, we have shown in Figure 3-4C that the H4 Lys12 is important for the H4 tail binding to Imp β , Kap β 2, Imp4 and Imp7, and Imp9. Pull-down binding assays were performed using immobilized synthetic acetylated-H3 and acetylated-H4 tail peptides (biotin-H3 tail(K14Ac), biotin-H3 tail(K18Ac) and biotin-H4 tail(K5Ac/K12Ac)) with Imp β , Kap β 2, Imp4, Imp5, Imp7, Imp9 and Imp α (Figures 3-5A and 3-5B). H3 tail(K14Ac) shows decreased binding to all six Importins and to Imp α by 40-60% compared to wild-type H3 tail (Figure 3-5A). H3 tail(K18Ac) showed ~40% decrease in binding for Imp β but has little effect on binding with the other Importins and with Imp α . H4 tail(K5Ac/K12Ac) showed only mild (20-30%) decreases in binding for all the Importins except Imp β (70% decrease) and Imp5 (55% decrease). These results suggest that acetylation of H3 Lys14 decreases the binding of the H3 tail to Imp β , Kap β 2, Imp4, Imp5, Imp7, Imp9 and Imp α . In contrast, acetylation of the H4 tail on Lys5 and Lys12, which are marks of newly synthesized histones, seems to have little effect on binding to most Importins.

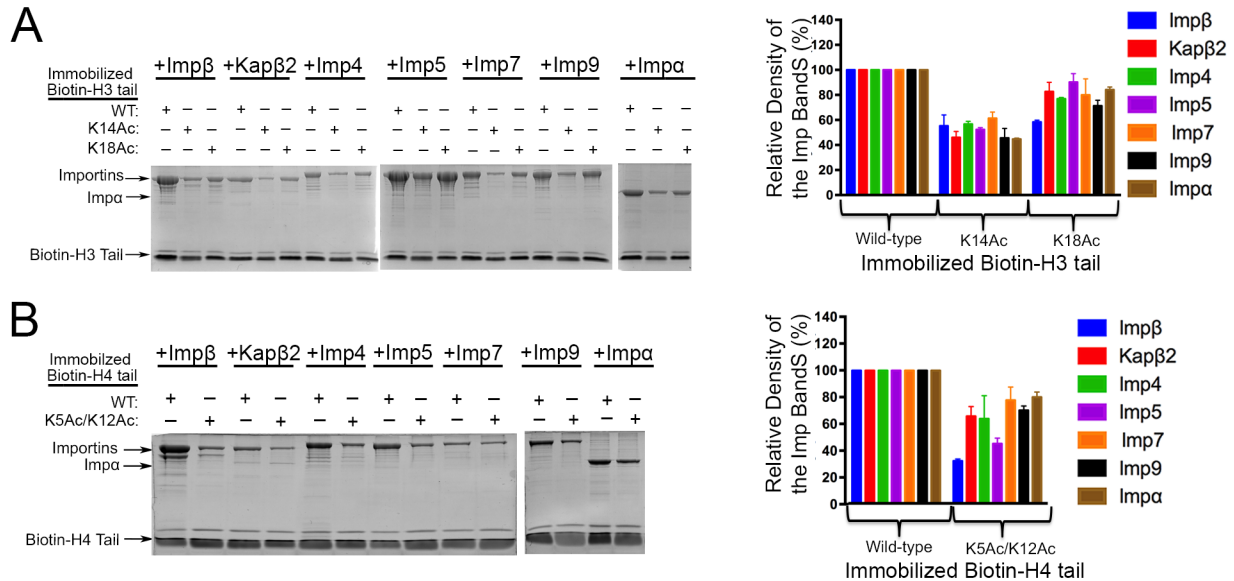


Fig. 3-5. Interactions of acetylation H3 tail and H4 tail peptides with Importins.

Pull-down assays of Imp β , Kap β 2, Imp4, Imp5, Imp7, Imp9 and Imp α with immobilized Biotin-tagged acetylated histone H3 tail and H4 tail peptides (SDS-PAGE/Coomassie staining). Relative intensities of the gel bands from experiments performed in triplicate are plotted in histograms. **A**) Pull-down binding assays of biotin-H3 tails acetylated at either K14 or K18Ac. **B**) Pull-down binding assays of biotin-H4 tail acetylated at both K5 and K12.

Discussion

The N-terminal tails of H3 and H4 can bind multiple Importins to be imported into the nucleus even though neither contains obvious classical-NLSs, PY-NLSs or Importin β -binding (IBB) sequences that are known to bind specifically to Imp α , Kap β 2 and Imp β , respectively (Dingwall et al. 1982; Kalderon et al. 1984a; Lanford and Butel 1984; Lange et al. 2007; Lange et al. 2010; Xu et al. 2010; Chook and Suel 2011; Marfori et al. 2011; Twyffels et al. 2014; Soniat and Chook 2015). Furthermore, little is known about sequence elements that bind Imp4, Imp7 and Imp9 (Chook and Suel 2011). Using biochemical approaches, we have mapped binding elements in both the H3 and H4 tails for Imp β , Kap β 2, Imp4, Imp5, Imp7, Imp9 and Imp α . The information obtained informs on both the organization of NLSs in the histone tails and on the general sequence elements that are recognized by the different Importins.

The N-terminal basic segments of H3 and H4 tails are used to bind all seven Importins

The same H3 segment (residues 11-27) that binds Kap β 2 is also important for binding all the other Importins (Imp β , Imp4, Imp5, Imp7, Imp9 and Imp α). Here, the H3 Lys14 residue is a binding hotspot for Imp β , Kap β 2, Imp4, Imp7, and Imp9. The H3 segment of residues 11-27 seems to contribute most of the binding energy for binding Imp β , Kap β 2 and Imp4 but interactions with Imp5, Imp7, Imp9 and Imp α are slightly more complex as they also involve downstream basic elements in the C-terminal region of the H3 tail. The H4 tail also shows the same trend of using either one or two basic regions to bind multiple Importins. Imp β , Kap β 2, Imp4, Imp7, Imp9 and Imp α bind the basic segment between H4 residues 5-20 where Lys12 seems to be the binding hotspot. Imp5 binds to two segments of the H4 tail: the basic segment of residues 5-20 and a small C-terminal basic element. Proteins that are transported into the nucleus are generally thought to contain specific NLSs that bind one of the ten different Importins (Soniati and Chook 2015). However, two classes of highly abundant proteins, histones and ribosomal proteins, seem to be exceptions as they can bind multiple Importins to be imported them into the nucleus (Jakel and Gorlich 1998; Johnson-Saliba et al. 2000; Baake et al. 2001; Muhlhauser et al. 2001; Mosammamarast et al. 2002b; Greiner et al. 2004; Blackwell et al. 2007; Campos et al. 2010). For example, the ribosomal protein L23A (rpL23A) binds Imp α/β , Kap β 2, Imp5, and Imp7 through its β -like import receptor binding (BIB) sequence within residues 32-74 (Jakel and Gorlich 1998). Although rpL23A contains the only clear example of a BIB sequence, other ribosomal proteins like rpS7 and rpL5 also bind several different Importins and have been proposed to contain BIB-like sequences (Jakel and Gorlich 1998). Jäkel and Görlich suggested that BIB sequences originated from ancestral nuclear import signals that existed before Importins diverged to gain specialized and distinct NLS binding sites (Jakel and

Gorlich 1998). Even though individual Importins have evolved to recognize distinct signals, many of them probably still retain the ability to interact with these ancestral non-specialized BIB sequences. Like the BIB domain of rpL23A, the basic region of H3 tail in residues 11-27 and the basic region of H4 tail between residues 5-20 can also interact with multiple Importins. Furthermore, alignment of the rpL23A BIB (residues 32-74) with the H3 and H4 tails shows that residues ⁵⁹KYPRKSAPRRNK⁷⁰ of rpL23A shares sequence similarity with residues of ¹⁴KAPRKQLATKAAR²⁶ and ⁸KGLGKGGAKRHR²⁰ in H3 and H4 tails, respectively.

NLSs in the histone tails for different Importins

Like Kap β 2, Imp β and Imp4 seem to bind solely to the N-terminal basic segments of the H3 tail and the N4 tail. Imp β is known to bind directly to functionally diverse cargos that contain NLSs that have very different lengths, sequences, and structural elements (Cingolani et al. 2002; Xu et al. 2010; Chook and Suel 2011; Lott and Cingolani 2011; Soniat and Chook 2015). We showed that electrostatic interactions with the N-terminal basic regions of the H3 tail (residues 11-27) and the H4 tail (residues 8-20) are likely important for Imp β binding. Similarly, electrostatic interactions have been shown to be important for Imp β binding to the helical IBB (α IBB) of Imp α and to the extended NLS from parathyroid hormone-related protein (PTHrP) even though the two NLSs bind different sites on Imp β (Cingolani et al. 1999; Lam et al. 1999). In the absence of structural data for the histone tails binding to Imp β , we cannot predict their conformations when bound to the Importin nor the location of their binding sites on Imp β . There is no structural information available at this time for how Imp4 binds its cargoes/NLSs. However, our results showing that Imp4 likely binds solely to the N-terminal basic regions of the H3 and H4 tail suggest that Imp4 NLSs may be more compact than the sprawling sequences in

the H3 and H4 tails that bind Imp5, Imp7, Imp9 and Imp α . Structural analysis of Imp4 bound to its cargoes is needed to reveal requirements for NLS recognition in that system.

Interactions of the H3 tail with Imp5, Imp7, Imp9 and Imp α involve two segments of the H3 tail – the basic region between residues 11-27 and a C-terminal IK-NLS motif at ³⁵VKKPHR⁴⁰. Similarly, the H4 tail also uses two analogous elements to interact with Imp5: the basic segment of H4 residues 5-20 and a C-terminal IK-NLS-like motif ²⁹ITKP³². Bipartite interaction with Imp α is not unexpected as the import adaptor is known to bind bipartite classical-NLSs (Marfori et al. 2011). The signal in the H3 tail that binds Imp α , ¹¹TGGKAPRKQLATKAARK²⁷-----³⁵VKKPHR⁴⁰ (potential bipartite classical-NLS consensus residues are underlined), differ from the bipartite classical-NLS consensus sequence of (K/R)(K/R)X₁₀₋₁₂(K/R)3/5) only because the linker in H3 is either too short or too long. However, bipartite classical-NLSs with artificial linkers as short as eight residues and linkers up to 40 residues have been shown to bind Imp α and be imported (Dingwall et al. 1982; McLane et al. 2008; Giesecke and Stewart 2010; Lange et al. 2010; Marfori et al. 2011). The range of linker lengths in the consensus sequence for bipartite classical-NLS is probably too restrictive, and the H3 tail does indeed contain a classical bipartite-NLS. The C-terminal basic epitope of this bipartite classical-NLS in the H3 tail overlaps with the IK-NLS epitope (³⁵VKKPHR⁴⁰) that is used to bind Imp5. Structural analysis of Kap121 (yeast homolog of Imp5) suggested that the compact IK-NLS is the most important and prevalent binding element in Kap121 and Imp5 cargoes (Kobayashi and Matsuura 2013). Interestingly, our results suggest that the IK-NLS motifs of H3 and H4 are only a portion of the NLSs for Imp5. Energetic contribution of the IK-NLS epitope in H3 to Imp5 binding is relatively minor compared to that of the N-terminal basic region of H3. Although IK-NLSs in Kap121 cargoes Pho4p, Spo12p and binding partner Nup53p

seem to be specific for Kap121 (Kobayashi and Matsuura 2013), the IK-NLS motifs in H3 and H4 contribute the C-terminal part of bipartite classical NLSs to also bind Imp α . Finally, although Imp7 and Imp9 have not yet been structurally characterized, our results suggest that both can bind long sprawling and possibly extended NLSs that use multiple basic epitopes for binding the Importins.

Importin recognition beyond the histone tails

We have focused on studies of the H3 and H4 tails because they were reported to be necessary and sufficient for nuclear import of the histones (Johnson-Saliba et al. 2000; Baake et al. 2001; Muhlhauser et al. 2001; Mosammamarast et al. 2002b; Greiner et al. 2004; Blackwell et al. 2007; Campos et al. 2010). However, transport of newly translated histones H3 and H4 into the cell nucleus is a multi-step process that is thought to involve multiple protein players in addition to the Importins (Verreault et al. 1998; Alekseev et al. 2005; Murzina et al. 2008; Hartl and Hayer-Hartl 2009; Campos et al. 2010; Jasencakova et al. 2010; Ejlassi-Lassalette et al. 2011; Li et al. 2014) (Alekseev et al. 2005; Hartl and Hayer-Hartl 2009; Campos et al. 2010). In addition, H3 and H4 are likely never present in the cell as folded monomers. They are thought to form H3/H4 dimers, bind to the histone chaperone Asf1 and then bind Importins to cross the nuclear pore complex (Baake et al. 2001; Muhlhauser et al. 2001; Mosammamarast et al. 2002b; Greiner et al. 2004; English et al. 2005; Mousson et al. 2005; English et al. 2006; Blackwell et al. 2007; Natsume et al. 2007; Alvarez et al. 2011; Zhang et al. 2013). Asf1 binds the histone folds of the H3/H4 dimer, leaving the tails free for Importin-binding (English et al. 2006; Natsume et al. 2007). However, information on H3/H4-Asf1-Importin complexes is not available and it is unclear if one or both histone tails in the Asf1-H3/H4 complex engage Importin. We have shown here that the Kap β 2-H3 tail and with Imp5-H3 tail interactions are both high affinity interactions

with $K_{DS} < 100$ nM. Qualitative comparisons of the other Importins with H3 tail suggest that the other Importins (Imp β , Imp4, Imp7, Imp9, and Imp α) likely bind more weakly. Kap β 2-H4 tail and Imp5-H4 tail interactions are significantly weaker with K_{DS} in the 600-800 nM range. If the Asf1-H3/H4 complex engages only one Importin molecule, and the trend that H3 tail binds more tightly than the H4 tail holds for all Importins, then the H3 tail is likely to present the primary NLSs that are recognized for nuclear import.

Although many different Importins can bind and import H3 and H4 tails, previous reports have shown that Imp4 and its yeast homolog Kap123 are consistently the most abundant Importins that co-purify with H3 and H4 in immunoprecipitation experiments, suggesting that Imp4 is the major nuclear importer for the histone pair (Muhlhauser et al. 2001; Campos et al. 2010; Jasencakova et al. 2010; Alvarez et al. 2011). Our results of histone tail-Importin interactions show no specificity of Imp4 over the other Importins for the H3 or H4 tail. Imp4 is in fact one of the Importins that bind more weakly to the both histone tails. The specificity for Imp4 in cells must therefore be present outside of the histone tails, perhaps in the histone folds or in the H3/H4-Asf1 complex. It is also possible that the high concentrations of Imp4 in cells provide an advantage for Imp4-mediated histone import. Previous studies showed that Kap123, yeast homolog of Imp4, is the most abundant Importin in budding yeast (~ 5 μ M; five-fold higher than Kap121) (Timney et al. 2006). Kap123 also gave the highest nuclear import rate (5-12 fold more rapid than other Importins) and its abundance was thought to contribute significantly to its nuclear import efficiency (Timney et al. 2006).

Acetylation of H3 Lys14 impairs Importin binding

Finally, the basic segments in H3 and H4 tails that bind Importins contain several lysine residues such as the H3 Lys14, H3 Lys18, the H4 Lys5 and H4 Lys12, which have all been

shown to be acetylated to different extents in the cytoplasm (Verreault et al. 1998; Murzina et al. 2008; Campos et al. 2010; Jasencakova et al. 2010; Ejlassi-Lassalette et al. 2011; Li et al. 2014). So far, the role of acetylation in nuclear import is controversial as acetylation has been reported to promote nuclear import of the histones and acetylation has also been reported to inhibit nuclear import of the histones (Muhlhausser et al. 2001; Blackwell et al. 2007; Campos et al. 2010; Jasencakova et al. 2010). It is clear from our data that the H3 Lys14 is the binding hotspot for Imp β , Kap β 2, Imp4, Imp7, and Imp9 and consistently, we find that acetylation of the H3 tail at Lys14 decreased binding to Imp β , Kap β 2, Imp4, Imp5, Imp7, Imp9 and Imp α . These results suggest that acetylation of the H3 Lys14 can compromise Importin-histone interactions, and thus may be used to control nuclear import of the small pool of histones with acetylated H3 tail. Alternatively, Importin-H3 tail interactions could potentially sequester the H3 tails and prevent its acetylation in the cytoplasm.

Unlike H3 where only a small fraction of the histone is acetylated in the cytoplasm, H4 has been shown to be persistently acetylated prior to deposition in the nucleus. We find that acetylation of the H4 tail at Lys5 and Lys12 has little effect on binding to most Importins except Imp β and Imp5. However, the unacetylated H4 tail binds Importins weakly, likely with dissociation constants larger than 600 nM, and may thus contribute little towards nuclear import in the H3/H4 dimer. It is currently not known and difficult to predict how acetylation of the H3/H4 dimer or the H3/H4-Asf1 complex may affect their interactions with the Importins. Studies of Importin-histone complexes beyond N-terminal tails of the histones will be important to resolve current controversies regarding histone acetylation and nuclear import.

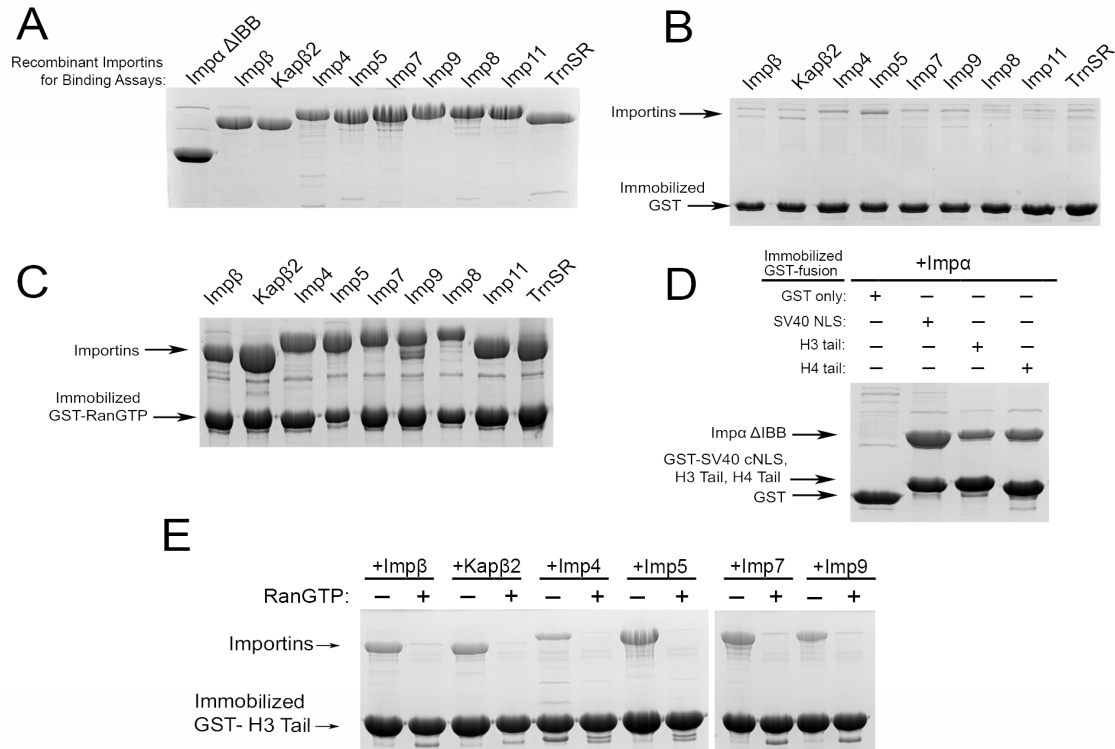


Fig. 3-6. Activity Controls for all Importins used and RanGTP Dissociation **A)** Recombinant Importins used for binding assays. **B)** Binding assays of Importins with immobilized GST protein. **C)** Binding assays of Importins with immobilized GST-RanGTP. **D)** Binding assays of Impα with immobilized GST-SV40 classical NLS, GST-H3 tail, and GST-H4 tail. **E)** Binding assays of immobilized GST-H3 tail with Impα, Impβ, Kapβ2, Imp4, Imp5, Imp7, and Imp9 in the presence and absence of RanGTP. All binding assays visualized by SDS-PAGE and Coomassie staining.

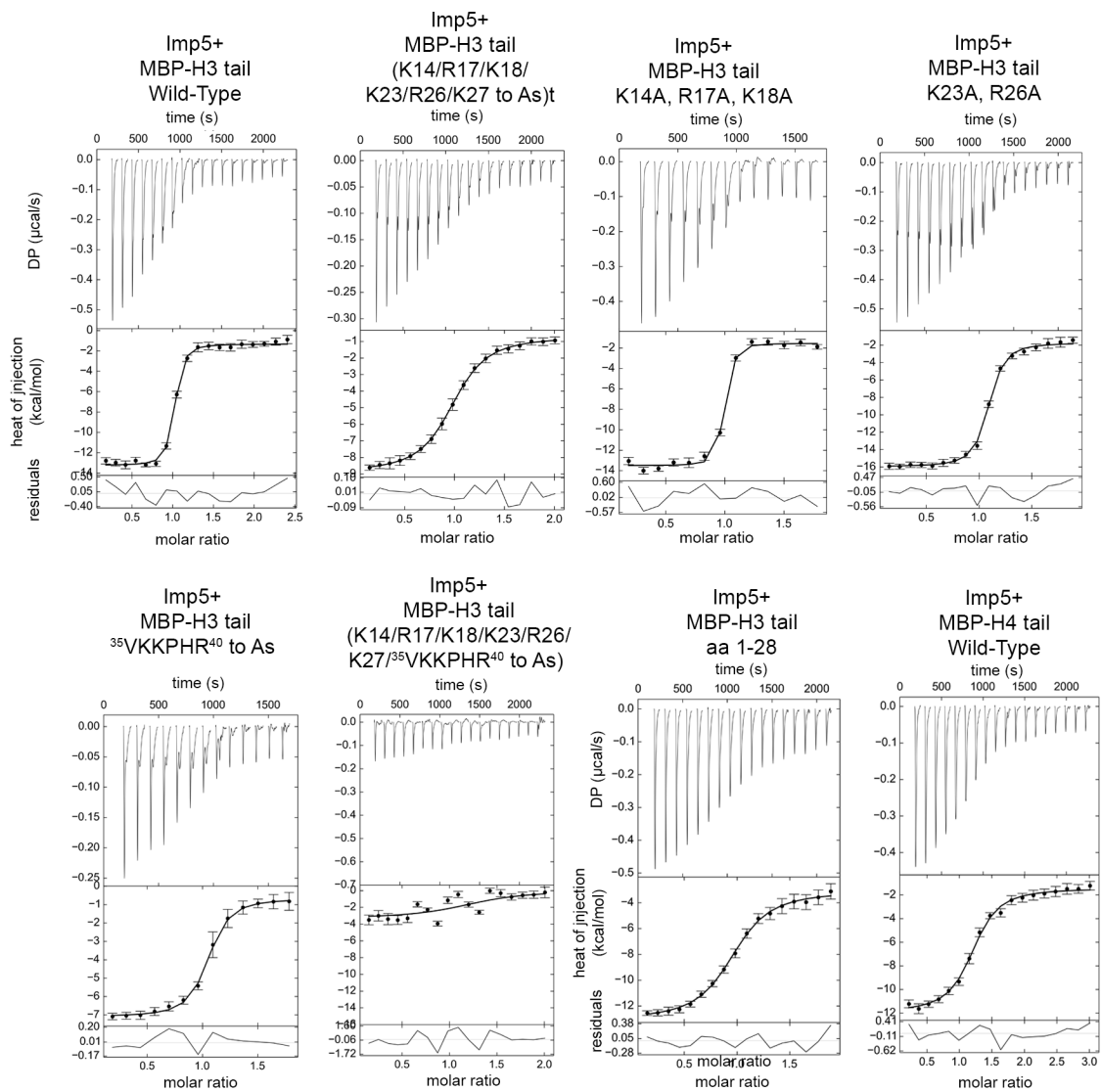


Fig. 3-7. Representative ITC measurements of MBP-H3 tail proteins binding to Imp5. After dialyzed against the same buffer, 200-400 μ M MBP-H3 and H4 tail proteins were titrated into a sample cell containing 20–40 μ M recombinant Imp5. ITC experiments were performed at 20°C with 19 rounds of 4- μ l injections. Data were plotted and analyzed using NITPIC and Sedphat. Data was visualized by GUSI.

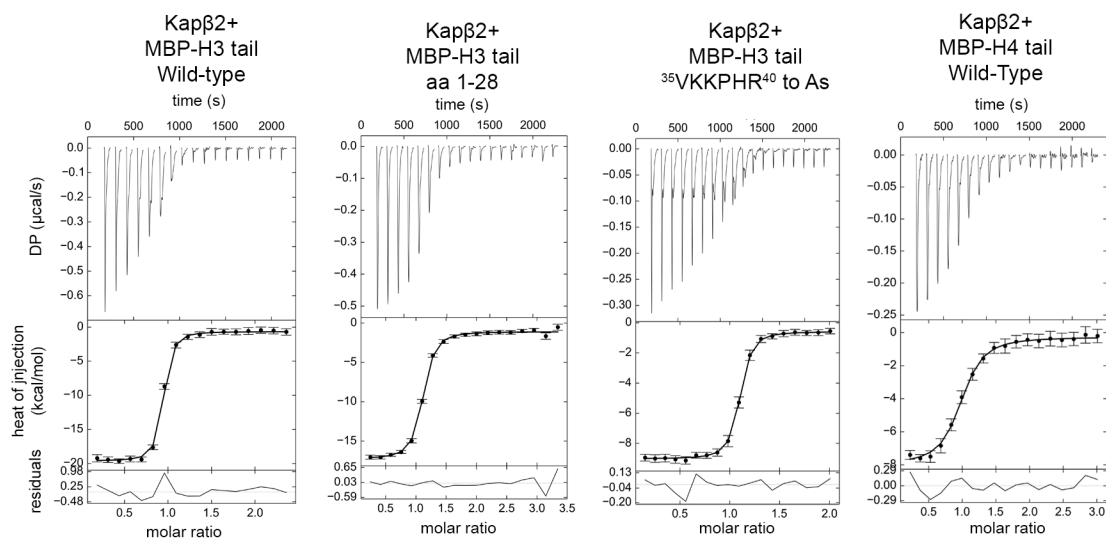


Fig. 3-8. Representative ITC measurements of MBP-H3 tail proteins binding to Kap β 2. After dialyzed against the same buffer, 200-400 μ M MBP- H3 and H4 tail proteins were titrated into a sample cell containing 20–40 μ M recombinant Kap β 2. ITC experiments were performed at 20°C with 19 rounds of 4- μ l injections. Data were plotted and analyzed using NITPIC and Sedphat. Data was visualized by GUSI.

CHAPTER 4

BIOCHEMICAL AND BIOPHYSICAL ANALYSIS OF THE IMPORTIN-ASF1-H3/H4 COMPLEX

Abstract

Multiple Importins were previously shown to transport newly synthesized core histones into the nucleus. Furthermore, I showed in the previous chapter that seven different Importins can bind the same basic epitopes in histone H3 and H4 tails. However, nothing is known about how the different Importins recognize the full-length H3/H4 dimer. Using biochemical and biophysical analysis, I show that the same seven Importins that binds H3 and H4 tails can bind the Asf1-H3/H4 complex and that RanGTP can dissociate the histone-histone-chaperone complex from each Importin. Previously, I found that the binding affinity trend (from high to low affinity) for N-terminal H3 tail is $\text{Kap}\beta 2, \text{Imp}5 > \text{Imp}\beta, \text{Imp}9, \text{Imp}\alpha > \text{Imp}4, \text{Imp}7$. The H4 tail binds Importins at least 10-fold weaker than the H3 tail, and the binding trend for Importins binding to the H4 tail is slightly different with $\text{Imp}5 > \text{Imp}9, \text{Imp}\alpha > \text{Imp}\beta, \text{Kap}\beta 2, \text{Imp}4, \text{Imp}7$. However, the binding trend for Asf1-H3/H4 is quite different, with: $\text{Imp}4, \text{Imp}5, \text{Imp}9 > \text{Imp}\beta, \text{Imp}7 > \text{Imp}\alpha, \text{Kap}\beta 2$. These results suggest that additional interactions with the histone fold domains

may be responsible for changing the Importin-full length histones specificity. I also show using small-angle X-ray analysis (SAXS) to show though there are two NLS binding sites on each H3/H4 dimer, only one Imp4 molecule is bound.

Introduction

Multiple Importins were previously shown to bind and mediate nuclear import of histones H3 and H4 (Baake, Bauerle, Doenecke, & Albig, 2001; Blackwell, Wilkinson, Mosammaparast, & Pemberton, 2007; Campos et al., 2010; Greiner, Caesar, & Schlenstedt, 2004; Johnson-Saliba, Siddon, Clarkson, Tremethick, & Jans, 2000; Mosammaparast, Guo, Shabanowitz, Hunt, & Pemberton, 2002; Muhlhausser, Muller, Otto, & Kutay, 2001). Histones H3 and H4 each consists of an N-terminal tail region followed by a globular histone fold domain, which is made up of a three helices connected by two loops (Luger, Mader, Richmond, Sargent, & Richmond, 1997; White, Suto, & Luger, 2001). We previously showed the N-terminal tails of H3 and H4 bind seven Importins (Imp α , Imp β , Kap β 2, Imp4, Imp5, Imp7, and Imp9) and binding for each Importin is through one or two basic regions within each tail. However, co-immunoprecipitation assays had shown that H3 and H4 are actually imported as a dimer in complex with the histone chaperone, Asf1 (Alvarez et al., 2011; Baake et al., 2001; Blackwell et al., 2007; English, Adkins, Carson, Churchill, & Tyler, 2006; Greiner et al., 2004; Mosammaparast et al., 2002; Mousson et al., 2005; Muhlhausser et al., 2001; Natsume et al., 2007; Zhang et al., 2013). It is not known if the Importins make additional interactions with the histone fold domain and/or with Asf1.

If H3 and H4 are imported as dimers and both have NLSs in their N-terminal tails, a single H3/H4 dimer should bind two Importins. It is not known at this time how many Importins

interact with each H3/H4 dimer. Additionally, since my previous studies looked just at Importin binding to the histone tails alone, it is not known if the Importin-histone tail interactions are used to bind the full length H3/H4 dimer. Lastly, previous studies of Kap114p (yeast homolog of Imp9) with H2A/H2B dimer showed that the H2A/H2B dimer is not dissociated from Kap114p by RanGTP (Mosammaparast et al., 2001). It is not known if the H3/H4 dimer can be dissociated from the Importins by RanGTP.

Materials and Method

Purification and assembly of Asf1-H3/H4 complexes: Recombinant *Xenopus* H3 and H4 were expressed in *E. coli* BL21 (DE3) pLysS as a His fusion protein using the pET3a vector. Expressed H3 and H4 were purified from inclusion bodies and refolded to obtain histone H3-H4 tetramers as previously described (Luger, Rechsteiner, & Richmond, 1999). Asf1 (aa 1-169 and full-length) were expressed in *E. coli* BL21 (DE3) as a GST fusion protein using the pGEX-Tev vector. Purification of Asf1 constructs were carried out using affinity chromatography and gel-filtration chromatography. GST-Asf1-H3/H4 complexes were assembled by mixing purified GST-Asf1 and H3/H4 in a 1:5 molar ratio followed by purification of the complex using gel-filtration chromatography as previously described (Natsume et al., 2007).

Purification and assembly of Imp4-Asf1-H3/H4 Complex: Imp4 was expressed in *E. coli* BL21 (DE3) as a GST fusion protein using the pGEX-Tev vector. Purification was carried out with affinity chromatography, proteolytic removal of GST followed by ion-exchange, and gel-filtration chromatography as previously described (Lee et al., 2006). Imp4-Asf1-H3/H4 complex was assembled by mixing purified Imp4 and immobilized GST-Asf1-H3/H4 in a 1:5 molar ratio followed by purification of the complex using gel-filtration chromatography. Purified Imp4-Asf1-H3/H4 Complex obtained was used for crystallization trials.

X-ray crystallography of the Imp4-Asf1-H3/H4 Complex: Initial crystallization trials of Imp4-Asf1-H3/H4 complexes were performed using purchased crystallization kits. Adjustment of pH, precipitant/salt/protein concentration, temperature, additives, and cryoprotection conditions are being used to optimize the crystals to get diffracting crystals. All X-ray data will be collected at the Advanced Photon Source (APS) at Argonne National Laboratory in Argonne, IL. Native crystallographic data will be collected and the available coordinates of Asf1-H3/H4 structures will be used as search models to solve the structures by molecular replacement (English et al., 2006; Natsume et al., 2007). However, if molecular replacement does not work, selenomethionine labeled Imp4 will be expressed and purified. Following histone complex assembly and crystallization, selenium anomalous data will be collected to solve H3/H4 complex. Crystallographic refinement and manual model building will be performed using PHENIX and COOT, respectively.

Small Angle X-ray Scattering (SAXS) Analysis

SAXS profiles of Imp4, H3-H4 tetramer, Asf1 (residues 1-169), and Imp4-Asf1-H3/H4 were obtained at concentrations of 0.5, 1.0, 1.5, 2.0, 5.0, and 10 mg/ml in 20 mM Tris pH 7.5, 150 mM NaCl, 5% Glycerol, 5 mM β -mercaptoethanol at 10°C, and twenty 1 s exposures were made for each protein sample. The buffer SAXS profile was obtained in the same manner and subtracted from a protein profile and molecular weights were calculated using PRIMUS.

Pull-down binding assays

Pull-down binding assays were performed by incubating immobilized GST-Asf1 alone or GST-Asf1-H3/H4 proteins with purified Importins in TB buffer for 30 min at 4°C, followed by extensive washing with the same buffer. Approximately 10-20 μ g of immobilized GST-H3 and H4 tail proteins were incubated with ~60 μ g of purified Importins.

For RanGTP dissociations assays, ~40 µg of purified RanGTP was incubated with immobilized GST- Asf1-H3/H4 bound to Importins, followed by extensive washing. Activity of Impβ, Kapβ2, Imp4, Imp5, Imp7, and Imp9 were verified by their binding to RanGTP and activity of Impα was verified by binding to the classical-NLS of the SV40 T antigen. Bound proteins were visualized using SDS-PAGE and Coomassie blue staining. Gels were subject to densitometry analysis using ImageJ. The density of the Importin band in each gel lane was divided by the density of the GST-histone tail band in the same lane. The ratios were then normalized to the ratio of the Importin band over the wild-type GST-H3 and H4 tail wild-type bands. Relative band intensities of experiments performed in triplicate are plotted with standard errors in histograms generated with GraphPad Prism.

Results

Purification and analysis of Imp4-H3/H4 complex

I purified the Imp4-H3/H4 complex to better understand how Imp4 recognizes the full-length H3/H4 dimer. I first purified H3/H4 from inclusion bodies (as previously described), which elutes as a heterotetramer. The H3/H4 tetramer was mixed with Imp4 in a 1:5 Imp4:histone ratio and purified by size-exclusion chromatography (SEC) as shown in Figure 4-1 (Luger, Rechsteiner, & Richmond, 1999). Whether Imp4 binds a dimer or tetramer of H3/H4 cannot be determined from SEC. To determine the molecular weight and overall shape, I sent the purified Imp4-H3/H4 complex to our collaborator Dr. Seung Joong Kim (postdoc, Andrej Sali Lab at UCSF) for SAXS data collection at the Advanced Light Source (ALS). When compared to Imp4 alone the overall shape of the Imp4-H3/H4 complex was elongated and extra density was seen in the center of the complex suggesting density for H3/H4 (Figure 4-2A and 4-2C). The molecular weight for this complex was determined to be 170.5 kDa, which is 25 kDa larger from

the calculated molecular weight for one Imp4 bound to a H3/H4 tetramer (Table 4-1). Since molecular weight of a H3/H4 tetramer is 52.9 kDa, a molecular weight of 170.5 kDa for Imp4-H3/H4 may also account for a complex of one Imp4 bound to one H3/H4 dimer. Further analysis is needed to verify molecular weight info from SAXS analysis.

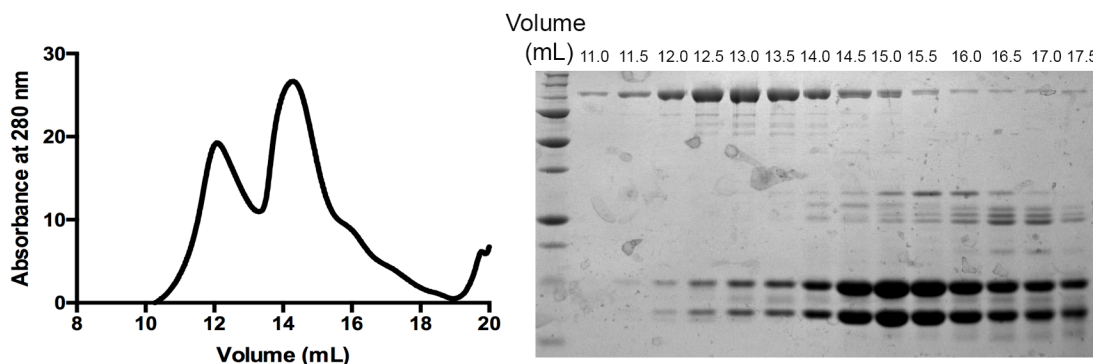


Figure 4-1 Size exclusion chromatography of Imp4-H3/H4 complex. SDS-page/Coomassie-stained gel.

Only one Imp4 molecule binds the Asf1-H3/H4 complex

The H3/H4 dimer has two N-terminal tails that each contain an NLS that can bind Importins. However, whether one or two Importins bind a H3/H4 dimer is not known. I purified Imp4, Asf1, H3/H4 heterotetramer, Imp4-H3 tail complex, Imp4-H3/H4 complex, and the Imp4-Asf1-H3/H4 complex, for SAXS analysis by Seung Joong Kim (postdoc, Andrej Sali Lab at UCSF). From the SAXS data we were able to determine an *ab initio* envelope of the proteins and also determine their molecular weights (Table 4-1). Experimental molecular weights of Asf1 alone, H3/H4 tetramers alone and Imp4 alone all agreed well to the calculated molecular weights showing the accuracy of SAXS in determining molecular weights (Table 4-1). We next calculated the molecular envelopes and molecular weights for Imp4 alone, the Imp4-H3 tail complex, Imp4-H3/H4, and the Imp4-Asf1-H3/H4 complex (Table 4-1; Figure 4-2A-D). We saw that the overall shape for Imp4-H3 tail did not change much from that of Imp4 alone and the

experimental molecular weight of Imp4-H3 tail from SAXS is in good agreement with its calculated molecular weight (-19.1 kDa). (Table-1; Figure 4-2B). The overall shape for Imp4-Asf1-H3/H4 is slightly elongated and extra density was seen in the center of the complex when compared to density for Imp4 alone, suggesting that the extra density is Asf1-H3/H4 (Figure 4-2D). The experimental molecular weight for Imp4-Asf1-H3/H4 complex is 184.2 kDa, which is within 20 kDa of the calculated molecular weight if only one Imp4 is bound to the complex (Table 4-1). These results suggest that even though there are potentially two NLSs within each H3/H4 dimer (one on the H3 tail and the other on the H4 tail), only one Imp4 molecule is bound to each Asf1-H3/H4 complex.

We calculated Kratky plots for each of the Imp4 complexes (Figure 4-2E). The Kratky plot is informative to check globularity and flexibility of the protein samples. The Kratky plot of a well-folded globular protein will exhibit a bell-shape peak at low q (scattering vector) and converges to the x-axis at high q . However, the Kratky plot will not converge to the x-axis if the protein has a pronounced disorder/flexibility. The Kratky plots that we obtained for Imp4 alone, the Imp4-H3/H4 complex, and the Imp4-Asf1-H3/H4 complex suggest compact assemblies but the Kratky plot for the Imp4-H3 tail suggests that complex is much more flexible.

Table 4-1 Molecular Weight Determination using SAXS of Imp4-Asf1-H3/H4 Complex

Sample	Calculated MW (kDa)	Experimental MW (kDa)	Difference (kDa)
Importin-4	118.7	136.6	+17.9
H3-H4 Tetramer	53.9	52.9	-1.0
Asf1	19.1	18.6	-0.5

Imp4-H3 tail	123.7	104.6	-19.1
Imp4-H3/H4	145.4	170.5	+25.1
Imp4-Asf1-H3/H4	164.6	184.2	+19.6

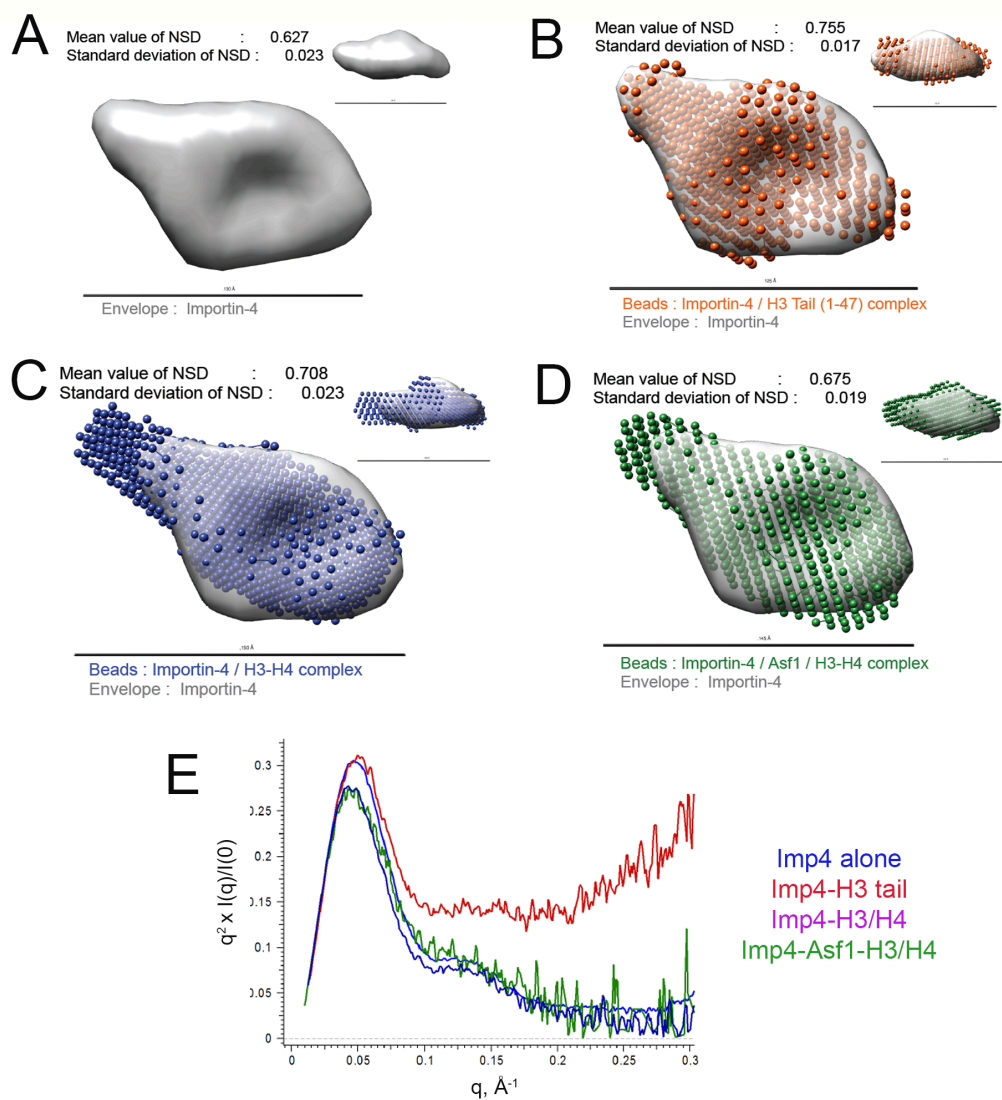


Figure 4-2 SAXS Analysis of Imp4-Histone Complexes. A) ab initio molecular envelope of Imp4. B-D) Comparison of Imp4 (envelope) with B) Imp4-H3 tail complex C) Imp4-H3/H4 complex D) Imp4-Asf1-H3/H4 complex (shown in beads). E) Kratky plots of Imp4, Imp4-H3 tail complex, Imp4-H3/H4 complex, and Imp4-Asf1-H3/H4 complex.

Importin binding trend with Asf1-H3/H4 complex is different from the trend with histone tails

To study interactions between Importins and the Asf1-H3/H4 complex, we performed pull-down binding assays using immobilized GST-Asf1-H3/H4 with the six different recombinant human Importins - Imp β , Kap β 2, Imp4, Imp5, Imp7, Imp9 and the Importin adaptor Imp α (Figure 4-3). Binding was observed using Coomassie Blue staining, and we saw that the binding trend is different from what we saw with the N-terminal H3 and H4 tails alone (Fig 3-1C). Previously, the binding trend for N-terminal tails went (from high to low affinity): Kap β 2, Imp5 > Imp β , Imp9, Imp α > Imp4, Imp7. However the binding trend for Asf1-H3/H4 has changed to Imp4, Imp5, Imp9 > Imp β , Imp7 > Imp α , Kap β 2 (Figure 4-3C). These results suggest that the histone fold domain and/or the histone chaperone Asf1 are very likely also important for Importin-histone binding. Pull-down assays showed no binding between Importins to immobilized GST-Asf1 alone (Figure 4-3B).

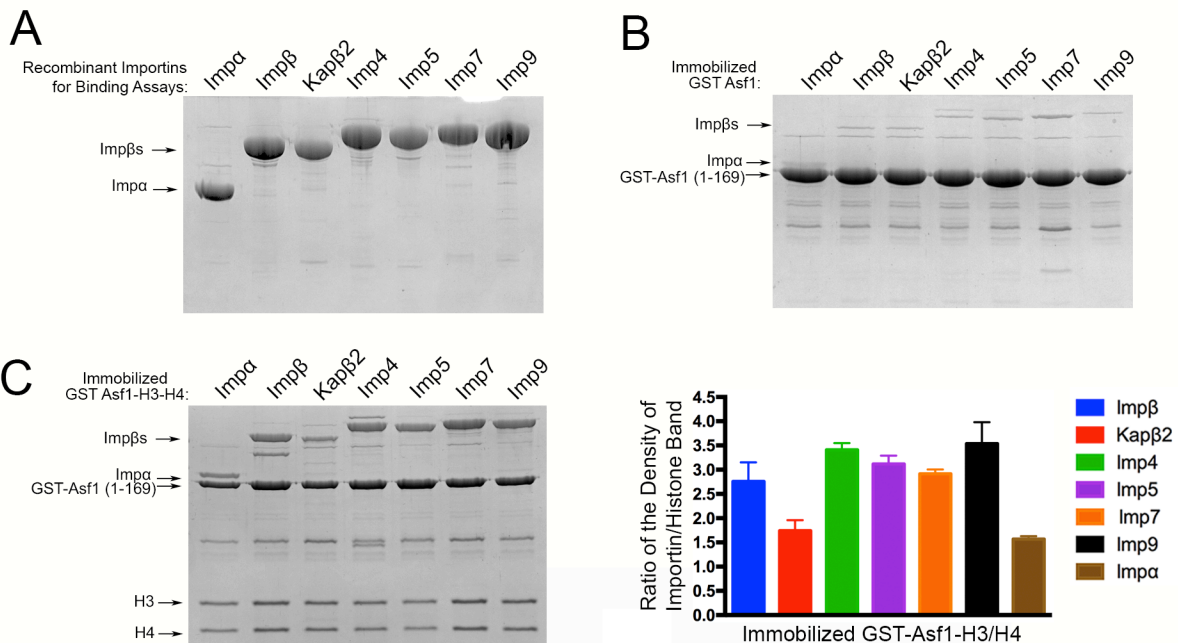


Figure 4-3 Seven Importins can bind Asf1-H3/H4 complex **A)** Recombinant Importins used for binding assays. **B-C)** Pull-down binding assays of immobilized **B)** GST-Asf1 (aa 1-169) **C)** GST-Asf1 (aa 1-169)-H3/H4. Relative band intensities from three separate experiments are plotted in histograms.

Asf1-H3/H4 complex is dissociated from Importins by RanGTP

Previous studies showed that Kap114-H2A/H2B complex is insensitive to RanGTP suggesting that other factors may be needed to release the H2A/H2B dimer from Kap114 (Mosammaparast et al., 2001). However it was not known if RanGTP can dissociate the H3/H4 dimer from Importins. I performed RanGTP dissociation assays by adding RanGTP to immobilized GST-Asf1-H3/H4 bound to each Importin (Fig 4-4). Unlike Kap114-H2A/H2B complex, RanGTP easily dissociates Asf1-H3/H4 from each of the seven Importins.

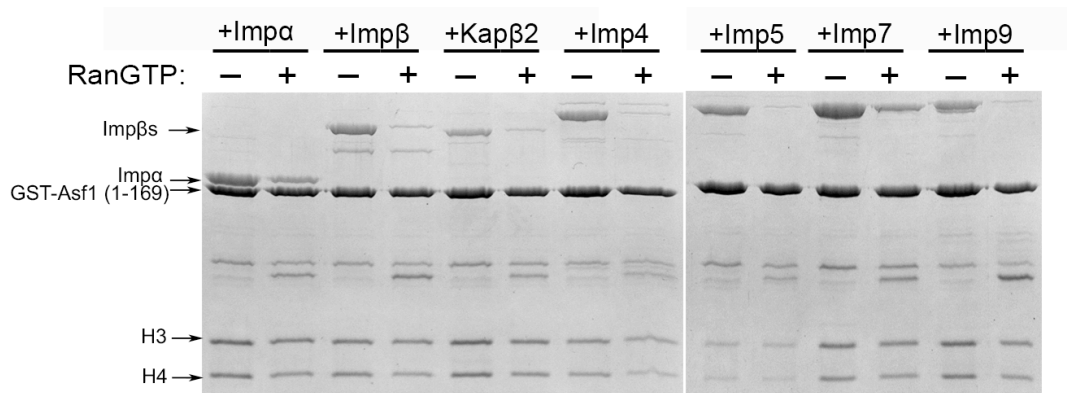


Figure 4-4 Binding assays of immobilized GST-Asf1-H3/H4 with Imp α , Imp β , Kap β 2, Imp4, Imp5, Imp7, and Imp9 in the presence and absence of RanGTP. All binding assays visualized by SDS-PAGE and Coomassie staining.

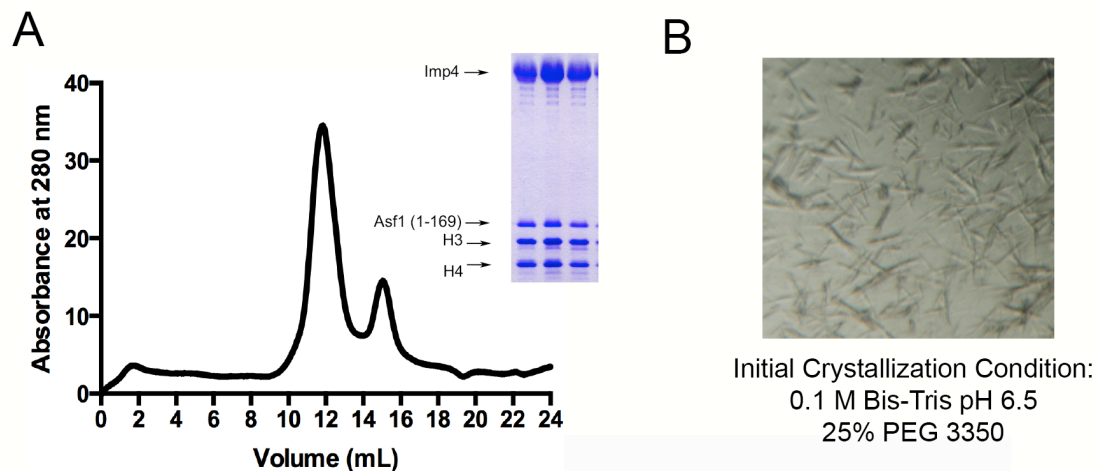


Figure 4-5 **A)** Size exclusion chromatography of Imp4-Asf1-H3/H4 complex. SDS-page/Coomassie-stained gel showing 10 μ L samples of volumes at 11, 12, 13 mL. **B)** Initial crystals of Imp4-Asf1-H3/H4 complex

Complex Formation and Crystallization of Imp4-Asf1-H3/H4 complex

To better understand how and Importin recognizes histones H3 and H4, I attempted to determine the structure of Imp4 in complex with Asf1-H3/H4. I purified the Imp4-Asf1-H3/H4 by first purifying the histones from inclusion bodies (previously described) and then mixing the H3/H4 with GST-Asf1 and purifying the complex by size-exclusion chromatography (Luger, Rechsteiner, & Richmond, 1999). Imp4 was then mixed with the purified GST-Asf1-H3/H4 in a 1:5 Imp4:histone ratio followed by removal of GST tag and size-exclusion chromatography (Fig 4-5A). The complex was concentrated to 10 mg/mL and crystal trials were performed with pre-made crystallization screens. I found an initial crystal hit with well solution containing 0.1 Bis-Tris pH 6.5/25% PEG 3350 (Fig 4-5B). More work is needed to optimize crystals to determine structure of Imp4-Asf1-H3/H4 complex.

Discussion

We show that all seven Importins (Imp α , Imp β , Kap β 2, Imp4, Imp5, Imp7, and Imp9) that can bind the N-terminal tails of H3 and H4 can also bind the H3/H4 dimer. However the

binding trend is very different than with the N-terminal tails alone. The binding trend for the N-terminal tails was $\text{Kap}\beta 2, \text{Imp}5 > \text{Imp}\alpha, \text{Imp}\beta, \text{Imp}9 > \text{Imp}4, \text{Imp}7$. In contrast, the binding trend for the Asf1-H3/H4 complex was: $\text{Imp}4, \text{Imp}5, \text{Imp}9 > \text{Imp}\beta, \text{Imp}7 > \text{Imp}\alpha, \text{Kap}\beta 2$. I showed that Asf1 alone does not bind any of the Importins. These results suggest that the histone fold domain and/or the Asf1-histone fold complex are important for Importin-histone recognition. Structural work of the Imp4-Asf1-H3/H4 complex will allow us to determine what in the histone fold domain is important for Imp4 recognition. I was able to get initial crystals of this complex but more work is needed to get diffracting crystals. I also showed that each of the Importin-Asf1-H3/H4 complexes can be dissociated by RanGTP in contrast to what was seen for the Kap114-H2A/H2B complex.

Using SAXS analysis, I showed that only one Imp4 molecule binds one H3/H4 dimer. However whether none, one, or both H3 and H4 tails are used to bind Imp4 is still unknown. Our previous ITC results showed that the H3 tail has a 10-fold higher affinity for Importins than the H4 tail, suggesting that if only one of the tails is used it is most likely be the H3 tail but more work is needed for verification.

CHAPTER 5

CRYSTAL STRUCTURE OF HUMAN KARYOPHERIN β 2 BOUND TO THE PY-NLS OF *SACCHAROMYCES CEREVISIAE* NAB2²

Abstract

Import-Karyopherin or Importin proteins bind nuclear localization signals (NLSs) to mediate the import of proteins into the cell nucleus. Karyopherin β 2 or Kap β 2, also known as Transportin, is a member of this transporter family responsible for the import of numerous RNA binding proteins. Kap β 2 recognizes a targeting signal termed the PY-NLS that lies within its cargos to target them through the nuclear pore complex. The recognition of PY-NLS by Kap β 2 is conserved throughout eukaryotes. Kap104, the Kap β 2 homolog in *Saccharomyces cerevisiae*, recognizes PY-NLSs in cargos Nab2, Hrp1, and Tfg2. I have determined the crystal structure of Kap β 2 bound to the PY-NLS of the mRNA processing protein Nab2 at 3.05-Å resolution. A seven-residue segment of the PY-NLS of Nab2 is observed to bind Kap β 2 in an extended conformation and occupies the same PY-NLS binding site observed in other Kap β 2-PY-NLS structures.

²Originally published in *Journal of Structural and Functional Genomics*. **2013**, 14(2), 31-35.

Introduction

Karyopherin β proteins (Kaps; also known as Importins and Exportins) are responsible for the majority of nucleocytoplasmic transport in eukaryotic cells. At least 20 members of the Kap family have been identified in humans, whereas 14 Kaps are known in *S. cerevisiae*. Each Kap binds a unique set of cargos and targets them to the nuclear pore complex. Kaps bind nuclear localization signals (NLSs) or nuclear export signals (NESs) in cargo proteins to direct them in and out of the nucleus, respectively. Kap-cargo interactions and transport directionality are in turn regulated by the Ran GTPase nucleotide cycle (Weis 2003).

The Karyopherin $\beta 2$ (Kap $\beta 2$; also known as Transportin) importin recognizes a class of NLS in its cargos termed the PY-NLS (Lee et al. 2006; Xu et al. 2010; Chook and Suel 2011). These 15- to 100-residue long sequences are diverse and cannot be sufficiently described by a traditional consensus sequence. PY-NLSs are instead described by a collection of physical rules that include the requirements for intrinsic structural disorder, overall basic character, and a set of sequence motifs. PY-NLS motifs consist of an N-terminal hydrophobic or basic motif and a C-terminal RX₂₋₅PY motif (Lee et al. 2006; Cansizoglu et al. 2007; Zhang and Chook 2012).

The shuttling heterogeneous nuclear ribonucleoprotein Nab2 is essential for mRNA export in *Saccharomyces cerevisiae*. Nab2 recognizes poly(A) RNA and binds to the nuclear pore-associated protein myosin-like protein 1 (Mlp1), which functions in both mRNA export and quality control (Fasken et al. 2008). Nab2 contains a PY-NLS, which is recognized by the yeast homolog of Kap $\beta 2$, Kap104, for import into the nucleus (Figure 5-1A) (Suel et al. 2008). The binding of cytosolic Kap104 to the PY-NLS of Nab2 has been implicated in the release of DEAD-box RNA helicase Dbp5 from mRNA to allow for translation (Lee and Aitchison 1999; Tran et al. 2007b). Following Nab2 release, the Kap104–Nab2 complex is translocated through

the nuclear pore complex into the nucleus, where RanGTP and mRNA act cooperatively to dissociate Nab2 from Kap104.

All previous structures of PY-NLSs bound to Kap β 2 are of signals that contain the canonical PY dipeptide motif. The PY-NLS of Nab2 is unusual in that it contains a homologous PL dipeptide motif at its C-terminus. Mutagenesis studies suggest that some PY dipeptides in PY-NLSs can be replaced by P ϕ dipeptides where ϕ is any hydrophobic residue without losing binding affinity for the Kap (Suel et al. 2008). Here I report the 3.05-Å-crystal structure of Kap β 2 bound to the PY-NLS of Nab2, which shows for the first time the homologous PL dipeptide motif. The structure explains how an aliphatic hydrophobic residue is able to substitute structurally for the conserved tyrosine in a PY-NLS.

Materials and Methods

Protein Expression, Purification, and Complex Assembly.

Human Kap β 2 (Uniprot ID U72069) was expressed in pGEX-TEV vector [pGEX-4T3 (GE Healthcare) with a TEV cleavage site] as a GST fusion protein and purified as previously described (Lee et al. 2006). Kap β 2 with a truncated loop, which does not interfere with NLS binding, was used for crystallization (residues 337– 367 of Kap β 2 were replaced with a GGSGGSG linker) (Lee et al. 2006). Residues 205-242 of *S. cerevisiae* Nab2 (^{Nab2}PY-NLS; Nab2, Uniprot ID P32505) were also expressed as a GST fusion protein (Suel et al. 2008). GST-^{Nab2}PY-NLS was purified by affinity and ion exchange chromatography. GST-^{Nab2}PY-NLS and Kap β 2 were mixed at molar ratio of 5:1. The GST tag was removed with TEV protease and the complex further purified by gel filtration in buffer composed of 20 mM HEPES, pH 7.3, 110 mM potassium acetate, 2 mM DTT, 2 mM magnesium acetate, and 1 mM EGTA with 20% (v/v) glycerol. The complex was concentrated to 13 mg/mL for crystallization.

Crystallization and structure determination of the Kap β 2-Nab2PY-NLS complex

Purified Kap β 2-Nab2PY-NLS complex was screened against MCSG1-4 (Microlytic North America, USA) and ProComplex (Qiagen, USA) crystallization screens *via* sitting drop vapor diffusion at 20°C (0.4 μ L protein + 0.4 μ L reservoir solution) using a Phoenix (Art Robins, USA) liquid handling system. Crystals with well-formed morphology were obtained in several conditions. Many crystals did not yield useful diffraction, but crystals grown with crystallization condition MCSG3-H11 (700 mM sodium citrate tribasic and 100 mM Bis-trispropane pH 7.0) diffracted to 3.05-Å resolution. Crystals were cryo-protected by addition of ~20% (v/v) glycerol, and flash-cooled by immersion in liquid nitrogen. Diffraction data, recorded at the X29A beamline at the Brookhaven National Laboratory at a wavelength of 1.0705 Å, were processed using HKL3000 (Minor et al. 2006). The structure was determined by molecular replacement using PHASER M(Adams et al. 2010) with a search model of human Kap β 2 from the PDB Code 2QMR (A chain) (Cansizoglu and Chook 2007). Several rounds of refinement using REFMAC5 (Collaborative Computational Project 1994) and manual model building with COOT (Emsley et al. 2010) were performed. The high resolution structure of Kap β 2 bound to the PY-NLS of Fused in Sarcoma protein (PDB code 4FDD) (Zhang and Chook 2012) was used to guide manual model building. Residues 234-240 of Nab2 were built into the electron density maps at the last stages of the refinement [Figure 5-1A]. The final model of the Kap β 2-Nab2PY-NLS complex shows excellent stereochemical parameters (Chen et al. 2010)(Table 5-I). Illustrations were prepared with PyMol (<http://www.pymol.org>).

Results and Discussion

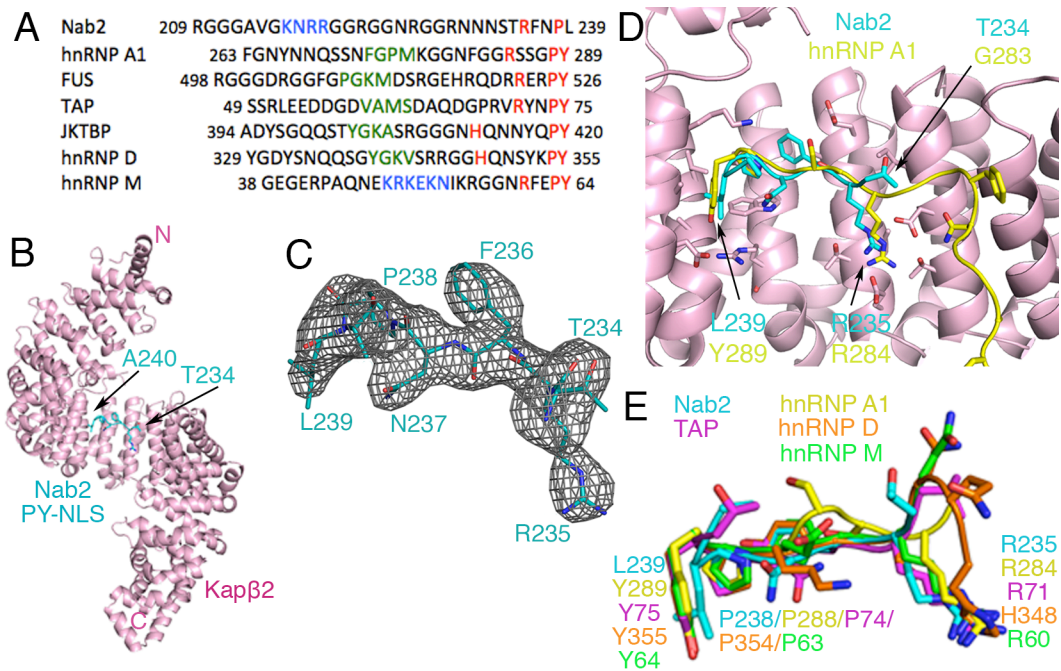


Fig. 5-1 Structure and comparative analysis of $Nab2$ PY-NLS. (A) Sequence alignment of several PY-NLSs. This signal consists of an N-terminal hydrophobic or basic motif (green and blue, respectively) and a C-terminal $RX_{2-5}PY$ motif (red). (B) Overall structure of the $Kap\beta 2$ - $Nab2$ PY-NLS complex. The karyopherin is in pink and the PY-NLS cyan. (C) mFo-DFc difference map, contoured at 2.0σ (grey), at the PY-NLS binding site of $Kap\beta 2$ before the $Nab2$ PY-NLS residues were included in the model. The final refined model of $Nab2$ PY-NLS residues Thr234 to Ala240 are in cyan. (D) Superposition of $Kap\beta 2$ residues 301-634 for $Kap\beta 2$ s bound to PY-NLSs from cargos Nab2 and hnRNP A1 (PDB ID 2H4M; C α rmsd 0.35 Å). $Kap\beta 2$ of the Nab2 complex is shown in pink. The Nab2 PY-NLS is in cyan and the hnRNP A1 PY-NLS is in yellow. (E) Similar superpositions of $Kap\beta 2$ as in D, to compare PY-NLSs from Nab2 (cyan), hnRNP A1 (yellow), hnRNP M (green), hnRNP D (orange), and TAP/NXF1 (purple)

Structure of the $Kap\beta 2$ - $Nab2$ PY-NLS complex

We have determined the 3.05 Å crystal structure of human $Kap\beta 2$ bound to the PY-NLS segment of *S. cerevisiae* Nab2 that spans residues 205-242 (Figure 5-1B). $Kap\beta 2$, as shown previously is a superhelical protein composed of 20 α -helical HEAT repeats (Cansizoglu and

Chook 2007; Imasaki et al. 2007). Each HEAT repeat is composed of two antiparallel α -helices, A and B, each lining the convex and concave sides of the superhelix, respectively. Seven residues of the ^{Nab2}PY-NLS (residues 234-240) are modeled (Figure 5-1C) and shown to bind the previously described PY-NLS binding site in the C-terminal arch of Kap β 2 (Lee et al. 2006; Cansizoglu et al. 2007; Imasaki et al. 2007; Zhang and Chook 2012). Residues 234-240 of the ^{Nab2}PY-NLS peptide bind in extended conformation, tracing a path along the concave surface of Kap β 2 similar to other structurally characterized PY-NLSs, such as that from hnRNP A1 (Figure 5-1D and 5-1E) (Lee et al. 2006). Residues 204-233 and 241-242 of the bound ^{Nab2}PY-NLS peptide were not modeled due to lack of electron density.

Residues ²³⁴TRFNPL²⁴⁰ of Nab2 occupy the same binding site on Kap β 2 as the ²⁸⁴RX₂₅PY²⁸⁹ motifs of other PY-NLSs such as those from cargos hnRNP A1, hnRNP D, hnRNP M, and TAP/NXF1 (Figure 5-1E) (Lee et al. 2006; Cansizoglu et al. 2007; Imasaki et al. 2007). All previous structures of PY-NLSs are of peptides that contain the canonical PY dipeptide. This Nab2 PY-NLS structure shows for the first time the homologous PL dipeptide motif. Like PY motifs, the PL motif of the ^{Nab2}PY-NLS also makes numerous contacts with hydrophobic residues of Kap β 2 (Figure 3-2A). Pro-238 of Nab2 interacts primarily through hydrophobic interactions with the sidechains Leu-419, Ile-457, and Trp-460 of Kap β 2. Leu-239 of the Nab2 PL motif makes hydrophobic interactions with Leu-419, Ala-381, Ala-422, and Trp-460 of Kap β 2. Previous mutational analysis showed that mutation of the PL motif (wildtype ^{Nab2}PY-NLS binds Kap β 2 with $K_D=37$ nM) in Nab2 to PY improved binding affinity to Kap104 by about three-fold ($K_D=13$ nM for the PY mutant of Nab2) (Suel et al. 2008). This increase in binding energy may be due to the aromatic ring of tyrosine making additional hydrophobic contacts with Kap β 2 side chains and/or the tyrosine making polar interactions with Arg-464 of Kap β 2 as seen

in other Kap β 2-PY-NLS structures (PDB ID: hnRNP A1, 2H4M; hnRNP M, 2OT8; TAP, 2Z5K; hnRNP D, 2Z5N).

Further N-terminus, Phe-236 also makes hydrophobic interactions with Ala-499, Glu-498 and Trp-460 sidechains of Kap β 2. The Phe236 sidechain is also positioned close to Pro-238 (within 4.5 Å). Similar conformations were observed for the equivalent position in PY-NLSs of hnRNP D, hnRNP M and TAP/NXF1 where a phenylalanine is also present (Figure 5-2B) (Lee et al. 2006; Cansizoglu et al. 2007; Imasaki et al. 2007). Previous biochemical studies have shown that Phe-236 contributes significantly to Kap104-Nab2 interactions and that a hydrophobic residue at this position is important (Suel et al. 2008). Phe-236 likely contributes entropically through intramolecular interactions that preorganize the PL motif for Kap β 2 binding. The neighboring Arg-235, which is the N-terminal arginine of the RX₂₋₅PY/L motif, makes multiple salt bridges and hydrogen bonds with Asp-543, Thr-506, Glu-509, and Thr-547 of Kap β 2 (Figure 5-2A). Beyond residue Thr-234, electron density is too weak to model the N-terminal portion of the Nab2 PY-NLS.

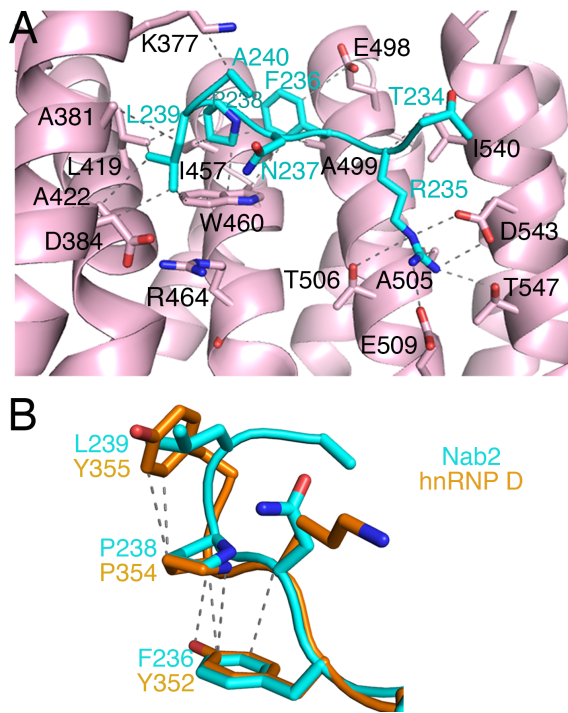


Fig. 5-2 The Kap β 2-^{Nab2}PY-NLS Interface. (A) The ^{Nab2}PY-NLS (cyan) makes numerous hydrophobic contacts with Kap β 2 (pink). In addition, Arg-235 of the ^{Nab2}PY-NLS makes multiple salt bridges and hydrogen bonds with Kap β 2. Interacting residues on Kap β 2 are labeled in black and contacts (4.0 Å or less) are indicated by dashed lines. (B) Comparison of the PY motifs of PY-NLSs from Nab2 (cyan) and hnRNP D (orange). Intramolecular contacts (4.0 Å or less) in hnRNP D are shown with dashed lines.

Table 5-I. Crystallographic statistics for HsKap β 2-^{ScNab2}PY-NLS complex.**Crystal Parameters**

Space group	<i>P2₁2₁2</i>
Cell dimensions:	
a, b, c (Å)	132.2, 172.4, 68.4
α , β , γ (°)	90, 90, 90
Matthew's coefficient (Å ³ /Da)	4.14
Solvent content (%)	70

Data Collection

Wavelength (Å)	1.0750
Resolution (Å)	50.00-3.05 (3.29-3.05) ^a
R _{sym} (%)	12.3
Number of unique reflections	30,914 (1536) ^a
Number of reflections in R _{free} set	1538
Mean Redundancy	8.8 (9.0) ^a
Overall Completeness (%)	100.0 (100.0)
Mean I/ σ	16.6 (1.18) ^a

Refinement Residuals

R _{free} (%)	23.7
R _{work} (%)	18.4
Completeness (%)	99.5 (94.6)

Model Quality

RMSD bond lengths (Å)	0.0109
RMSD bond angles (°)	1.5380
Molprobit Ramachandran:	
Favored region (%)	94.8
Allowed region (%)	99.9
Mean overall B-factor	
HsKap β 2 (Å ²)	104.7
ScNAB2-NLS (Å ²)	101.7

Model Contents

Protomers in ASU	
HsKap β 2	1
No. of HsKap β 2 residues	840
No. of HsKap β 2 atoms	6676
ScNAB2-NLS	1
No. of ScNAB2-NLS residues	7
No. of ScNAB2-NLS atoms	57
No. of water atoms	0

PDB accession code 4H1K^a Values in parenthesis correspond to the highest-resolution shell

CHAPTER 6

CONCLUSIONS AND FUTURE PERSPECTIVES

There are at least 10 different Importins in human cells that bind distinct nuclear localization signals (NLSs) in their cargos to target them to the nuclear pore complex (Chook and Suel 2011; Soniat and Chook 2015). Most known cargoes contain an NLS that is recognized and imported by one or a few Importins. However, two classes of cargoes have been shown to be imported by multiple Importins: ribosomal proteins and the core histones. My work focused on understanding how the histones, particularly histones H3 and H4, are recognized by the Importins.

During S-phase, newly synthesized histone H2A/H2B dimers and H3/H4 dimers are imported into the nucleus to be assembled into nucleosomes (Eickbush and Moudrianakis 1978; Luger et al. 1997; Campos and Reinberg 2009; Burgess and Zhang 2013). It was previously shown that multiple Importins can bind the N-terminal tails of histone H3 and H4; however, nothing was known about how the different Importins recognize the same histone tails (Mosammamarast et al. 2002b). Using pull-down assays, we showed that seven Importins, Imp α , Imp β , Kap β 2, Imp4, Imp5, Imp7 and Imp9, are able to bind the N-terminals tails of H3 and H4. We determined the crystal structure of the H3 tail bound to Kap β 2, which identified residues 11-

27 of the H3 tail as the binding element for this Importin. Like other known PY-NLSs, the H3 tail contains an N-terminal basic region and an arginine similar to the conserved Arg of the R-X₂-₃-P-Y consensus motif. However the H3 tail does not contain the P-Y or the homologous P-Φ motif. These results revealed the first example of a PY-less PY-NLS variant.

We found that the same basic segment (residues 11-27) in H3 was also important for binding six Importins (Imp α , Imp β , Kap β 2, Imp4, Imp7, and Imp9) where this segment is the sole binding element for Imp β , Kap β 2, and Imp4. Within this basic segment, Lys14 is a critical hotspot for binding Imp β , Kap β 2, Imp4, Imp7, and Imp9. The N-terminal basic segment in the H3 tail is used along with a C-terminal IK-NLS motif (residues 35-40) to bind Imp5, Imp7, Imp9 and Imp α . We showed that H4 tail also binds the same seven Importins and the H4 tail uses an N-terminal epitope that spans residues 8-20, where Lys12 is a hotspot for Importin binding. Additionally, Imp5 recognizes a C-terminal IK-NLS-like epitope in the H4 tail that spans residues 29-32.

While identifying the binding determinants in the H3 and H4 tails for the different Importins, we also studied the effects of histone tail acetylation on Importin-histone binding. We discovered that acetylation of Lys14 of the H3 tail impairs binding to all seven Importins while acetylation of Lys18 of H3 tail and acetylation of Lys5 and Lys12 of the H4 tail had only mild effects on Importin binding. These results show that acetylation of H3 Lys14 can compromise Importin-histone interaction and can potentially regulate nuclear import of histones. However previous mass spectrometry analysis found that only ~20-30% of histone H3 in the cytoplasm is acetylated at Lys14 and/or Lys18, suggesting that that the modifications are not prevalent in the cytoplasm (Jasencakova et al. 2010). Therefore, at best only a fraction of H3 may be acetylated in a way that could impair nuclear import. In contrast, histone H4 is always acetylated at Lys5

and Lys12 prior to nuclear import (Jasencakova et al. 2010). However, H4 Ly5/Lys12 diacetylation has little effect the H4 tail binding to Importins. Our results of Importins binding to acetylated H3 and H4 tail peptides suggest that acetylation of the histone tails may not be important in regulating histone nuclear import but these modifications that occur in the cytoplasm may instead be important for downstream nuclear events in histone biogenesis.

In addition to analyses with the N-terminal tails, I studied Importin-binding to the Asf1-H3/H4 complex. I showed that the Importin-histone binding trend for Asf1-H3/H4 is different from the trend for the histone tails alone. The binding trend for Importins binding to the H3 tail, from high to low affinity, is Kap β 2, Imp5 > Imp β , Imp9, Imp α > Imp4, Imp7. The H4 tail binds Importins at least 10-fold weaker than the H3 tail, and the binding trend for Importins binding to the H4 tail is slightly different with Imp5 > Imp9, Imp α > Imp β , Kap β 2, Imp4, Imp7. However, the binding trend for Asf1-H3/H4 complex is quite different, with Imp4, Imp5, Imp9 > Imp β and Imp7 > Imp α and Kap β 2. These results suggest that either the dimeric histone folds and/or Asf1 are interacting with the Importins. Finally, using SAXS, we determined that only one Imp4 is bound per H3/H4 dimer suggesting that at most only one histone tail in the dimer engages the Importin.

Future Perspectives

Kap β 2 cargoes that may contain the PY-less PY-NLS variant

Although the N-terminal H3 and H4 tails bind Kap β 2, neither contains a recognizable PY-NLSs (Lee et al. 2006). There are other Kap β 2 cargoes like the H3 and H4 tails that do not have recognizable PY-NLS. These proteins may lack the P-Y motif and bind Kap β 2 by using only two of the three PY-NLS epitopes, like the H3 tail. Such PY-less PY-NLS cargoes may not have evolved a P-Y motif or may have lost it through evolution. Alternatively, non-PY-NLS

cargoes may use PY-NLS Epitope 1 and 2 in combination with an Epitope 3 that does not resemble the P-Y motif. For example, it has been suggested that a E-R dipeptide in the RNA binding protein ADAR1 binds in place of the P-Y dipeptide of a typical PY-NLS in the P-Y site of Kap β 2. Finally, non-PY-NLS cargoes may contain a completely different signal that binds a different site of Kap β 2. Additional structural and biochemical analysis of these non-PY cargoes (include histone tails H2A, H2B and H4, transcription factor FOXO4, RNA-editing enzyme ADAR1, and viral proteins HIV-1 REV, HPV E6 and Adenovirus Ad2) are needed (Mosammaparast et al. 2001; Soniat and Chook 2015). Understanding how these cargoes are recognized by Kap β 2 will allow us to determine which of the three modes of binding (described above) is used and to understand how PY-less PY-NLSs maintain sufficient binding energy for Kap β 2.

Ribosomal proteins also bind multiple Importins

Along with core histones, another class of proteins that is known to be recognized by multiple Importins are ribosomal proteins (Jakel and Gorlich 1998). For example, previous studies by Jakel and Görlich of the ribosomal protein L23A (rpL23A) showed that it can bind Imp α / β , Kap β 2, Imp5, and Imp7 through β -like import receptor binding (BIB) sequences. The authors proposed that BIB sequences originated from ancestral NLS that existed before Importins developed distinct NLS binding sites (Jakel and Gorlich 1998). Alignment of the rpL23A BIB sequence with the H3 and H4 tails showed that residues ⁵⁹KYPRKSAPRRNK⁷⁰ of rpL23A shares sequence similarity with residues of ¹⁴KAPRKQLATKAAR²⁶ and ⁸KGLGKGGAKRHR²⁰ in H3 and H4 tails, respectively. Structural studies of rpL23A bound to the Importins are needed to better understand what is important for Importin-BIB recognition. Additional studies of other ribosomal proteins, such as rpS7 and rpL5, and the other histones,

such as H2A and H2B, are needed to further determine a consensus sequence for BIB sequences (Jakel and Gorlich 1998; Mosammaparast et al. 2001).

Structure determination of other Importin-histone complexes

Along with crystals of Kap β 2-H3 tail complex, we were able to crystallize Imp4 in complex with the H3 tail, but the crystals were not suitable for structure determination. Future work should focus on crystallization optimization of the complex to get better crystals to obtain a high-resolution structure. Imp4 is the main importer of the H3/H4 dimer in cells and structural work will reveal how Imp4 recognizes the N-terminal H3 tails and also increase our understanding of Importin-histone interactions (Muhlhauser et al. 2001; Campos et al. 2010; Jasencakova et al. 2010; Alvarez et al. 2011). An Imp4-H3 tail structure will allow us to better compare Imp4-H3 interaction to Kap β 2-H3 interactions to determine similarities and differences in recognition by different Importins. Structural work of Imp4-H3 tail complex will also allow us to gain insight into the class of NLS that bind Imp4, which is currently unknown. Additional structural work is also needed of the other Importins (Imp α , Imp β , Imp5, Imp7, and Imp9) with the H3 tail to get a more detailed understanding of Importin-H3 interactions.

Along with Imp4-H3 crystals, we were also able to get crystals of Imp5 in complex with the H3 tail but these never diffracted better than 4 Å resolution. Previously studies suggested that the compact IK-NLS is the most important element in Kap121/Imp5 cargoes for binding the Importin (Kobayashi and Matsuura 2013). However our results showed that the IK-NLS motifs in H3 and H4 only contribute a small portion to Imp5 binding. A structure of the Imp5-H3 complex would allow us to better understand how Imp5 recognizes the N-terminal basic epitope of H3. Additional epitopes that are important for binding may be found in other Imp5 cargoes but these epitopes may be more dynamic than the IK-NLS motif. Previous Kap121p-cargo

structural work found only small IK-NLS motifs in Pho4p, Ste12p, and Nup53p binding to the Importin, suggesting that additional epitopes, if they exist in these cargoes, bind in a dynamic fashion and thus are not observed in the crystal structures (Kobayashi and Matsuura 2013). It is also possible that the region of the NLS that used for crystallization did not contain these epitopes (Kobayashi and Matsuura 2013).

The role of Acetylation in Nuclear Import of Histones

Our results showed that acetylation of H3 Lys14 can compromise Importin-H3 tail interactions but whether acetylation is used to regulate nuclear import of histones is unknown. Furthermore, why or how or if acetylation is used to regulate the histones import is not clear. If acetylation is used to regulate nuclear import of histones, does acetylation add specificity and allow the H3/H4 dimer to be preferably bound by a one or a smaller set of Importins? Or will acetylation specify which histone tail the Importins should bind? Yet another possibility is that acetylation may be used to prevent nuclear import of premature or incompletely processed histone complexes such as histone monomers or H3/H4 dimers that are not bound to the histone chaperone, Asf1. Perhaps once the H3/H4 dimer is bound to Asf1, deacetylation of one of the H3 or H4 tails may finally allow Importins to bind and allow nuclear import to proceed.

Further experiments are needed to verify the importance of acetylation in nuclear import of histones. We have only studied the effect of acetylation on Importin binding in the context of the histone H3 and H4 tails. More work is needed to understand the effect of acetylation on Importin binding with the H3/H4 dimers. Future work using either acetylation mimics (K to Q mutations) of these important lysines or using the sortase-mediated reactions to link synthetically made acetylated histone tail peptides to the histone fold domain of H3 and H4 is needed.

Structure determination of the Imp4-Asf1-H3/H4 Complex

Other than with the N-terminal tails, the Importins may make additional interactions with the histone fold domain of H3 and H4. To better understand these Importin-histone interactions, we have purified the Imp4-Asf1-H3/H4 complex and attempted to obtain a high-resolution structure this complex. We have been able to get initial crystals of the Imp4-Asf1-H3/H4 complex but further optimization of these crystals is needed to get diffracting crystals for structure determination. The Imp4-Asf1-H3/H4 structure will allow us to understand Importin-interactions with the histone fold domain. Furthermore, our SAXS analysis showed that only one Imp4 molecule binds each H3/H4 dimer. Our ITC results showed that of the two tails, the H3 tail binds Importins at least 10-fold more tightly, suggesting that in the H3/H4 dimer, the H3 tail is more likely to bind Importins but more work is needed to verify this idea. A structure of Imp4-Asf1-H3/H4 will allow us to determine whether both of the tails are recognized, one of the tails or none of the tails are used to bind Importins. Additionally, an Imp4-Asf1-H3/H4 structure will allow us to understand potential effects of acetylation on Importin binding.

Overall, we have determined Importin-histone recognition elements within the histones H3 and H4 tail and shown that acetylation H3 Lys12 affects Importin-histone binding.

BIBLIOGRAPHY

- Adam EJ, Adam SA. 1994. Identification of cytosolic factors required for nuclear location sequence-mediated binding to the nuclear envelope. *The Journal of cell biology* **125**: 547-555.
- Adams PD, Afonine PV, Bunkoczi G, Chen VB, Davis IW, Echols N, Headd JJ, Hung LW, Kapral GJ, Grosse-Kunstleve RW et al. 2010. PHENIX: a comprehensive Python-based system for macromolecular structure solution. *Acta crystallographica Section D, Biological crystallography* **66**: 213-221.
- Adkins MW, Carson JJ, English CM, Ramey CJ, Tyler JK. 2007. The histone chaperone anti-silencing function 1 stimulates the acetylation of newly synthesized histone H3 in S-phase. *The Journal of biological chemistry* **282**: 1334-1340.
- Ahmad K, Henikoff S. 2002. The histone variant H3.3 marks active chromatin by replication-independent nucleosome assembly. *Molecular cell* **9**: 1191-1200.
- Alekseev OM, Widgren EE, Richardson RT, O'Rand MG. 2005. Association of NASP with HSP90 in mouse spermatogenic cells: stimulation of ATPase activity and transport of linker histones into nuclei. *The Journal of biological chemistry* **280**: 2904-2911.
- Allemand E, Dokudovskaya S, Bordonne R, Tazi J. 2002. A conserved Drosophila transportin-serine/arginine-rich (SR) protein permits nuclear import of Drosophila SR protein splicing factors and their antagonist repressor splicing factor 1. *Molecular biology of the cell* **13**: 2436-2447.
- Alvarez F, Munoz F, Schilcher P, Imhof A, Almouzni G, Loyola A. 2011. Sequential establishment of marks on soluble histones H3 and H4. *The Journal of biological chemistry* **286**: 17714-17721.
- Andrews AJ, Chen X, Zevin A, Stargell LA, Luger K. 2010. The histone chaperone Nap1 promotes nucleosome assembly by eliminating nonnucleosomal histone DNA interactions. *Molecular cell* **37**: 834-842.
- Annunziato AT. 2013. Assembling chromatin: the long and winding road. *Biochimica et biophysica acta* **1819**: 196-210.
- Arnold M, Nath A, Hauber J, Kehlenbach RH. 2006. Multiple importins function as nuclear transport receptors for the Rev protein of human immunodeficiency virus type 1. *The Journal of biological chemistry* **281**: 20883-20890.
- Baake M, Bauerle M, Doenecke D, Albig W. 2001. Core histones and linker histones are imported into the nucleus by different pathways. *European journal of cell biology* **80**: 669-677.
- Barraud P, Banerjee S, Mohamed WI, Jantsch MF, Allain FH. 2014. A bimodular nuclear localization signal assembled via an extended double-stranded RNA-binding domain acts as an RNA-sensing signal for transportin 1. *Proceedings of the National Academy of Sciences of the United States of America* **111**: E1852-1861.
- Bauerle M, Doenecke D, Albig W. 2002. The requirement of H1 histones for a heterodimeric nuclear import receptor. *The Journal of biological chemistry* **277**: 32480-32489.
- Belotserkovskaya R, Oh S, Bondarenko VA, Orphanides G, Studitsky VM, Reinberg D. 2003. FACT facilitates transcription-dependent nucleosome alteration. *Science* **301**: 1090-1093.
- Bernis C, Swift-Taylor B, Nord M, Carmona S, Chook YM, Forbes DJ. 2014. Transportin acts to regulate mitotic assembly events by target binding rather than Ran sequestration. *Molecular biology of the cell* **25**: 992-1009.

- Bhaumik SR, Smith E, Shilatifard A. 2007. Covalent modifications of histones during development and disease pathogenesis. *Nature structural & molecular biology* **14**: 1008-1016.
- Bjorkblom B, Maple-Grodem J, Puno MR, Odell M, Larsen JP, Moller SG. 2014. Reactive oxygen species-mediated DJ-1 monomerization modulates intracellular trafficking involving karyopherin beta2. *Molecular and cellular biology* **34**: 3024-3040.
- Blackwell JS, Jr., Wilkinson ST, Mosammamarast N, Pemberton LF. 2007. Mutational analysis of H3 and H4 N termini reveals distinct roles in nuclear import. *The Journal of biological chemistry* **282**: 20142-20150.
- Blazek E, Meisterernst M. 2006. A functional proteomics approach for the detection of nuclear proteins based on derepressed importin alpha. *Proteomics* **6**: 2070-2078.
- Bono F, Cook AG, Grunwald M, Ebert J, Conti E. 2010. Nuclear import mechanism of the EJC component Mago-Y14 revealed by structural studies of importin 13. *Molecular cell* **37**: 211-222.
- Burgess RJ, Zhang Z. 2013. Histone chaperones in nucleosome assembly and human disease. *Nature structural & molecular biology* **20**: 14-22.
- Cairo LV, Ptak C, Wozniak RW. 2013. Mitosis-specific regulation of nuclear transport by the spindle assembly checkpoint protein Mad1p. *Molecular cell* **49**: 109-120.
- Campos EI, Fillingham J, Li G, Zheng H, Voigt P, Kuo WH, Seepany H, Gao Z, Day LA, Greenblatt JF et al. 2010. The program for processing newly synthesized histones H3.1 and H4. *Nature structural & molecular biology* **17**: 1343-1351.
- Campos EI, Reinberg D. 2009. Histones: annotating chromatin. *Annu Rev Genet* **43**: 559-599.
- Cansizoglu AE, Chook YM. 2007. Conformational heterogeneity of karyopherin beta2 is segmental. *Structure* **15**: 1431-1441.
- Cansizoglu AE, Lee BJ, Zhang ZC, Fontoura BM, Chook YM. 2007. Structure-based design of a pathway-specific nuclear import inhibitor. *Nature structural & molecular biology* **14**: 452-454.
- Catimel B, Teh T, Fontes MR, Jennings IG, Jans DA, Howlett GJ, Nice EC, Kobe B. 2001. Biophysical characterization of interactions involving importin-alpha during nuclear import. *The Journal of biological chemistry* **276**: 34189-34198.
- Chadwick BP, Valley CM, Willard HF. 2001. Histone variant macroH2A contains two distinct macrochromatin domains capable of directing macroH2A to the inactive X chromosome. *Nucleic Acids Res* **29**: 2699-2705.
- Chang CW, Counago RL, Williams SJ, Boden M, Kobe B. 2012. Crystal structure of rice importin-alpha and structural basis of its interaction with plant-specific nuclear localization signals. *The Plant cell* **24**: 5074-5088.
- Chang CW, Counago RM, Williams SJ, Boden M, Kobe B. 2013. Distinctive conformation of minor site-specific nuclear localization signals bound to importin-alpha. *Traffic* **14**: 1144-1154.
- Chaves SR, Blobel G. 2001. Nuclear import of Spo12p, a protein essential for meiosis. *The Journal of biological chemistry* **276**: 17712-17717.
- Chen MH, Ben-Efraim I, Mitrousis G, Walker-Kopp N, Sims PJ, Cingolani G. 2005. Phospholipid scramblase 1 contains a nonclassical nuclear localization signal with unique binding site in importin alpha. *The Journal of biological chemistry* **280**: 10599-10606.
- Chen VB, Arendall WB, 3rd, Headd JJ, Keedy DA, Immormino RM, Kapral GJ, Murray LW, Richardson JS, Richardson DC. 2010. MolProbity: all-atom structure validation for

- macromolecular crystallography. *Acta crystallographica Section D, Biological crystallography* **66**: 12-21.
- Choi S, Yamashita E, Yasuhara N, Song J, Son SY, Won YH, Hong HR, Shin YS, Sekimoto T, Park IY et al. 2014. Structural basis for the selective nuclear import of the C2H2 zinc-finger protein Snail by importin beta. *Acta crystallographica Section D, Biological crystallography* **70**: 1050-1060.
- Chook YM, Blobel G. 1999. Structure of the nuclear transport complex karyopherin-beta2-Ran x GppNHp. *Nature* **399**: 230-237.
- . 2001. Karyopherins and nuclear import. *Current opinion in structural biology* **11**: 703-715.
- Chook YM, Jung A, Rosen MK, Blobel G. 2002. Uncoupling Kapbeta2 substrate dissociation and ran binding. *Biochemistry* **41**: 6955-6966.
- Chook YM, Suel KE. 2011. Nuclear import by karyopherin-betas: recognition and inhibition. *Biochimica et biophysica acta* **1813**: 1593-1606.
- Christ F, Thys W, De Rijck J, Gijssbers R, Albanese A, Arosio D, Emiliani S, Rain JC, Benarous R, Cereseto A et al. 2008. Transportin-SR2 imports HIV into the nucleus. *Current biology : CB* **18**: 1192-1202.
- Cingolani G, Bednenko J, Gillespie MT, Gerace L. 2002. Molecular basis for the recognition of a nonclassical nuclear localization signal by importin beta. *Molecular cell* **10**: 1345-1353.
- Cingolani G, Petosa C, Weis K, Muller CW. 1999. Structure of importin-beta bound to the IBB domain of importin-alpha. *Nature* **399**: 221-229.
- Collaborative Computational Project N. 1994. The CCP4 suite: programs for protein crystallography. *Acta crystallographica Section D, Biological crystallography* **50**: 760-763.
- Conti E, Izaurralde E. 2001. Nucleocytoplasmic transport enters the atomic age. *Current opinion in cell biology* **13**: 310-319.
- Conti E, Muller CW, Stewart M. 2006. Karyopherin flexibility in nucleocytoplasmic transport. *Current opinion in structural biology* **16**: 237-244.
- Conti E, Uy M, Leighton L, Blobel G, Kuriyan J. 1998. Crystallographic analysis of the recognition of a nuclear localization signal by the nuclear import factor karyopherin alpha. *Cell* **94**: 193-204.
- Cook A, Bono F, Jinek M, Conti E. 2007. Structural biology of nucleocytoplasmic transport. *Annual review of biochemistry* **76**: 647-671.
- Cook AJ, Gurard-Levin ZA, Vassias I, Almouzni G. 2011. A specific function for the histone chaperone NASP to fine-tune a reservoir of soluble H3-H4 in the histone supply chain. *Molecular cell* **44**: 918-927.
- Cutress ML, Whitaker HC, Mills IG, Stewart M, Neal DE. 2008. Structural basis for the nuclear import of the human androgen receptor. *Journal of cell science* **121**: 957-968.
- Das C, Tyler JK, Churchill ME. 2010. The histone shuffle: histone chaperones in an energetic dance. *Trends Biochem Sci* **35**: 476-489.
- de Barros AC, Takeda AA, Chang CW, Kobe B, Fontes MR. 2012. Structural basis of nuclear import of flap endonuclease 1 (FEN1). *Acta crystallographica Section D, Biological crystallography* **68**: 743-750.
- De Iaco A, Luban J. 2011. Inhibition of HIV-1 infection by TNPO3 depletion is determined by capsid and detectable after viral cDNA enters the nucleus. *Retrovirology* **8**: 98.

- De Iaco A, Santoni F, Vannier A, Guipponi M, Antonarakis S, Luban J. 2013. TNPO3 protects HIV-1 replication from CPSF6-mediated capsid stabilization in the host cell cytoplasm. *Retrovirology* **10**: 20.
- Dean KA, von Ahsen O, Gorlich D, Fried HM. 2001. Signal recognition particle protein 19 is imported into the nucleus by importin 8 (RanBP8) and transportin. *Journal of cell science* **114**: 3479-3485.
- Delahodde A, Pandjaitan R, Corral-Debrinski M, Jacq C. 2001. Pse1/Kap121-dependent nuclear localization of the major yeast multidrug resistance (MDR) transcription factor Pdr1. *Molecular microbiology* **39**: 304-312.
- Desmond CR, Atwal RS, Xia J, Truant R. 2012. Identification of a karyopherin beta1/beta2 proline-tyrosine nuclear localization signal in huntingtin protein. *The Journal of biological chemistry* **287**: 39626-39633.
- Dias SM, Wilson KF, Rojas KS, Ambrosio AL, Cerione RA. 2009. The molecular basis for the regulation of the cap-binding complex by the importins. *Nature structural & molecular biology* **16**: 930-937.
- Dingwall C, Sharnick SV, Laskey RA. 1982. A polypeptide domain that specifies migration of nucleoplamin into the nucleus. *Cell* **30**: 449-458.
- Dishinger JF, Kee HL, Jenkins PM, Fan S, Hurd TW, Hammond JW, Truong YN, Margolis B, Martens JR, Verhey KJ. 2010. Ciliary entry of the kinesin-2 motor KIF17 is regulated by importin-beta2 and RanGTP. *Nature cell biology* **12**: 703-710.
- Dong X, Biswas A, Suel KE, Jackson LK, Martinez R, Gu H, Chook YM. 2009. Structural basis for leucine-rich nuclear export signal recognition by CRM1. *Nature* **458**: 1136-1141.
- Dormann D, Haass C. 2011. TDP-43 and FUS: a nuclear affair. *Trends in neurosciences* **34**: 339-348.
- Dormann D, Madl T, Valori CF, Bentmann E, Tahirovic S, Abou-Ajram C, Kremmer E, Ansorge O, Mackenzie IR, Neumann M et al. 2012. Arginine methylation next to the PY-NLS modulates Transportin binding and nuclear import of FUS. *The EMBO journal* **31**: 4258-4275.
- Downs JA, Lowndes NF, Jackson SP. 2000. A role for *Saccharomyces cerevisiae* histone H2A in DNA repair. *Nature* **408**: 1001-1004.
- Eickbush TH, Moudrianakis EN. 1978. The histone core complex: an octamer assembled by two sets of protein-protein interactions. *Biochemistry* **17**: 4955-4964.
- Ejlassi-Lassalette A, Mocquard E, Arnaud MC, Thiriet C. 2011. H4 replication-dependent diacetylation and Hat1 promote S-phase chromatin assembly in vivo. *Molecular biology of the cell* **22**: 245-255.
- Elsasser SJ, D'Arcy S. 2013. Towards a mechanism for histone chaperones. *Biochimica et biophysica acta* **1819**: 211-221.
- Emsley P, Lohkamp B, Scott WG, Cowtan K. 2010. Features and development of Coot. *Acta crystallographica Section D, Biological crystallography* **66**: 486-501.
- English CM, Adkins MW, Carson JJ, Churchill ME, Tyler JK. 2006. Structural basis for the histone chaperone activity of Asf1. *Cell* **127**: 495-508.
- English CM, Maluf NK, Tripet B, Churchill ME, Tyler JK. 2005. ASF1 binds to a heterodimer of histones H3 and H4: a two-step mechanism for the assembly of the H3-H4 heterotetramer on DNA. *Biochemistry* **44**: 13673-13682.

- Faast R, Thonglairoam V, Schulz TC, Beall J, Wells JR, Taylor H, Matthaei K, Rathjen PD, Tremethick DJ, Lyons I. 2001. Histone variant H2A.Z is required for early mammalian development. *Current biology : CB* **11**: 1183-1187.
- Fasken MB, Stewart M, Corbett AH. 2008. Functional significance of the interaction between the mRNA-binding protein, Nab2, and the nuclear pore-associated protein, Mlp1, in mRNA export. *The Journal of biological chemistry* **283**: 27130-27143.
- Favre N, Camps M, Arod C, Chabert C, Rommel C, Pasquali C. 2008. Chemokine receptor CCR2 undergoes transportin1-dependent nuclear translocation. *Proteomics* **8**: 4560-4576.
- Foltz DR, Jansen LE, Bailey AO, Yates JR, 3rd, Bassett EA, Wood S, Black BE, Cleveland DW. 2009. Centromere-specific assembly of CENP-a nucleosomes is mediated by HJURP. *Cell* **137**: 472-484.
- Fontes MR, Teh T, Jans D, Brinkworth RI, Kobe B. 2003a. Structural basis for the specificity of bipartite nuclear localization sequence binding by importin-alpha. *The Journal of biological chemistry* **278**: 27981-27987.
- Fontes MR, Teh T, Kobe B. 2000. Structural basis of recognition of monopartite and bipartite nuclear localization sequences by mammalian importin-alpha. *Journal of molecular biology* **297**: 1183-1194.
- Fontes MR, Teh T, Toth G, John A, Pavo I, Jans DA, Kobe B. 2003b. Role of flanking sequences and phosphorylation in the recognition of the simian-virus-40 large T-antigen nuclear localization sequences by importin-alpha. *The Biochemical journal* **375**: 339-349.
- Forwood JK, Lange A, Zachariae U, Marfori M, Preast C, Grubmuller H, Stewart M, Corbett AH, Kobe B. 2010. Quantitative structural analysis of importin-beta flexibility: paradigm for solenoid protein structures. *Structure* **18**: 1171-1183.
- Fritz J, Strehblow A, Taschner A, Schopoff S, Pasierbek P, Jantsch MF. 2009. RNA-regulated interaction of transportin-1 and exportin-5 with the double-stranded RNA-binding domain regulates nucleocytoplasmic shuttling of ADAR1. *Molecular and cellular biology* **29**: 1487-1497.
- Fukumoto M, Sekimoto T, Yoneda Y. 2011. Proteomic analysis of importin alpha-interacting proteins in adult mouse brain. *Cell structure and function* **36**: 57-67.
- Fung HY, Chook YM. 2014. Atomic basis of CRM1-cargo recognition, release and inhibition. *Seminars in cancer biology* **27**: 52-61.
- Giesecke A, Stewart M. 2010. Novel binding of the mitotic regulator TPX2 (target protein for Xenopus kinesin-like protein 2) to importin-alpha. *The Journal of biological chemistry* **285**: 17628-17635.
- Goldberg AD, Banaszynski LA, Noh KM, Lewis PW, Elsaesser SJ, Stadler S, Dewell S, Law M, Guo X, Li X et al. 2010. Distinct factors control histone variant H3.3 localization at specific genomic regions. *Cell* **140**: 678-691.
- Gorlich D. 1998. Transport into and out of the cell nucleus. *The EMBO journal* **17**: 2721-2727.
- Gorlich D, Kutay U. 1999. Transport between the cell nucleus and the cytoplasm. *Annual review of cell and developmental biology* **15**: 607-660.
- Gorlich D, Prehn S, Laskey RA, Hartmann E. 1994. Isolation of a protein that is essential for the first step of nuclear protein import. *Cell* **79**: 767-778.
- Greiner M, Caesar S, Schlenstedt G. 2004. The histones H2A/H2B and H3/H4 are imported into the yeast nucleus by different mechanisms. *European journal of cell biology* **83**: 511-520.

- Guttler T, Madl T, Neumann P, Deichsel D, Corsini L, Monecke T, Ficner R, Sattler M, Gorlich D. 2010. NES consensus redefined by structures of PKI-type and Rev-type nuclear export signals bound to CRM1. *Nature structural & molecular biology* **17**: 1367-1376.
- Hartl FU, Hayer-Hartl M. 2009. Converging concepts of protein folding in vitro and in vivo. *Nature structural & molecular biology* **16**: 574-581.
- Hirano H, Matsuura Y. 2011. Sensing actin dynamics: structural basis for G-actin-sensitive nuclear import of MAL. *Biochemical and biophysical research communications* **414**: 373-378.
- Huang X, Zhang L, Qi H, Shao J, Shen J. 2013. Identification and functional implication of nuclear localization signals in the N-terminal domain of JMJD5. *Biochimie* **95**: 2114-2122.
- Hurd TW, Fan S, Margolis BL. 2011. Localization of retinitis pigmentosa 2 to cilia is regulated by Importin beta2. *Journal of cell science* **124**: 718-726.
- Imasaki T, Shimizu T, Hashimoto H, Hidaka Y, Kose S, Imamoto N, Yamada M, Sato M. 2007. Structural basis for substrate recognition and dissociation by human transportin 1. *Molecular cell* **28**: 57-67.
- Isoyama T, Murayama A, Nomoto A, Kuge S. 2001. Nuclear import of the yeast AP-1-like transcription factor Yap1p is mediated by transport receptor Pse1p, and this import step is not affected by oxidative stress. *The Journal of biological chemistry* **276**: 21863-21869.
- Ito D, Seki M, Tsunoda Y, Uchiyama H, Suzuki N. 2011. Nuclear transport impairment of amyotrophic lateral sclerosis-linked mutations in FUS/TLS. *Annals of neurology* **69**: 152-162.
- Jakel S, Gorlich D. 1998. Importin beta, transportin, RanBP5 and RanBP7 mediate nuclear import of ribosomal proteins in mammalian cells. *The EMBO journal* **17**: 4491-4502.
- Jakel S, Mingot JM, Schwarzmaier P, Hartmann E, Gorlich D. 2002. Importins fulfil a dual function as nuclear import receptors and cytoplasmic chaperones for exposed basic domains. *The EMBO journal* **21**: 377-386.
- Janiszewska M, De Vito C, Le Bitoux MA, Fusco C, Stamenkovic I. 2010. Transportin regulates nuclear import of CD44. *The Journal of biological chemistry* **285**: 30548-30557.
- Jasencakova Z, Scharf AN, Ask K, Corpet A, Imhof A, Almouzni G, Groth A. 2010. Replication stress interferes with histone recycling and predeposition marking of new histones. *Molecular cell* **37**: 736-743.
- Johnson-Saliba M, Siddon NA, Clarkson MJ, Tremethick DJ, Jans DA. 2000. Distinct importin recognition properties of histones and chromatin assembly factors. *FEBS letters* **467**: 169-174.
- Kaffman A, Rank NM, O'Shea EK. 1998. Phosphorylation regulates association of the transcription factor Pho4 with its import receptor Pse1/Kap121. *Genes & development* **12**: 2673-2683.
- Kahle J, Baake M, Doenecke D, Albig W. 2005. Subunits of the heterotrimeric transcription factor NF-Y are imported into the nucleus by distinct pathways involving importin beta and importin 13. *Molecular and cellular biology* **25**: 5339-5354.
- Kahle J, Piaia E, Neimanis S, Meisterernst M, Doenecke D. 2009. Regulation of nuclear import and export of negative cofactor 2. *The Journal of biological chemistry* **284**: 9382-9393.
- Kalderon D, Richardson WD, Markham AF, Smith AE. 1984a. Sequence requirements for nuclear location of simian virus 40 large-T antigen. *Nature* **311**: 33-38.

- Kalderon D, Roberts BL, Richardson WD, Smith AE. 1984b. A short amino acid sequence able to specify nuclear location. *Cell* **39**: 499-509.
- Kataoka N, Bachorik JL, Dreyfuss G. 1999. Transportin-SR, a nuclear import receptor for SR proteins. *The Journal of cell biology* **145**: 1145-1152.
- Keck KM, Pemberton LF. 2012. Histone chaperones link histone nuclear import and chromatin assembly. *Biochimica et biophysica acta* **1819**: 277-289.
- Kimmins S, Sassone-Corsi P. 2005. Chromatin remodelling and epigenetic features of germ cells. *Nature* **434**: 583-589.
- Kimura M, Kose S, Okumura N, Imai K, Furuta M, Sakiyama N, Tomii K, Horton P, Takao T, Imamoto N. 2013a. Identification of cargo proteins specific for the nucleocytoplasmic transport carrier transportin by combination of an in vitro transport system and stable isotope labeling by amino acids in cell culture (SILAC)-based quantitative proteomics. *Molecular & cellular proteomics : MCP* **12**: 145-157.
- Kimura M, Okumura N, Kose S, Takao T, Imamoto N. 2013b. Identification of cargo proteins specific for importin-beta with importin-alpha applying a stable isotope labeling by amino acids in cell culture (SILAC)-based in vitro transport system. *The Journal of biological chemistry* **288**: 24540-24549.
- Kobayashi J, Matsuura Y. 2013. Structural basis for cell-cycle-dependent nuclear import mediated by the karyopherin Kap121p. *Journal of molecular biology* **425**: 1852-1868.
- Kobe B. 1999. Autoinhibition by an internal nuclear localization signal revealed by the crystal structure of mammalian importin alpha. *Nature structural biology* **6**: 388-397.
- Kosugi S, Hasebe M, Matsumura N, Takashima H, Miyamoto-Sato E, Tomita M, Yanagawa H. 2009a. Six classes of nuclear localization signals specific to different binding grooves of importin alpha. *The Journal of biological chemistry* **284**: 478-485.
- Kosugi S, Hasebe M, Tomita M, Yanagawa H. 2009b. Systematic identification of cell cycle-dependent yeast nucleocytoplasmic shuttling proteins by prediction of composite motifs. *Proceedings of the National Academy of Sciences of the United States of America* **106**: 10171-10176.
- Kouzarides T. 2007. Chromatin modifications and their function. *Cell* **128**: 693-705.
- Kraemer DM, Strambio-de-Castillia C, Blobel G, Rout MP. 1995. The essential yeast nucleoporin NUP159 is located on the cytoplasmic side of the nuclear pore complex and serves in karyopherin-mediated binding of transport substrate. *The Journal of biological chemistry* **270**: 19017-19021.
- Kressler D, Bange G, Ogawa Y, Stjepanovic G, Bradatsch B, Pratte D, Amlacher S, Strauss D, Yoneda Y, Katahira J et al. 2012. Synchronizing nuclear import of ribosomal proteins with ribosome assembly. *Science* **338**: 666-671.
- Lai MC, Kuo HW, Chang WC, Tarn WY. 2003. A novel splicing regulator shares a nuclear import pathway with SR proteins. *The EMBO journal* **22**: 1359-1369.
- Lai MC, Lin RI, Huang SY, Tsai CW, Tarn WY. 2000. A human importin-beta family protein, transportin-SR2, interacts with the phosphorylated RS domain of SR proteins. *The Journal of biological chemistry* **275**: 7950-7957.
- Lai MC, Lin RI, Tarn WY. 2001. Transportin-SR2 mediates nuclear import of phosphorylated SR proteins. *Proceedings of the National Academy of Sciences of the United States of America* **98**: 10154-10159.

- Lam MH, Briggs LJ, Hu W, Martin TJ, Gillespie MT, Jans DA. 1999. Importin beta recognizes parathyroid hormone-related protein with high affinity and mediates its nuclear import in the absence of importin alpha. *The Journal of biological chemistry* **274**: 7391-7398.
- Lanford RE, Butel JS. 1984. Construction and characterization of an SV40 mutant defective in nuclear transport of T antigen. *Cell* **37**: 801-813.
- Lange A, McLane LM, Mills RE, Devine SE, Corbett AH. 2010. Expanding the definition of the classical bipartite nuclear localization signal. *Traffic* **11**: 311-323.
- Lange A, Mills RE, Lange CJ, Stewart M, Devine SE, Corbett AH. 2007. Classical nuclear localization signals: definition, function, and interaction with importin alpha. *The Journal of biological chemistry* **282**: 5101-5105.
- Lau CK, Delmar VA, Chan RC, Phung Q, Bernis C, Fichtman B, Rasala BA, Forbes DJ. 2009. Transportin regulates major mitotic assembly events: from spindle to nuclear pore assembly. *Molecular biology of the cell* **20**: 4043-4058.
- Lee BJ, Cansizoglu AE, Suel KE, Louis TH, Zhang Z, Chook YM. 2006. Rules for nuclear localization sequence recognition by karyopherin beta 2. *Cell* **126**: 543-558.
- Lee DC, Aitchison JD. 1999. Kap104p-mediated nuclear import. Nuclear localization signals in mRNA-binding proteins and the role of Ran and Rna. *The Journal of biological chemistry* **274**: 29031-29037.
- Lee MS, Huang YH, Huang SP, Lin RI, Wu SF, Li C. 2009. Identification of a nuclear localization signal in the polo box domain of Plk1. *Biochimica et biophysica acta* **1793**: 1571-1578.
- Lee SJ, Matsuura Y, Liu SM, Stewart M. 2005. Structural basis for nuclear import complex dissociation by RanGTP. *Nature* **435**: 693-696.
- Lee SJ, Sekimoto T, Yamashita E, Nagoshi E, Nakagawa A, Imamoto N, Yoshimura M, Sakai H, Chong KT, Tsukihara T et al. 2003. The structure of importin-beta bound to SREBP-2: nuclear import of a transcription factor. *Science* **302**: 1571-1575.
- Leslie DM, Grill B, Rout MP, Wozniak RW, Aitchison JD. 2002. Kap121p-mediated nuclear import is required for mating and cellular differentiation in yeast. *Molecular and cellular biology* **22**: 2544-2555.
- Leslie DM, Zhang W, Timney BL, Chait BT, Rout MP, Wozniak RW, Aitchison JD. 2004. Characterization of karyopherin cargoes reveals unique mechanisms of Kap121p-mediated nuclear import. *Molecular and cellular biology* **24**: 8487-8503.
- Li Q, Burgess R, Zhang Z. 2012. All roads lead to chromatin: Multiple pathways for histone deposition. *Biochimica et biophysica acta* **1819**: 238-246.
- Li Q, Zhou H, Wurtele H, Davies B, Horazdovsky B, Verreault A, Zhang Z. 2008. Acetylation of histone H3 lysine 56 regulates replication-coupled nucleosome assembly. *Cell* **134**: 244-255.
- Li Y, Zhang L, Liu T, Chai C, Fang Q, Wu H, Agudelo Garcia PA, Han Z, Zong S, Yu Y et al. 2014. Hat2p recognizes the histone H3 tail to specify the acetylation of the newly synthesized H3/H4 heterodimer by the Hat1p/Hat2p complex. *Genes & development* **28**: 1217-1227.
- Liu WH, Roemer SC, Port AM, Churchill ME. 2012. CAF-1-induced oligomerization of histones H3/H4 and mutually exclusive interactions with Asf1 guide H3/H4 transitions among histone chaperones and DNA. *Nucleic Acids Res* **40**: 11229-11239.

- Lott K, Bhardwaj A, Sims PJ, Cingolani G. 2011. A minimal nuclear localization signal (NLS) in human phospholipid scramblase 4 that binds only the minor NLS-binding site of importin alpha1. *The Journal of biological chemistry* **286**: 28160-28169.
- Lott K, Cingolani G. 2011. The importin beta binding domain as a master regulator of nucleocytoplasmic transport. *Biochimica et biophysica acta* **1813**: 1578-1592.
- Loyola A, Bonaldi T, Roche D, Imhof A, Almouzni G. 2006. PTMs on H3 variants before chromatin assembly potentiate their final epigenetic state. *Molecular cell* **24**: 309-316.
- Luger K, Dechassa ML, Tremethick DJ. 2012. New insights into nucleosome and chromatin structure: an ordered state or a disordered affair? *Nat Rev Mol Cell Biol* **13**: 436-447.
- Luger K, Mader AW, Richmond RK, Sargent DF, Richmond TJ. 1997. Crystal structure of the nucleosome core particle at 2.8 Å resolution. *Nature* **389**: 251-260.
- Luger K, Rechsteiner TJ, Richmond TJ. 1999. Preparation of nucleosome core particle from recombinant histones. *Methods Enzymol* **304**: 3-19.
- Luk E, Vu ND, Patteson K, Mizuguchi G, Wu WH, Ranjan A, Backus J, Sen S, Lewis M, Bai Y et al. 2007. Chz1, a nuclear chaperone for histone H2AZ. *Molecular cell* **25**: 357-368.
- Lusk CP, Makhnevych T, Marelli M, Aitchison JD, Wozniak RW. 2002. Karyopherins in nuclear pore biogenesis: a role for Kap121p in the assembly of Nup53p into nuclear pore complexes. *The Journal of cell biology* **159**: 267-278.
- Ly-Huynh JD, Lieu KG, Major AT, Whiley PA, Holt JE, Loveland KL, Jans DA. 2011. Importin alpha2-interacting proteins with nuclear roles during mammalian spermatogenesis. *Biology of reproduction* **85**: 1191-1202.
- Maertens GN, Cook NJ, Wang W, Hare S, Gupta SS, Oztop I, Lee K, Pye VE, Cosnefroy O, Snijders AP et al. 2014. Structural basis for nuclear import of splicing factors by human Transportin 3. *Proceedings of the National Academy of Sciences of the United States of America* **111**: 2728-2733.
- Makhnevych T, Lusk CP, Anderson AM, Aitchison JD, Wozniak RW. 2003. Cell cycle regulated transport controlled by alterations in the nuclear pore complex. *Cell* **115**: 813-823.
- Mallet PL, Bachand F. 2013. A proline-tyrosine nuclear localization signal (PY-NLS) is required for the nuclear import of fission yeast PAB2, but not of human PABPN1. *Traffic* **14**: 282-294.
- Marfori M, Lonhienne TG, Forwood JK, Kobe B. 2012. Structural basis of high-affinity nuclear localization signal interactions with importin-alpha. *Traffic* **13**: 532-548.
- Marfori M, Mynott A, Ellis JJ, Mehdi AM, Saunders NF, Curmi PM, Forwood JK, Boden M, Kobe B. 2011. Molecular basis for specificity of nuclear import and prediction of nuclear localization. *Biochimica et biophysica acta* **1813**: 1562-1577.
- Matsuura Y, Lange A, Harreman MT, Corbett AH, Stewart M. 2003. Structural basis for Nup2p function in cargo release and karyopherin recycling in nuclear import. *The EMBO journal* **22**: 5358-5369.
- Matsuura Y, Stewart M. 2005. Nup50/Npap60 function in nuclear protein import complex disassembly and importin recycling. *The EMBO journal* **24**: 3681-3689.
- McLane LM, Pulliam KF, Devine SE, Corbett AH. 2008. The Ty1 integrase protein can exploit the classical nuclear protein import machinery for entry into the nucleus. *Nucleic Acids Res* **36**: 4317-4326.
- Mehrotra PV, Ahel D, Ryan DP, Weston R, Wiechens N, Kraehenbuehl R, Owen-Hughes T, Ahel I. 2011. DNA repair factor APLF is a histone chaperone. *Molecular cell* **41**: 46-55.

- Mingot JM, Kostka S, Kraft R, Hartmann E, Gorlich D. 2001. Importin 13: a novel mediator of nuclear import and export. *The EMBO journal* **20**: 3685-3694.
- Minor W, Cymborowski M, Otwinowski Z, Chruszcz M. 2006. HKL-3000: the integration of data reduction and structure solution--from diffraction images to an initial model in minutes. *Acta crystallographica Section D, Biological crystallography* **62**: 859-866.
- Mitrousis G, Olia AS, Walker-Kopp N, Cingolani G. 2008. Molecular basis for the recognition of snurportin 1 by importin beta. *The Journal of biological chemistry* **283**: 7877-7884.
- Miyamoto Y, Baker MA, Whiley PA, Arjomand A, Ludeman J, Wong C, Jans DA, Loveland KL. 2013. Towards delineation of a developmental alpha-importome in the mammalian male germline. *Biochimica et biophysica acta* **1833**: 731-742.
- Mor A, White MA, Fontoura BM. 2014. Nuclear trafficking in health and disease. *Current opinion in cell biology* **28**: 28-35.
- Moroianu J, Blobel G, Radu A. 1995. Previously identified protein of uncertain function is karyopherin alpha and together with karyopherin beta docks import substrate at nuclear pore complexes. *Proceedings of the National Academy of Sciences of the United States of America* **92**: 2008-2011.
- Mosammaparast N, Ewart CS, Pemberton LF. 2002a. A role for nucleosome assembly protein 1 in the nuclear transport of histones H2A and H2B. *The EMBO journal* **21**: 6527-6538.
- Mosammaparast N, Guo Y, Shabanowitz J, Hunt DF, Pemberton LF. 2002b. Pathways mediating the nuclear import of histones H3 and H4 in yeast. *The Journal of biological chemistry* **277**: 862-868.
- Mosammaparast N, Jackson KR, Guo Y, Brame CJ, Shabanowitz J, Hunt DF, Pemberton LF. 2001. Nuclear import of histone H2A and H2B is mediated by a network of karyopherins. *The Journal of cell biology* **153**: 251-262.
- Mosammaparast N, Pemberton LF. 2004. Karyopherins: from nuclear-transport mediators to nuclear-function regulators. *Trends in cell biology* **14**: 547-556.
- Mousson F, Lautrette A, Thuret JY, Agez M, Courbeyrette R, Amigues B, Becker E, Neumann JM, Guerois R, Mann C et al. 2005. Structural basis for the interaction of Asf1 with histone H3 and its functional implications. *Proceedings of the National Academy of Sciences of the United States of America* **102**: 5975-5980.
- Muhlhauser P, Muller EC, Otto A, Kutay U. 2001. Multiple pathways contribute to nuclear import of core histones. *EMBO reports* **2**: 690-696.
- Murzina NV, Pei XY, Zhang W, Sparkes M, Vicente-Garcia J, Pratap JV, McLaughlin SH, Ben-Shahar TR, Verreault A, Luisi BF et al. 2008. Structural basis for the recognition of histone H4 by the histone-chaperone RbAp46. *Structure* **16**: 1077-1085.
- Mynott AV, Harrop SJ, Brown LJ, Breit SN, Kobe B, Curmi PM. 2011. Crystal structure of importin-alpha bound to a peptide bearing the nuclear localisation signal from chloride intracellular channel protein 4. *The FEBS journal* **278**: 1662-1675.
- Nakagawa T, Bulger M, Muramatsu M, Ito T. 2001. Multistep chromatin assembly on supercoiled plasmid DNA by nucleosome assembly protein-1 and ATP-utilizing chromatin assembly and remodeling factor. *The Journal of biological chemistry* **276**: 27384-27391.
- Natsume R, Eitoku M, Akai Y, Sano N, Horikoshi M, Senda T. 2007. Structure and function of the histone chaperone CIA/ASF1 complexed with histones H3 and H4. *Nature* **446**: 338-341.

- Neumann M, Bentmann E, Dormann D, Jawaid A, DeJesus-Hernandez M, Ansorge O, Roeber S, Kretzschmar HA, Munoz DG, Kusaka H et al. 2011. FET proteins TAF15 and EWS are selective markers that distinguish FTLD with FUS pathology from amyotrophic lateral sclerosis with FUS mutations. *Brain : a journal of neurology* **134**: 2595-2609.
- Niu C, Zhang J, Gao F, Yang L, Jia M, Zhu H, Gong W. 2012. FUS-NLS/Transportin 1 complex structure provides insights into the nuclear targeting mechanism of FUS and the implications in ALS. *PloS one* **7**: e47056.
- O'Reilly AJ, Dacks JB, Field MC. 2011. Evolution of the karyopherin-beta family of nucleocytoplasmic transport factors; ancient origins and continued specialization. *PloS one* **6**: e19308.
- Palmer DK, O'Day K, Wener MH, Andrews BS, Margolis RL. 1987. A 17-kD centromere protein (CENP-A) copurifies with nucleosome core particles and with histones. *The Journal of cell biology* **104**: 805-815.
- Park KE, Inerowicz HD, Wang X, Li Y, Koser S, Cabot RA. 2012. Identification of karyopherin alpha1 and alpha7 interacting proteins in porcine tissue. *PloS one* **7**: e38990.
- Pehrson JR, Fried VA. 1992. MacroH2A, a core histone containing a large nonhistone region. *Science* **257**: 1398-1400.
- Pemberton LF, Paschal BM. 2005. Mechanisms of receptor-mediated nuclear import and nuclear export. *Traffic* **6**: 187-198.
- Ploski JE, Shamsher MK, Radu A. 2004. Paired-type homeodomain transcription factors are imported into the nucleus by karyopherin 13. *Molecular and cellular biology* **24**: 4824-4834.
- Portela A, Esteller M. 2010. Epigenetic modifications and human disease. *Nat Biotechnol* **28**: 1057-1068.
- Pumroy RA, Cingolani G. 2015. Diversification of importin-alpha isoforms in cellular trafficking and disease states. *The Biochemical journal* **466**: 13-28.
- Pumroy RA, Ke S, Hart DJ, Zachariae U, Cingolani G. 2015. Molecular Determinants for Nuclear Import of Influenza A PB2 by Importin alpha Isoforms 3 and 7. *Structure* **23**: 374-384.
- Putker M, Madl T, Vos HR, de Ruiter H, Visscher M, van den Berg MC, Kaplan M, Korswagen HC, Boelens R, Vermeulen M et al. 2013. Redox-dependent control of FOXO/DAF-16 by transportin-1. *Molecular cell* **49**: 730-742.
- Quan Y, Ji ZL, Wang X, Tartakoff AM, Tao T. 2008. Evolutionary and transcriptional analysis of karyopherin beta superfamily proteins. *Molecular & cellular proteomics : MCP* **7**: 1254-1269.
- Radu A, Blobel G, Moore MS. 1995. Identification of a protein complex that is required for nuclear protein import and mediates docking of import substrate to distinct nucleoporins. *Proceedings of the National Academy of Sciences of the United States of America* **92**: 1769-1773.
- Ray-Gallet D, Quivy JP, Scamps C, Martini EM, Lipinski M, Almouzni G. 2002. HIRA is critical for a nucleosome assembly pathway independent of DNA synthesis. *Molecular cell* **9**: 1091-1100.
- Roman N, Christie M, Swarbrick CM, Kobe B, Forwood JK. 2013. Structural characterisation of the nuclear import receptor importin alpha in complex with the bipartite NLS of Prp20. *PloS one* **8**: e82038.

- Rona G, Marfori M, Borsos M, Scheer I, Takacs E, Toth J, Babos F, Magyar A, Erdei A, Bozoky Z et al. 2013. Phosphorylation adjacent to the nuclear localization signal of human dUTPase abolishes nuclear import: structural and mechanistic insights. *Acta crystallographica Section D, Biological crystallography* **69**: 2495-2505.
- Rout MP, Blobel G, Aitchison JD. 1997. A distinct nuclear import pathway used by ribosomal proteins. *Cell* **89**: 715-725.
- Sarma K, Reinberg D. 2005. Histone variants meet their match. *Nat Rev Mol Cell Biol* **6**: 139-149.
- Sawatsubashi S, Murata T, Lim J, Fujiki R, Ito S, Suzuki E, Tanabe M, Zhao Y, Kimura S, Fujiyama S et al. 2010. A histone chaperone, DEK, transcriptionally coactivates a nuclear receptor. *Genes & development* **24**: 159-170.
- Schones DE, Cui K, Cuddapah S, Roh TY, Barski A, Wang Z, Wei G, Zhao K. 2008. Dynamic regulation of nucleosome positioning in the human genome. *Cell* **132**: 887-898.
- Senger B, Simos G, Bischoff FR, Podtelejnikov A, Mann M, Hurt E. 1998. Mtr10p functions as a nuclear import receptor for the mRNA-binding protein Npl3p. *The EMBO journal* **17**: 2196-2207.
- Shi Q, Han Y, Jiang J. 2014. Suppressor of fused impedes Ci/Gli nuclear import by opposing Trn/Kapbeta2 in Hedgehog signaling. *Journal of cell science* **127**: 1092-1103.
- Shin SH, Lee EJ, Chun J, Hyun S, Kim YI, Kang SS. 2012. The nuclear localization of glycogen synthase kinase 3beta is required its putative PY-nuclear localization sequences. *Molecules and cells* **34**: 375-382.
- Smith S, Stillman B. 1991. Stepwise assembly of chromatin during DNA replication in vitro. *The EMBO journal* **10**: 971-980.
- Soniat M, Chook YM. 2015. Nuclear localization signals for four distinct karyopherin-beta nuclear import systems. *The Biochemical journal* **468**: 353-362.
- Soniat M, Chook YM. 2016. Recognition elements in the histone H3 and H4 tails for seven different Importins. *Manuscript Submitted*.
- Soniat M, Sampathkumar P, Collett G, Gizzi AS, Banu RN, Bhosle RC, Chamala S, Chowdhury S, Fiser A, Glenn AS et al. 2013. Crystal structure of human Karyopherin beta2 bound to the PY-NLS of *Saccharomyces cerevisiae* Nab2. *Journal of structural and functional genomics* **14**: 31-35.
- Su D, Hu Q, Li Q, Thompson JR, Cui G, Fazly A, Davies BA, Botuyan MV, Zhang Z, Mer G. 2012. Structural basis for recognition of H3K56-acetylated histone H3-H4 by the chaperone Rtt106. *Nature* **483**: 104-107.
- Suel KE, Cansizoglu AE, Chook YM. 2006. Atomic resolution structures in nuclear transport. *Methods* **39**: 342-355.
- Suel KE, Chook YM. 2009. Kap104p imports the PY-NLS-containing transcription factor Tfg2p into the nucleus. *The Journal of biological chemistry* **284**: 15416-15424.
- Suel KE, Gu H, Chook YM. 2008. Modular organization and combinatorial energetics of proline-tyrosine nuclear localization signals. *PLoS biology* **6**: e137.
- Tagami H, Ray-Gallet D, Almouzni G, Nakatani Y. 2004. Histone H3.1 and H3.3 complexes mediate nucleosome assembly pathways dependent or independent of DNA synthesis. *Cell* **116**: 51-61.
- Tai LR, Chou CW, Lee IF, Kirby R, Lin A. 2013. The quantitative assessment of the role played by basic amino acid clusters in the nuclear uptake of human ribosomal protein L7. *Experimental cell research* **319**: 367-375.

- Takeda AA, de Barros AC, Chang CW, Kobe B, Fontes MR. 2011. Structural basis of importin-alpha-mediated nuclear transport for Ku70 and Ku80. *Journal of molecular biology* **412**: 226-234.
- Thiriet C, Hayes JJ. 2001. A novel labeling technique reveals a function for histone H2A/H2B dimer tail domains in chromatin assembly in vivo. *Genes & development* **15**: 2048-2053.
- Timney BL, Tetenbaum-Novatt J, Agate DS, Williams R, Zhang W, Chait BT, Rout MP. 2006. Simple kinetic relationships and nonspecific competition govern nuclear import rates in vivo. *The Journal of cell biology* **175**: 579-593.
- Tran EJ, Bolger TA, Wentz SR. 2007a. SnapShot: nuclear transport. *Cell* **131**: 420.
- Tran EJ, Zhou Y, Corbett AH, Wentz SR. 2007b. The DEAD-box protein Dbp5 controls mRNA export by triggering specific RNA:protein remodeling events. *Molecular cell* **28**: 850-859.
- Trojer P, Reinberg D. 2007. Facultative heterochromatin: is there a distinctive molecular signature? *Molecular cell* **28**: 1-13.
- Trowitzsch S, Viola C, Scheer E, Conic S, Chavant V, Fournier M, Papai G, Ebong IO, Schaffitzel C, Zou J et al. 2015. Cytoplasmic TAF2-TAF8-TAF10 complex provides evidence for nuclear holo-TFIID assembly from preformed submodules. *Nature communications* **6**: 6011.
- Twyffels L, Gueydan C, Kruijs V. 2014. Transportin-1 and Transportin-2: protein nuclear import and beyond. *FEBS letters* **588**: 1857-1868.
- Twyffels L, Wauquier C, Soin R, Decaestecker C, Gueydan C, Kruijs V. 2013. A masked PY-NLS in Drosophila TIS11 and its mammalian homolog tristetraprolin. *PloS one* **8**: e71686.
- Tyler JK, Adams CR, Chen SR, Kobayashi R, Kamakaka RT, Kadonaga JT. 1999. The RCAF complex mediates chromatin assembly during DNA replication and repair. *Nature* **402**: 555-560.
- Ueta R, Fukunaka A, Yamaguchi-Iwai Y. 2003. Pse1p mediates the nuclear import of the iron-responsive transcription factor Aft1p in *Saccharomyces cerevisiae*. *The Journal of biological chemistry* **278**: 50120-50127.
- Venkatesh S, Workman JL. 2015. Histone exchange, chromatin structure and the regulation of transcription. *Nat Rev Mol Cell Biol* **16**: 178-189.
- Verreault A, Kaufman PD, Kobayashi R, Stillman B. 1998. Nucleosomal DNA regulates the core-histone-binding subunit of the human Hat1 acetyltransferase. *Current biology : CB* **8**: 96-108.
- Waldmann I, Walde S, Kehlenbach RH. 2007. Nuclear import of c-Jun is mediated by multiple transport receptors. *The Journal of biological chemistry* **282**: 27685-27692.
- Walker P, Doenecke D, Kahle J. 2009. Importin 13 mediates nuclear import of histone fold-containing chromatin accessibility complex heterodimers. *The Journal of biological chemistry* **284**: 11652-11662.
- Wang L, Li M, Cai M, Xing J, Wang S, Zheng C. 2012. A PY-nuclear localization signal is required for nuclear accumulation of HCMV UL79 protein. *Medical microbiology and immunology* **201**: 381-387.
- Weis K. 2003. Regulating access to the genome: nucleocytoplasmic transport throughout the cell cycle. *Cell* **112**: 441-451.
- White CL, Suto RK, Luger K. 2001. Structure of the yeast nucleosome core particle reveals fundamental changes in internucleosome interactions. *The EMBO journal* **20**: 5207-5218.

- Winkler DD, Zhou H, Dar MA, Zhang Z, Luger K. 2012. Yeast CAF-1 assembles histone (H3-H4)₂ tetramers prior to DNA deposition. *Nucleic Acids Res* **40**: 10139-10149.
- Wodrich H, Cassany A, D'Angelo MA, Guan T, Nemerow G, Gerace L. 2006. Adenovirus core protein pVII is translocated into the nucleus by multiple import receptor pathways. *Journal of virology* **80**: 9608-9618.
- Xu D, Farmer A, Chook YM. 2010. Recognition of nuclear targeting signals by Karyopherin-beta proteins. *Current opinion in structural biology* **20**: 782-790.
- Xu S, Zhang Z, Jing B, Gannon P, Ding J, Xu F, Li X, Zhang Y. 2011. Transportin-SR is required for proper splicing of resistance genes and plant immunity. *PLoS genetics* **7**: e1002159.
- Yang SN, Takeda AA, Fontes MR, Harris JM, Jans DA, Kobe B. 2010. Probing the specificity of binding to the major nuclear localization sequence-binding site of importin-alpha using oriented peptide library screening. *The Journal of biological chemistry* **285**: 19935-19946.
- Yarbrough ML, Mata MA, Sakthivel R, Fontoura BM. 2014. Viral subversion of nucleocytoplasmic trafficking. *Traffic* **15**: 127-140.
- Yaseen NR, Blobel G. 1997. Cloning and characterization of human karyopherin beta3. *Proceedings of the National Academy of Sciences of the United States of America* **94**: 4451-4456.
- Yun CY, Velazquez-Dones AL, Lyman SK, Fu XD. 2003. Phosphorylation-dependent and -independent nuclear import of RS domain-containing splicing factors and regulators. *The Journal of biological chemistry* **278**: 18050-18055.
- Zhang W, Tyl M, Ward R, Sobott F, Maman J, Murthy AS, Watson AA, Fedorov O, Bowman A, Owen-Hughes T et al. 2013. Structural plasticity of histones H3-H4 facilitates their allosteric exchange between RbAp48 and ASF1. *Nature structural & molecular biology* **20**: 29-35.
- Zhang ZC, Chook YM. 2012. Structural and energetic basis of ALS-causing mutations in the atypical proline-tyrosine nuclear localization signal of the Fused in Sarcoma protein (FUS). *Proceedings of the National Academy of Sciences of the United States of America* **109**: 12017-12021.
- Zhang ZC, Satterly N, Fontoura BM, Chook YM. 2011. Evolutionary development of redundant nuclear localization signals in the mRNA export factor NXF1. *Molecular biology of the cell* **22**: 4657-4668.